PROTEASE-ACTIVATED RECEPTOR SIGNALING IN CELLULAR DIFFERENTIATION FOLLOWING VASCULAR AND HEPATIC INJURY

A thesis

submitted by

Karyn M. Austin

In partial fulfillment of the requirements
for the degree of

Doctor of Philosophy

in

Genetics

TUFTS UNIVERSITY

Sackler School of Graduate Biomedical Sciences

May 2013

ADVISER: Athan Kuliopulos MD,PhD

ABSTRACT

Protease-activated receptors (PARs) are a family of G protein coupled receptors whose aberrant activation influences a variety of disease states including cardiovascular disease, liver fibrosis, arthritis, sepsis, and cancer. This thesis focuses on the pathologic role of PAR1 and PAR2 signaling following vascular and hepatic injury.

Atherothrombotic disease remains the leading cause of death in the United States, Europe and Western nations. PAR1, also known as the high-affinity thrombin receptor, has emerged as a new drug target in patients undergoing percutaneous coronary intervention (PCI) for treatment of atherothrombotic disease. However, studies with direct thrombin inhibitors have not demonstrated a beneficial effect in preventing restenosis of culprit lesions post-PCI. Here, we identify matrix metalloprotease-1 (MMP-1) as a non-canonical PAR1 agonist that specifically stimulates smooth muscle cell (SMC) de-differentiation, hyperplasia and migration, resulting in phenotypic alterations that favor a restenotic program. In contrast, thrombin-PAR1 signaling promotes a differentiated, contractile phenotype in vascular SMCs. Unlike thrombin blockade, inhibition of MMP1-activity leads to marked suppression of restenosis in mouse models of arterial wire-injury. These findings suggest a MMP1-driven phenotypic switch via PAR1 with therapeutic implications for suppressing post-injury restenosis.

Non-alcoholic fatty liver disease (NAFLD), and the more severe non-alcoholic steatohepatitis (NASH), are liver manifestations of obesity and insulin resistance. The prevalence of NAFLD in the general population is estimated between 10-46%. PAR2-driven activation and differentiation of hepatic stellate cells has been implicated in the pathogenesis of NAFLD and NASH. Using a cell-penetrating PAR2 antagonist pepducin, we demonstrate decreased steatosis and hepatic inflammation in animal models of

NASH, providing critical evidence for the use of PAR2 inhibitors in the treatment of NAFLD/NASH.

ACKNOWLEDGEMENTS

I would like to thank my adviser, Dr. Athan Kuliopulos, for his guidance and support throughout the completion of my thesis. I would also like to sincerely thank Dr. Lidija Covic for her scientific expertise and contributions to experimental design and manuscript editing. A special thanks to my outside examiner, Dr. John Keaney. I appreciate you taking the time to read my thesis and contributing to my development as a physician-scientist. I thank my thesis committee, doctors Gordon Huggins, Grace Gill, and Janis Lem for their support, direction, and scientific guidance over the years.

To Dr. Anika Agarwal, who is not only my colleague, but my friend; you have helped me through a number of hard times and I truly value our friendship. To the remainder of the Kuliopulos Lab, past and present, in particular: Leila Sevigny, Caitlin Foley, Katie O'Callaghan, and George Koukos. They have been wonderful friends and lab-mates throughout my years at Tufts, and we have shared a number of laughs that I will always remember (like when George's thumb was chopped off!). A special thanks to Nga Nguyen for whom the lab would not exist without. I would like to thank my sister, Carlye Austin, PhD, and my boyfriend, Chris Parkin MS, for their help with proof-reading and editing.

I would also like to thank Dr. Goli Javid for histological specimens from the Tufts Medical Center Department of Pathology. To the Genetics and MD/PhD programs for making my PhD thesis as painless as possible. To my family and friends, and the countless people along my path who have helped and inspired me; I dedicate this to you all.

TABLE OF CONTENTS

LIST OF TABLES

LIST OF FIGURES

I. Introduction

II. Chapter 1

III. Chapter 2

V. Appendix

LIST OF ABBREVIATIONS

ACS: acute coronary syndrome

ALT: alanine aminotransferase

APC: activated protein C

ERK: extracellular-signal regulated kinase

FAK: focal adhesion kinase

FFA: free fatty acid

GPCR: G protein coupled receptor

H&E: hematoxylin and eosin

HFD: high fat diet

HLI: hind limb ischemia

HSC: hepatic stellate cell

IP3: inositol triphosphate

KO: knock-out

MCD: methionine-choline deficient

MLC: myosin light chain

MMP: matrix metalloprotease

NAFLD: non-alcoholic fatty liver disease

NAS: NASH activity score

NASH: non-alcoholic steatohepatitis

PAD: peripheral artery disease

PAR: protease activated receptor

PCI: percutaneous coronary intervention

PECAM: CD31

PLC: phospholipase C

PTx: pertussis toxin

RT-qPCR: reverse transcriptase- quantitative polymerase chain reaction

RWJ: RWJ-56110

SMA: smooth muscle actin

SMC: smooth muscle cell

TM: transmembrane

TZD: thiazolidinedione

WT: wild-type

I. Chapter 1: Introduction

Over two decades ago, the classic ligand-initiated paradigm of G protein coupled receptor (GPCR) signaling was challenged with the discovery of protease-activated receptors (PARs). Unlike canonical GPCR activation, which requires a soluble ligand, PARs are enzymatically cleaved at their N-terminus to free a tethered ligand, which subsequently activates the receptor and downstream signaling.[1] The elucidation of this unique activation mechanism has transformed how we think about GPCR signaling, and more importantly, emphasizes the critical role of proteases in influencing cellular behavior. This thesis focuses on the contributions of protease-activated receptors -1 and -2 (PAR1 and PAR2) to cellular injury and repair, with a special focus on matrix metalloprotease-PAR1 signaling and cellular differentiation in cardiovascular and hepatic pathophysiology. The following introductory reading will summarize the current literature on PARs and matrix metalloproteases (MMPs), and bring the reader up to date on PAR1 and PAR2 signaling in the cardiovascular and hepatic systems, respectively.

I.1 G protein coupled receptors

GPCRs represent the largest protein family in the human genome, and include upwards of 800 distinct receptors which account for approximately 30% of current drug targets.[2, 3] GPCRs are characterized by their distinctive seven-transmembrane topology, and are grouped into five major families based on amino acid sequence: Rhodopsin, Adhesion, Secretin, Glutamate, and Frizzled. They are further subdivided based on homology; PARs belong to the 'delta' subgroup of the Rhodopsin family.

I.2 Protease-activated receptors (PARs)

Proteases comprise approximately 2% of the human genome and contribute to cell signaling through zymogen/ligand activation, degradation/inactivation of soluble ligands, and activation/inactivation of cell-surface receptors.[4, 5] PARs are a subfamily of GPCRs that are cleaved and activated by an array of proteases including those associated with coagulation, inflammatory cells, the digestive tract, and matrix remodeling.[5] PARs signal through heterotrimeric G proteins to activate a multitude of signaling outputs that influence cell behavior and function (**Figure 1.1**). Aberrant PAR signaling has been implicated in thrombosis, in-stent restenosis, heart failure, sepsis, arthritis, inflammation, wound-healing, and cancer among others.[1] This section will summarize the cloning, receptor activation, signal termination, and physiological roles PARs, with a focus on PAR1 and PAR2.

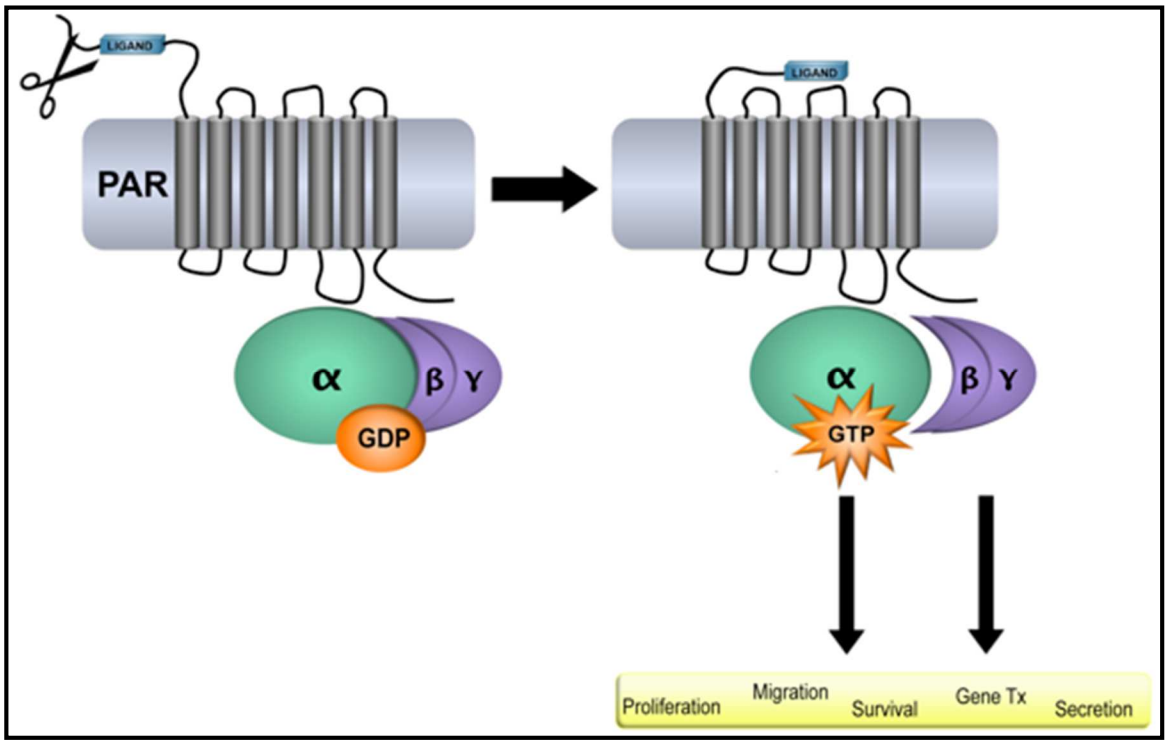

Figure 1.1. Mechanism of PAR activation. PARs are activated through proteolytic cleavage of the N-terminus, which liberates a tethered ligand that is then capable of interacting with extracellular loop 2, resulting in conformational changes in the transmembrane regions that activate G-protein signaling. Activation of the receptor results in the exchange of GDP for GTP in the Gα subunit, resulting in dissociation of the α and βγ subunits. Both the α and βγ subunits are capable of activating downstream signaling cascades that are cell type- and context-specific.

I.2.1 Molecular cloning of PARs

PARs were initially cloned following the observation that thrombin, a coagulation protease, is an extremely potent activator of platelet aggregation.[6] The search for a *thrombin receptor* was initiated through expression vector screening using cDNA's derived from thrombin-sensitive cells.[7] Examination of positively identified clones produced a 3.5 kb fragment of cDNA whose sequence revealed that it belonged to the seven-transmembrane GPCR superfamily of proteins. The novel receptor was initially termed the thrombin receptor, but later named protease-activated receptor-1 (PAR1) following identification of other PARs.

Further analysis of PAR1 identified a sequence in the N-terminus that closely mimicked the thrombin cleavage site in the coagulation factor, activated protein C (APC), suggesting that the receptor was a direct proteolytic target of thrombin.[7] Vu and colleagues postulated that thrombin cleavage at the N-terminus unmasked a tethered ligand that subsequently was capable of activating the receptor. Mutational analysis of the proposed cleavage site rendered the receptor unresponsive to thrombin, providing crucial support for their proposed mechanism. Additional studies revealed a hirudin-like sequence distal to the thrombin cleavage site (**Figure 1.2**), which binds to exosite I in thrombin and results in a conformational change that lowers thrombin's activation energy for cleavage.[8] Hirudin, is a naturally occurring leech anti-coagulant and potent thrombin inhibitor. It was later shown that the hirudin-like sequence increases the efficiency of thrombin-PAR1 interactions and cleavage, as its absence, such as in PAR4 (discussed below), results in decreased affinity between the enzyme and receptor.[7-9] Experiments conducted in parallel on hamster isolates resulted in the discovery of hamster PAR1; similar to Vu *et al.*, a thrombin cleavage site was identified in the N-terminus along with an acidic hirudin-like sequence.[10] It was therefore proposed that thrombin binds to the hirudin-like sequence and cleaves the N-terminus of the receptor, liberating a tethered

ligand that is capable of activating the receptor. Proof of concept was obtained when Coughlin and his group showed that an exogenous peptide corresponding to the cleaved tethered ligand could be used to activate PAR1.[7]

Following the discovery of PAR1, further investigation hinted at the existence of additional protease-activated receptors. First, it was observed that exogenous activating peptides alone could not completely recapitulate all of the functions of thrombin in platelets. Second, keratinocytes were found to be responsive to a thrombin-generated activating peptide, but not to thrombin itself.[11, 12] These findings suggested that an alternative receptor was responsible for the observed discrepancies. Hybridization studies utilizing primers to the bovine substance K GPCR against a mouse genomic library resulted in a positive hit, the sequence of which was most closely related to the human thrombin receptor, PAR1. Exogenous expression in *Xenopus* oocytes, however, did not result in a thrombin-responsive phenotype. Surprisingly, the alternate serine protease, trypsin, triggered robust intracellular calcium mobilization, suggesting the existence of an alternative receptor that is sensitive to trypsin.[13] Additional studies confirmed the presence of a human homologue of the trypsin receptor, now known as PAR2.[11]

The discovery of a second thrombin-sensitive receptor came after the creation of *Par1* $^{-/-}$ mice. Although nearly half of these animals die around embryonic day 9, those that survive have platelets that are capable of responding to thrombin, despite germline PAR1 deletion.[14] Subsequent studies resulted in the cloning of the PAR3 receptor.[15] Unlike PAR1 and PAR2, exogenous addition of the cleavage-generated peptide did not result in PAR3 receptor activation.[115] Furthermore, it was found that human platelets do not express PAR3, in stark contrast to murine platelets which express high levels of the receptor.[16] Additionally, the signaling of PAR3 appears to be drastically different depending on the interrogated species; thrombin is able to activate human PAR3,

whereas mouse Par3 is unresponsive to thrombin cleavage.[15, 17] Since PAR3 contains a hirudin-like sequence that promotes thrombin association and cleavage, it has been suggested that mouse Par3 functions as an anchoring protein for thrombin-driven activation of Par4 (which lacks a hirudin-like sequence), as opposed to being a direct thrombin target.[17]

The last PAR identified, PAR4, was discovered independently by two groups in the late 1990s. The first used an *in silico* approach and performed a homology BLAST against both the public DNA database dbEST and the Incyte EST database using the previously identified PARs1-3 as the query sequences.[18] A partial sequence was identified in the screen, and the full length cDNA was cloned from a lymphoma cell library.[18] The second group proposed the existence of a fourth receptor due to the fact that platelets from *Par3*$^{-/-}$ mice were still capable of responding to thrombin despite their inability to express PAR1. A BLAST search of the mouse GenBank revealed the presence of PAR4, which was confirmed after showing that *Par3*$^{-/-}$ platelets were activated by exogenous addition of the PAR4-derived agonist peptide.[19]

PARs 1-3 are clustered on the long arm of human chromosome 5, whereas PAR4 is located on chromosome 19.[20] PAR1 and PAR2 are less than 100 kb downstream from one another, suggesting that PAR2 most likely arose from a recent gene duplication.[21] The PARs are similarly structured, in that they contain two exons; the first encodes a signal peptide and the second encodes the entire functional receptor.[22] Because of the structural and genetic similarities among PARs, it has been proposed that they evolved from a common ancestor.[23]

I.2.2 Mechanism of receptor activation and structural insights

PARs are activated through irreversible proteolytic cleavage of the N-terminus allowing for extracellular interactions between the newly created tethered ligand and extracellular loop 2 of the receptor (**Figure 1.1**).[1, 7] Subsequent conformational changes in the transmembrane and intracellular portions of the receptor translate information regarding the extracellular proteolytic environment to a functional second messenger or effector protein.[1]

Cleavage of PAR1 by thrombin occurs at a canonical R_{41}-S_{42} bond in the N-terminal region (**Figure 1.2**). Exogenous addition of synthetic peptides corresponding to the thrombin-generated tethered-ligand (*e.g.*, S/TFLLRN) are able to stimulate signaling outputs that mimic proteolytic activation of the receptor,[7] thus providing critical evidence that PARs carry their own ligand. Additionally, it has been observed that the peptide agonist, SFLLRN, is capable of activating both PAR1 and PAR2 either through a direct heterodimer or close membrane proximity; however, replacement of the serine for threonine at the first position in the tethered ligand shows a predilection for PAR1 signaling only.[1, 24]

Thrombin cleavage of PAR1 is facilitated by a $K_{51}YEPF_{55}$ motif in the receptor that resembles the C-terminus of hirudin (**Figure 1.2**).[25] Binding of thrombin's exosite I to the hirudin-like sequence of PAR1 results in allosteric changes to the protease that lower the activation energy necessary for cleavage at the LDPR-S canonical site on PAR1 (**Figure 1.2**).[26] Mutational analysis of the thrombin cleavage site identified the Leu_{38} and Pro_{40} residues as critical for proper cleavage of PAR1.[27, 28] By comparison, the low-affinity PAR4 receptor lacks the functional hirudin-like sequence found in PAR1, and therefore is a less potent thrombin receptor.[29] Instead, PAR4 contains an anionic cluster in its exodomain, which slows the dissociation rate of PAR4 from the cationic thrombin.[29]

A high-resolution crystal structure of PAR1 was recently published, and this has strengthened our understanding of the structure-function relationship of PARs in general.[30] Two major differences between PAR1 and other Rhodopsin family GPCRs occur at conserved sites in transmembrane (TM) regions 6 and 7.[30] A highly conserved motif in TM6, FXXCWXP (where X is any residue), acts as a toggle switch in the majority of GPCRs[31]; interestingly, PAR1 has a substituted Phe for Trp in this motif. Additionally, the NPXXY motif in TM7, which helps stabilize the open-state conformation in other GPCRs, has a replacement of the asparagine for aspartate.[30] These structural changes suggest that PAR1, and perhaps other PARs by extension, differ quite drastically from other GPCRs in how they transmit the extracellular signal to the associated heterotrimeric G protein complex. Consistent with this hypothesis is the observation that mutations at and near the extracellular surface drastically reduce PAR1 activation, suggesting that PAR1 agonist peptides may bind and activate the receptor more superficially than has been observed with other GPCR peptide agonists (*e.g.*, opioid receptors).[30]

PAR2 is activated by a similar mechanism, with the distinction that PAR2 is not responsive to thrombin but is instead activated by trypsin and trypsin-like proteases (mast cell tryptase, Factor Xa, and matriptase[1]). N-terminal PAR2 cleavage occurs at the R_{34}-S_{35} peptide bond and results in a ligand corresponding to SLIGKV.[24] Similar to PAR1, the addition of exogenous peptides corresponding to the human and mouse sequences is able to activate PAR2-dependent signaling cascades.

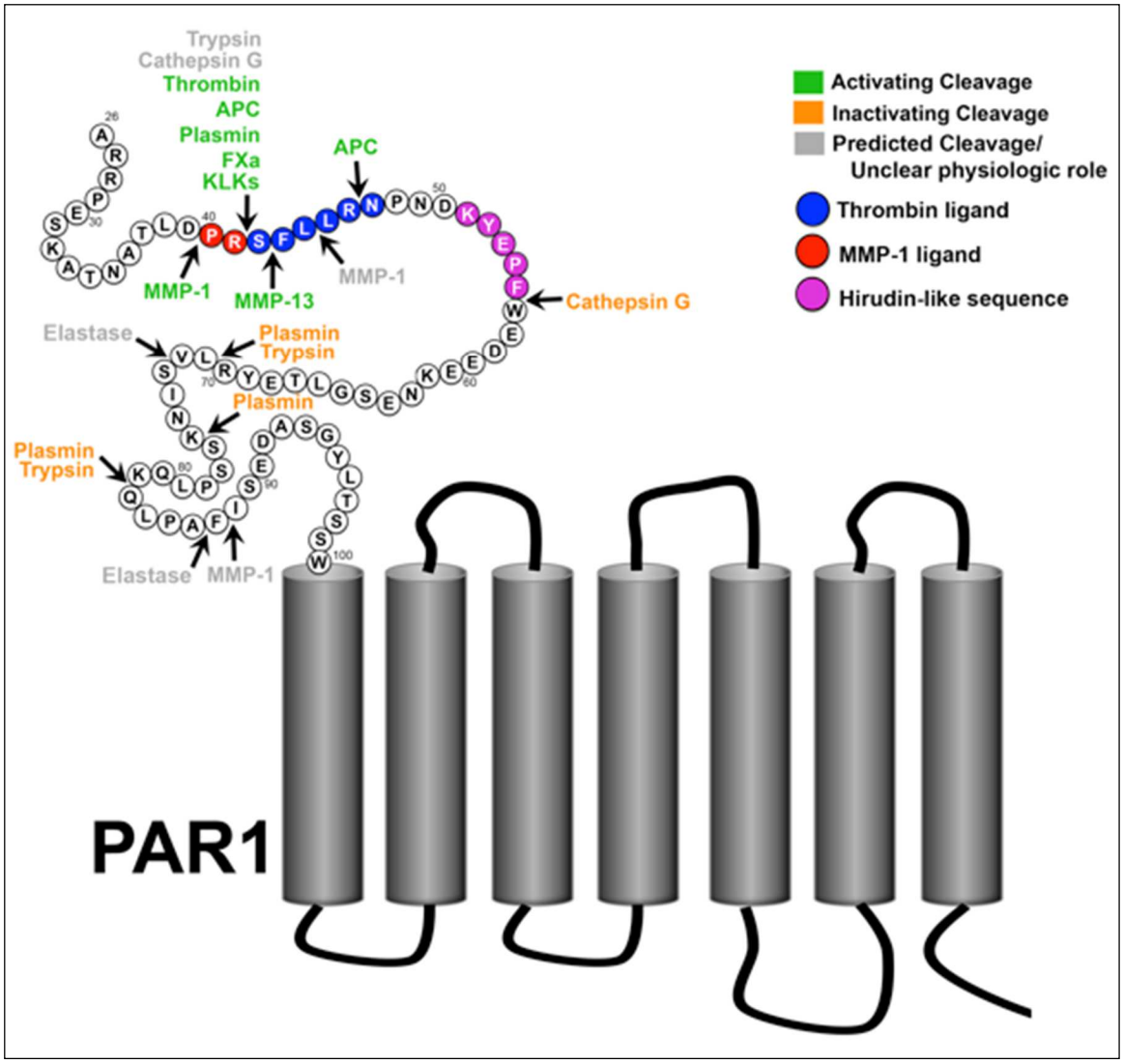

Figure 1.2. Activating and Inactivating cleavages in PAR1. Schematic of enzymatic cleavages of PAR1. Enzymes shown in green are confirmed activating cleavages, those shown in orange are inactivating cleavages. Enzymes shown in grey are either predicted cleavage sites, or sites that have been shown to activate/inactivate with unknown physiologic significance. Blue residues correspond to the canonical thrombin ligand, whereas red residues show the non-canonical MMP-1 generated peptide which is two amino acids longer than the classic thrombin ligand. Activated protein C (APC); Factor Xa (FXa), Kalikreins (KLKs); Matrix metalloprotease (MMP). It should be noted that other proteases have been shown to inactivate PAR1 (ADAM17 and Protease 3) although only functional cleavage and exact cleavage sites have not been identified.

I.2.3 PAR signaling and termination

I.2.3.1 Signaling

PARs exert their effects through activation of various G protein constituents. Specifically, PAR1 has been shown to activate the G_i, G_q, and $G_{12/13}$ families of G proteins (**Figure 1.3**).[1, 5] The exact nature of each interaction and the functional consequences that result from G protein activation are cell type- and environment-specific. Most studies attempting to identify specific interactions have relied on G protein-blocking antibodies or have utilized cells derived from G protein knock-out animals. Therefore, although there are general guidelines to PAR1-dependent G protein signaling, it is by no means comprehensive. A recent study attempted to ectopically express both PAR1 and PAR2 in the PAR-null Cos7 cell line to elucidate how PARs couple to G proteins under similar cellular conditions. The researchers found that PAR1 and PAR2 both signal through G_q and G_{12}, whereas only PAR1 signaled through G_i.[32] Although these results are intriguing, Cos7 cells are not human derived and the receptors are ectopically expressed, which are important limitations to the study.

One of the more prominent PAR1-coupled pathways involves G_q activation and subsequent PLC-β signaling (**Figure 1.3**). Fibroblasts, cancer cells, and platelets utilize this signaling cascade to mobilize intracellular calcium and stimulate calcium-dependent pathways. [1, 5] Activation of this signaling axis promotes proliferation, migration, and secretion, among others.[5] PAR1 is also capable of coupling to G_i dependent pathways in certain cell lines and cell types. In Chinese hamster ovary (CHO) cells, PAR1 signaling is almost entirely G_i-dependent, and stimulates PLC-β activation and arachidonic acid release through the $\beta\gamma$ subunits. G_i signaling is sensitive to inhibition by pertussis toxin, which is a useful reagent when interrogating G_i -dependent pathways. $G_{12/13}$ pathways are important for cytoskeletal reorganization and cellular shape change (**Figure 1.3**).

PAR1 couples to $G_{12/13}$ pathways in both platelets and endothelial cells, which results in platelet activation and endothelial barrier disruption, respectively.[33, 34] PAR1 has consistently been shown to activate MAP- kinase (MAPK) signaling pathways, although it is unclear whether this occurs through a specific G protein pathway, or is ubiquitous to all G proteins.[24, 34]

Although PAR2 G protein signaling has not been as thoroughly studied as PAR1, some similarities have been identified. PAR2 is known to couple to inositol triphosphate (IP_3)-calcium-dependent pathways in a number of cell types, suggesting that PAR2 probably couples to G_q.[1] Studies have not demonstrated pertussis toxin-sensitive PAR2 signaling, indicating that G_i is not a prominent pathway for PAR2.[1] Similar to PAR1, PAR2 strongly activates MAPK signaling, particularly the ERK1/2 pathway; the exact mechanism of MAPK activation is elusive, but arrestins are thought to play an important scaffolding role for PAR2.

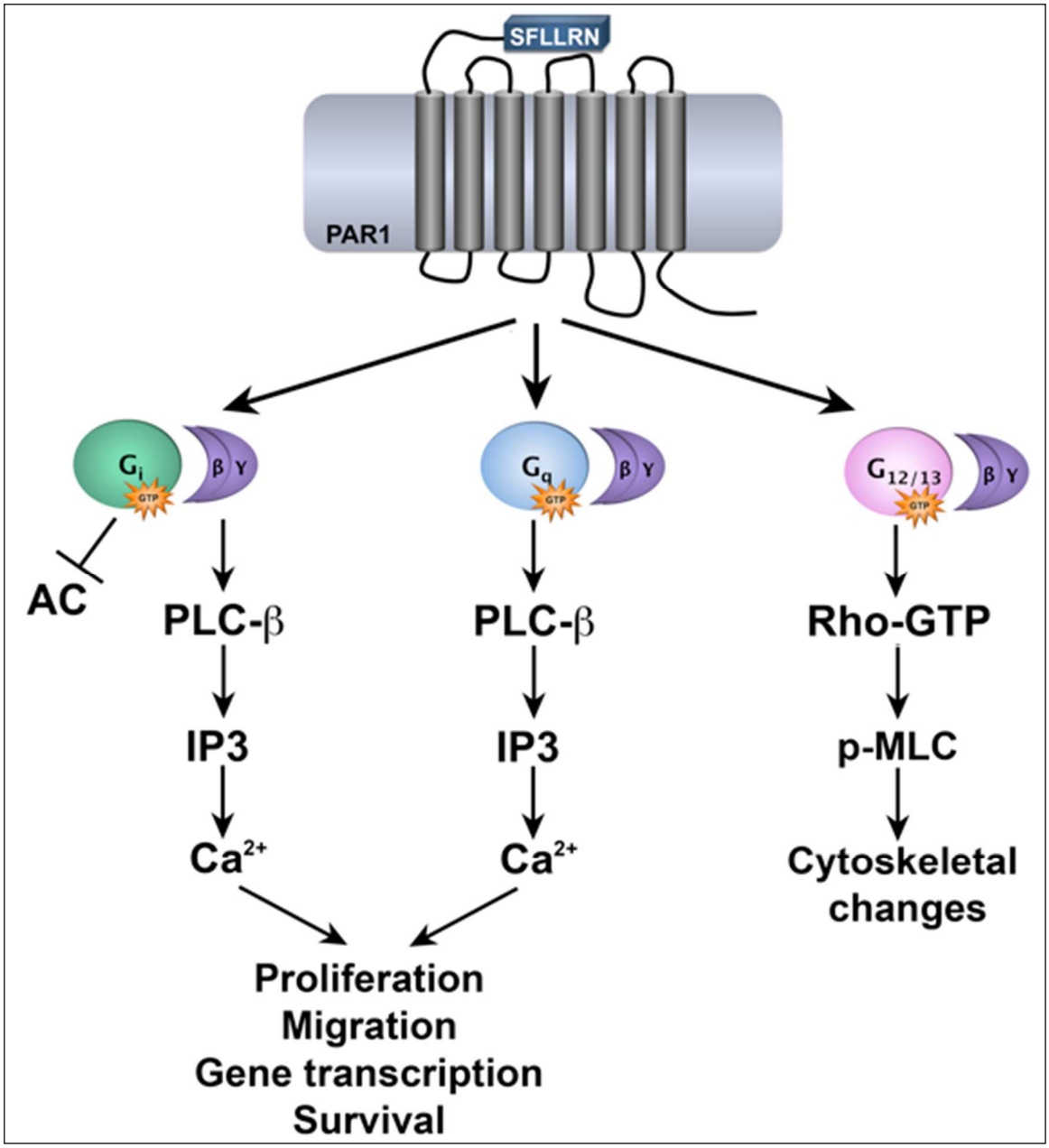

Figure 1.3. PAR1-G protein signaling. Schematic of G protein signaling pathways known to couple to PAR1: G_i, G_q, $G_{12/13}$. Adenylyl cyclase (AC), phospholipase C (PLC-β), inositol phosphate-3 (IP3), calcium (Ca^{2+}), phosphor-myosin light chain (MLC). For illustrative purposes, the tethered ligand is shown from N⇒C, from left to right.

I.2.3.2 Termination

Unlike classic ligand-receptor interactions, where signaling is dependent on the availability and concentration of the given ligand in the extracellular milieu, PARs have the unique ability to maintain an innate connection with their ligand due to N-terminal tethering. Given the constant availability of ligand, it would seem possible that PARs could signal indefinitely following proteolytic cleavage; surprisingly this is not the case. In fact, the accumulation of IP_3 is directly correlated to the absolute rate of PAR1 cleavage by thrombin.[35] Therefore, PARs utilize a precise form (or forms) of signal termination to regulate their signaling effects. This phenomenon can be readily observed by monitoring intracellular calcium flux in cells in response to various protease and peptide agonists. Following stimulation with a particular agonist, cells often become unresponsive to repeated stimulation, suggesting that some form of signal termination has occurred. Currently, two primary mechanisms of PAR inactivation exist.

Currently, there exist two primary mechanisms of PAR1 inactivation. The first mechanism involves inactivating cleavages in the N-terminus by other proteases (**Figure 1.2**). The best example of this takes place between trypsin and PAR1. Trypsin is capable of cleaving PAR1 at the canonical R_{41}-S_{42} peptide bond, and has also been shown to cleave at the 70-71 and 82-83 peptide bonds with similar kinetics.[36] Studies by Nakayama *et al*[37] showed that endothelial cells were unresponsive to thrombin with preceding trypsin treatment, which theoretically could result from trypsin-induced cleavage at any of the three primary sites. What they then observed was that the response to trypsin with preceding thrombin stimulation did not differ from that without thrombin, suggesting that the observed trypsin-signal was a result of PAR2 activation, since PAR1 desensitization was not observed following the initial thrombin treatment.[37] This led the investigators to hypothesize that trypsin is capable of cleaving PAR1, but that this cleavage does not result in functional PAR1 signaling. In fact, numerous

proteases have been found to cleave PAR1 at distal sites to the R_{41}-S_{42} bond, although it is not clear whether all of these cleavages are functionally relevant (**Figure 1.2**).

A second mechanism of signal termination is C-tail phosphorylation by G protein-coupled receptor kinases (GRKs). Studies utilizing overexpression systems of GRK3 and GRK5 have demonstrated increased PAR1 phosphorylation and inhibition of IP_3 accumulation.[38] In other GPCRs, phosphorylation by GRKs has been shown to enhance receptor binding to arrestins, which disrupts the interaction between the receptor and G proteins, thereby inhibiting the signal.[39] Studies of PAR1 signaling in β-arrestin1/2 null mouse embryonic fibroblasts (MEFs) show impaired desensitization following PAR1 activation, suggesting that a similar phosphorylation- β-arrestin pathway exists for PAR1.[40]

Phosphokinase C (PKC) appears to play an important role in PAR2-dependent desensitization. Cells activated with phorbol esters to stimulate PKC activity display inhibited PAR2-dependent calcium signaling.[41] Furthermore, C-terminal mutations in the putative PKC abolish the inhibition observed with phorbol ester treatment. These results suggest that PAR2 may have unique inactivating mechanisms independent of those established for PAR1.[5]

I.2.4 PAR1 and PAR2 in normal and pathophysiology

PAR-driven physiologic signaling represents a complex pathway that involves activating and inactivating proteases, receptors, receptor dimers, cofactors, various G proteins, and desensitizing pathways. Therefore, the functional outputs that result from PAR signaling are many and varied, and PARs have been implicated in the vast majority of pathological states including, but not limited to, cardiovascular disease, thrombosis, cancer, inflammation, fibrosis, and arthritis.[22] This section will summarize the roles of

PAR1 and PAR2 in both normal and pathophysiology, with particular focus on the cardiovascular and gastrointestinal/hepatic systems.

I.2.4.1 ***Cardiovascular system***

Considering that PARs were initially identified as thrombin receptors, their role in the vasculature is paramount.[42] PARs are expressed on nearly all cell types in the blood vessel wall and blood, the notable exception being red blood cells.[42] PAR1 is the high-affinity thrombin receptor and is expressed on the surface of endothelium, smooth muscle cells, platelets, neutrophils, macrophages, and leukemic white cells.[43, 44] Thrombin activation of PAR1 promotes platelet aggregation, shape change, adhesion, cell proliferation, chemokine production, and migration via G_q, G_i and $G_{12/13}$ pathways.[24] PAR1 is on platelets is activated under low concentrations of thrombin, subsequent increases in thrombin can result in the activation of the low-affinity receptor, PAR4.[45] Platelet activation results in granule release and adhesion, both of which are critical for proper clot formation.

Despite thrombin's important role in platelet-driven thrombosis, activation of platelets in patients with acute coronary syndromes often occurs under high shear-stress on sub-endothelial surfaces enriched with collagen fibrils.[46] Studies using whole human blood spiked with PAR1 inhibitors, such as a PAR1 pepducin,[47] have shown no effect on primary adhesion of platelets to immobilized collagen fibrils under arterial shear.[48] This led to the hypothesis that an alternative PAR1 activator was responsible for initial platelet activation and nucleation under high flow rates. It was subsequently shown that matrix metalloprotease-1 (MMP-1) is capable of cleaving and activating PAR1 on platelets.[48] Furthermore, it was demonstrated that the growth-rate of platelet aggregate "strings" was significantly attenuated by an MMP-1 inhibitor, FN-439, or PAR1 inhibitors.

Additionally direct antagonism of thrombin had little effect on early thrombogenesis on collagen surfaces under high arterial flow rates.[48] Several studies have previously shown that thrombin may be more important for later propagation and stability of platelet thrombi, and is not involved in initiating early thrombus growth at high arterial shear[49-51] unless tissue factor levels are extremely high.[52]

Both PAR1 and PAR2 are highly expressed on endothelium and vascular smooth muscle.[5] It has been proposed that PAR1 plays a critical role in cardiovascular development since the 50% embryonic lethality rate exhibited by *Par1*$^{-/-}$ mice can be corrected with re-expression of PAR1 in the endothelium.[14, 53] Activation of PAR1 and PAR2 in the vasculature has been shown to cause both vasoconstriction and dilation depending on the source of the blood vessel, presence or absence of endothelium, and the conditions under which the experiment was performed.

In the endothelium, activation of PAR1 results in endothelial contraction with loss of tight junctions and increased permeability resulting in edema and inflammation.[5] PAR1 activation also results in release of von Willibrand factor (VWF) and P-selectin cell surface expression to promote platelet and leukocyte rolling and adhesion.[45] Cleavage of endothelial PAR2 mediates proliferation and cytokine expression, and stimulates vasodilation.[22, 54] Human studies, in which PAR2-derived peptide agonists were injected into the forearm, showed dilation of resistance vessels and elevated blood flow, which occur through nitric oxide (NO)- and prostaglandin-dependent pathways. [5] PAR2 activation also induces edema and neutrophil infiltration, although this mechanism is thought to be primarily due to PAR2-$_{\text{elicited}}$ neuropeptide release from sensory neurons.[5]

PAR1 expression on vascular smooth muscle cells (SMCs) is increased following balloon catheter placement and in atherosclerotic plaques.[55, 56] Furthermore, studies have shown increased SMC surface expression of PAR1 after subarachnoid hemorrhage,[57] suggesting that up-regulation of PAR1 following vascular injury may be a

universal response in the SMC repair process. Thrombin-PAR1 activation in vascular SMCs results in mobilization of intracellular calcium, extracellular matrix (ECM) production, growth factor release, and increased proliferation.[58-61] Inhibition of PAR1 in models of vascular injury have produced mixed results; *Par1*$^{-/-}$ mice showed no statistical difference in neointima formation in wire injury models, and actually showed increased neointimal proliferation in ligation-injury models.[62, 63] Conversely, pharmacologic inhibitors of PAR1 have reduced neointima formation in animal models of vascular injury.[59, 62]

Similar to PAR1, PAR2 expression is also increased on SMCs following balloon-injury models.[64] Furthermore, *Par2*$^{-/-}$ mice show reduced neointima formation after wire-injury, although it was suggested that this effect was due to PAR2's role in leukocyte adhesion and a concomitant decreased inflammatory response in *Par2*$^{-/-}$ mice.[65] These results illustrate that PAR1 and PAR2 in the vasculature are important mediators of the repair process following injury, although it is unclear whether PAR1 propagates or ameliorates the hyperplastic response.

I.2.4.2 Gastrointestinal/hepatic system

Both PAR1 and PAR2 are expressed on a number of cell types throughout the gastrointestinal system. PAR1 is present on intestinal epithelial cells, SMCs of the gut, and enteric neurons. PAR2, on the other hand, has a broader expression pattern that includes enterocytes of the intestine and colon, liver, pancreas, SMCs, and enteric neurons. PAR2 activation of enterocytes results in IP_3 production, intracellular calcium mobilization, and prostaglandin release.[5] Stimulation of PAR2 on ductal cells of the pancreas regulates ion transport and protects against pancreatitis by increasing ductal secretions upon premature activation of trypsinogen. Consistent with PAR2's protective

role in pancreatitis, *Par2*$^{-/-}$ mice show increased acinar cell vacuolization and necrosis in models of acute pancreatitis.[66]

PAR2 also plays a detrimental role in infectious colitis through increased neutrophil infiltration, cytokine production, and bacterial translocation.[67] Genetic deletion of PAR2 reduces the inflammatory response in models of infectious colitis. In contrast, PAR1 appears to mediate an anti-inflammatory response in similar models, and studies have shown that administration of a PAR1 agonist or use of *Par1*$^{-/-}$ mice reduces the inflammatory response in colitis models.[1]

Both PAR1 and PAR2 have been implicated in injury-induced fibrotic responses in the liver. Kassel *et al*[68] showed that *Par1*$^{-/-}$ mice had reduced hepatic inflammation and steatosis in Western diet-induced models of liver steatosis. Other studies have shown that PAR1 antagonists dosed to rats reduced collagen expression in the liver.[69] \Genetic deletion of *Par2* protects against collagen deposition and hepatic stellate cell activation in experimental models of liver fibrosis.[70] Additionally,PAR2 blocking peptides have been used successfully to prevent acute liver injury in endotoxemia models in mice.[71]

I.2.4.3 ***Cancer***

PAR1 was initially identified as a potential oncogene in 1995 after a screen of cDNA libraries by the Whitehead Institute.[72] Dysregulated PAR1 and PAR2 expression has been linked to a wide variety of cancers, including lung, colorectal, prostate, breast, and ovarian.[1] Generally speaking, PAR1 expression and activation is associated with increased tumor invasion and metastasis as well as being a pro-angiogenic pathway. Activation of PAR1 on breast cancer cells enhances cell migration *in vitro*, and PAR1 knockdown in MDA-MB-231 breast cancer cells abolishes *in vivo* tumor formation in the mammary fat pad in xenograft models.[1] Furthermore, PAR1 activation by thrombin in

prostate cancer cells results in increased secretion of IL-8 and VEGF, both potent angiogenic factors.[73] PAR2 also appears to play a detrimental role in tumor progression. *Par2*$^{-/-}$ mice bred onto a spontaneous tumor background show delayed tumor onset and decreased metastasis.[1] PAR2 activation also promotes angiogenesis through production of pro-angiogenic factors.[1] Both PAR1 and PAR2 have been shown to increase proliferation in cancerous cell lines through MAPK-dependent pathways, suggesting that PARs may also play a role in cancer cell proliferation and survival.[1]

I.2.5 PAR inhibition

Given the importance of PARs in the vasculature, among other systems, there has been substantial interest in developing PAR-specific antagonists. The majority of antagonists have been directed at the prototypical receptor, PAR1, due to its critical role in platelet aggregation, and by extension antithrombotic therapeutic potential. The first class of receptor antagonists were peptide-mimetics in which modifications were made to the activating peptide sequence in order to retain peptide binding but prevent receptor activation. The most successful peptide-mimetics were developed based on a “three point pharmacophore model” which constricts the distances between three important functional groups.[59, 74-76] The resulting structure inhibits activation of the receptor by both enzymatic cleavage and peptide agonists. These compounds include BMS-200261 and RWJ-56110/58259, which are widely used experimentally.[22]

Blocking antibodies have also been used successfully to inhibit thrombin-induced platelet activation, although at high concentrations and in concert with PAR4 blocking antibodies.[77] Another class of inhibitors, pepducins, utilizes a completely different approach to receptor antagonism by inhibiting from the intracellular surface of the GPCR. Pepducins correspond to a sequence modeled after the intracellular loops of

their target receptor and contain a hydrophobic lipid to facilitate membrane anchoring. They mimic or antagonize the contacts between the targeted receptor and the associated G protein.[78] The first pepducins were targeted against both PAR1 and PAR4 and were shown to inhibit peptide-driven platelet aggregation.[79, 80] Most recently, a PAR1 antagonist pepducin, PZ-128, was shown to inhibit arterial thrombosis in guinea pig and baboon models.[81] PAR2 antagonist pepducins such as PZ-235 have been used in models of inflammation and edema, and are shown to inhibit neutrophil migration and infiltration.[63] Pepducins have also been successfully used in models of sepsis and cancer.

The next wave of inhibitors were non-peptide based small molecules discovered through screening of a combinatorial library.[82] The most successful were the two orally-active piperazine compounds, F16357 and F16618. Both compounds showed greater than 90% inhibition of calcium release and had antithrombotic effects in shunt models, although it is possible that these compounds also targeted non-PAR GPCRs.[82, 83] Currently, the two most successful small molecule inhibitors, SCH-530348 (vorapaxar) and E5555 (atopaxar), have progressed to phase 2 and 3 clinical trials. Vorapaxar is an orally active small molecule inhibitor based on the alkaloid himbacine isolated from the bark of the Australian magnolia.[82, 84] It was shown to be extremely efficacious in preventing thrombosis in non-human primate models of arterial thrombosis.[85] In 2009 a multi-center, randomized, double-blind, controlled phase 3 clinical trial was instated (TRACER: ***T***hrombin ***R***eceptor ***A***ntagonist for ***C***linical ***E***vent ***R***eduction in acute coronary syndrome)[86] to test the antithrombotic effects of vorapaxar in combination with current standard of care therapy (aspirin and/or clopidogrel). Due to observed increases in intracranial bleeding during TRACER, the trial was stopped and two subsections aimed at evaluating the efficacy and safety in (1) atherosclerotic disease and (2) prevention of thrombotic events in patients with a history of myocardial infarction (MI) was modified to

exclude patients with a history of stroke (TRA 2°P-TIMI 50).[87] For the evaluation of vorapaxar in prevention of atherothrombotic events, vorapaxar-treated patients showed a statistically significant decrease in the primary endpoint (cardiovascular death), although there was an increase in moderate to severe bleeding and intracranial hemorrhage.[88] The results from the TRA 2°P-TIMI 50 arm aimed at preventing thrombotic events in patients with a history of MI were recently published, and showed a significant decrease in cardiovascular death, myocardial infarction, and stroke in the vorapaxar-treated group versus control (in patients with a history of MI). Moderate or severe bleeding events were seen more frequently in the vorapaxar-treated arm.[89]

E5555 is a competitive antagonist of PAR1 that has been shown to inhibit platelet aggregation, without significantly increasing the bleeding risk.[84, 90] A small phase 2 clinical trial was established to evaluate safety, in which the drug was well tolerated and there was no increased risk of bleeding (J-LANCELOT: ***J***apanese-***L***esson from ***AN***tagonizing the ***CEL***lular effects ***O***f ***T***hrombin).[91]

PAR2 inhibitors have received very little attention compared to PAR1 inhibitors. Peptide-mimetics (FSLLRY-NH_2 and LSIGRL-NH_2) have been shown to block trypsin-mediated cleavage, although they have little effect on activating peptides.[1] GB88 is a small molecule inhibitor of PAR2 that is the first orally available, reversible agonist shown to specifically inhibit PAR2 signaling by both trypsin and activating peptides.[1] Given the prevalence of aberrant PAR2 signaling in disease (see Section I.2.4), further development of GB88 and similar antagonists is warranted.

I.3 Matrix metalloproteases

MMPs represent a family of proteases that were initially characterized by their ability to degrade ECM, although they have been revisited in recent years due to the overwhelming evidence of their importance in both normal and pathophysiology. Furthermore, two MMPs, MMP-1 and MMP-13, have recently been shown to cleave and activate PAR1 (**Figure 1.4a,b**). The following sections will summarize the current literature on MMPs and their role in PAR signaling and cardiovascular disease.

I.3.1 Classifications

MMPs comprise a family of 28 zinc-dependent endopeptidases, which are further subdivided based on their distinct, albeit overlapping, substrate specificity.[92] MMP-1, -8, and -13, otherwise known as the interstitial collagenases, are capable of initiating the degradation of fibrillar-type collagens by cleaving at a single site three-quarters of the distance away from the N-terminus.[93] The ensuing ¾ and ¼ fragments are subsequently denatured at body temperature and further degraded by the gelatinases. Collagen is the most abundant protein in the human body; therefore, the collagenases represent an essential enzyme class critical for normal development and tissue repair.[94] MMP-2 and -9 comprise the gelatinases -- the primary enzymes capable of degrading the gelatinous by-products of collagen degradation.[95] MMP-3, -7, -10, and -11 are members of the stromelysin subfamily, which degrade laminin, fibronectin, and elastin, among others.[96] MMP-12 is thought to be a distantly related metalloelastase, which primarily degrades elastin and is found predominantly in macrophages.[95, 97] The final class is composed of the membrane-tethered MMPs; these include MMP-14, -15, -16, -17, -24, and -25.[98]

Nearly all MMPs are secreted as zymogens, and acquire activity through removal of their auto-inhibitory pro-domain.[99] The pro-domain of MMPs contains a highly

conserved cysteine residue responsible for coordinating with the active-site zinc to lock the enzyme in an inactive state. Disruption of the cysteine-zinc interaction, either through chemical modification or by proteolytic release of the pro-domain, results in activation of the zymogen.[99]

To date, only two MMPs have been identified as having agonist activity against PAR1: MMP-1 and MMP-13.[100-103] MMP-1 and MMP-13 belong to the collagenase subfamily and share several important structural features, including classic signal peptide, pro-, catalytic, and hemopexin domains characteristic of this subgroup (**Figure 1.4a**). MMP-1 is expressed in most human tissues, including the majority of cell types in the blood vessel wall, inflammatory cells, and platelets, and is considered the primary enzyme responsible for collagen degradation.[104-106] Despite the pervasive basal expression of MMP-1, a number of disease states result in further up-regulation of MMP-1, a consequence that is often associated with poor outcomes.[95, 105, 107]

MMP-13 is more limited in its tissue expression profile compared to MMP-1, and is important to developing bone and periodontal tissues.[108, 109] Similar to MMP-1, MMP-13 is up-regulated in a number of pathologic states including atherosclerosis, rheumatoid arthritis, periodontitis, breast cancer, melanoma, and squamous cell carcinomas of the head and neck.[105, 110]

Although MMPs are classically categorized based on their extracellular-matrix substrate specificity, they also function as important signaling molecules through the cleavage of more than 100 extracellular ligands and proteins.[111] Important non-matrix substrates include osteopontin[112], SDF-1α[113], HB-EGF[114], IL-1β[115], and now PAR1.

I.3.2 MMP-1 cleavage of PAR1 and biased agonism

Recently, it was found that PAR1 is also a substrate for the collagenases, MMP-1 and MMP-13, which cleave PAR1 at non-canonical sites distinct from thrombin.[48, 103] The initial identification of the MMP-1 cleavage site of PAR1 stemmed from cleavage studies utilizing a synthetic 26-amino acid peptide (TR26) which spanned the N-terminal tethered ligand region of PAR1.[48] Incubation of nanomolar MMP-1 with TR26 yielded a peptide with a mass that corresponded to cleavage at the D_{39}-P_{40} peptide bond (**Figure 1.4b**). This cleavage resulted in a tethered-ligand two amino acids longer than the thrombin-generated ligand. To confirm that this cleavage event would result in productive PAR1 signaling, the longer MMP-1 ligand PR-SFLLRN peptide was synthesized and tested for platelet activity. The result was complete recapitulation of the signaling cascades activated by the authentic MMP-1 enzyme including platelet shape change, RhoA activation, and p38 phosphorylation; however, the peptide was a relatively weak agonist for stimulating intracellular calcium mobilization and platelet aggregation. These effects were all blocked by a small molecule inhibitor of PAR1, RWJ-56110, confirming that these are PAR1-dependent events.[48] Together, these data demonstrate that MMP1-PAR1 strongly activated Rho-GTP pathways, cell shape change, motility, and MAPK signaling in platelets.[48] Subsequent analysis of G protein signaling pathways presented the first evidence that MMP-1 and the PR-SFLLRN ligand are biased agonists that preferentially activate $G_{12/13}$, and thrombin preferentially activates G_q in human platelets.[48]

Blackburn *et al*[116] showed that MMP-1 and thrombin differentially activate MAPK signaling, with MMP1-driven signals delayed (15 min) compared to thrombin (5 min), both of which were inhibited by a PAR1-specific antagonist. In breast cancer cells, thrombin and MMP-1 activated PAR1-dependent phospho-Akt signals[117], with the peak Akt signal occurring at 5 min for thrombin and 1 h for MMP-1, showing that even with

identical signaling outputs, thrombin and MMP-1 display markedly divergent kinetics.[117] Perhaps more striking was the differential effects seen on PAR1-dependent gene expression of certain pro-angiogenic factors in endothelial cells.[116] The two enzymes individually increased expression of subsets that were independent of the other protease, suggesting that MMP1-PAR1 signaling may alter the phenotype of cells in a manner distinct from thrombin-PAR1 activation.[116]

Though thrombin is specific for the R_{41}-S_{42}FLLRN bond, MMP-1 generally prefers a hydrophobic residue at the C-terminal side (P1′) of the cleavage site, a basic or hydrophobic amino acid at P2′, and a small residue (alanine, glycine or serine) at P3′ which facilitates proper fit between the substrate and the S1′-S3' sites on the enzyme surface (**Figure 1.4b**).[118, 119] By placing the hydrophobic P_{40} residue at the P1′ position, the alignment of the PAR1 cleavage peptide resembles that seen in native substrates of the collagenases.[118, 119] Using x-ray structures of MMP-1 and MMP-8 bound to peptide inhibitors,[120, 121] we modeled the PAR1 ligand region consisting of the residues T_{37}LD-PRSFLLRN$_{47}$ bound to the active site cleft of human MMP-1 with the scissile D_{39}-P_{40} peptide bond carbonyl oxygen coordinated to the active site zinc (**Figure 1.4b**). Especially favorable hydrophobic interactions and geometry were observed for PAR1 P3 and P2 residues (T_{37}, L_{38}) and for the C-terminal cleavage site P1′-P_{40} within the active site groove surrounding the catalytic zinc of MMP-1. To provide evidence to support this model, we substituted the P1′-P_{40} residue with asparagine in both the full-length receptor (P40N-PAR1) and the cleavage peptide (TR26-P40N), a substitution which had previously been shown to substantially reduce cleavage of collagen peptides.[122] To inhibit proteolysis by thrombin, we mutated the P1′-S_{42} serine of the thrombin cleavage site to aspartate (S42D-PAR1), a mutation that suppresses cleavage by thrombin.[123] The P40N PAR1 mutant was fully cleaved by thrombin but was poorly cleaved by MMP-1.

Conversely, the S42D-PAR1 mutant was substantially cleaved by MMP-1 but was poorly cleaved by thrombin. These results are consistent with the mass spectrometry cleavage data, which show that MMP-1 cleaves PAR1 at D_{39}-P_{40}, and illustrate the ability to selectively uncouple MMP-1 cleavage of PAR1 from thrombin.

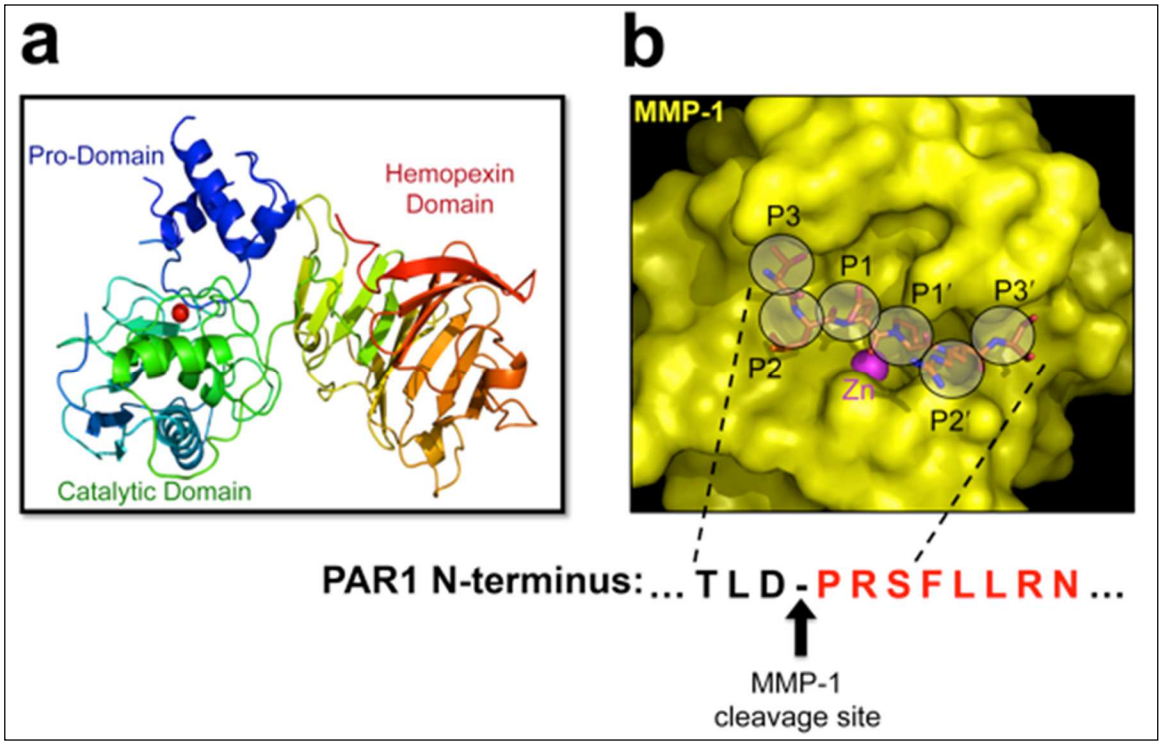

Figure 1.4. MMP-1 cleavage of PAR1. (a) Crystal structure of MMP-1 showing the pro, catalytic and hemopexin domains. The catalytic zinc is shown in red. **(b)** Model of the N-terminal region of PAR1 in the MMP-1 active site. The catalytic zinc is shown in magenta. MMP-1 favors a hydrophobic residue at the P1′ to facilitate fit into the catalytic groove. (Modeling performed in collaboration with Dr. Andrew Bohm; Modified from Austin et al. 2012)[124]

Two other MMP-1 cleavage sites in the PAR1 N-terminal exodomain have been described. Nesi *et al*.[125] showed that by using a longer incubation time and micromolar concentrations of MMP-1, recombinant PAR1 (A_{26}-L_{103}) exodomain[126] was cleaved at the L_{44}-L_{45} and F_{87}-I_{88} bonds, which could result in receptor desensitization due to loss of part or all of the tethered ligand (**Figure 1.2**). As the L_{44}-L_{45} and F_{87}-I_{88} MMP1-cleaved receptors have not been validated physiologically, it is unclear whether MMP-1 cleavage sites within or distal to the canonical ligand are capable of productive signaling. However, it was recently shown that APC may also cleave PAR1 at R_{46}-N_{47},[127] as opposed to the canonical R_{41}-S_{42} cleavage site.[126] Although cleavage at the C-terminus of the tethered ligand might be expected to severely impact signaling, the APC R_{46}-N_{47} cleavage event is capable of producing cytoprotective effects through PAR1, representing a new example of biased agonism for PAR1 (**Figure 1.2**).[127] This raises the question of whether additional proteases that cleave at distal sites may be capable of producing new kinds of signaling outputs from PARs either as homomers or in partnership with other PARs in heteromeric complexes, such as PAR1-PAR2 heterodimers.[34, 128] It is also possible that conformational changes or steric steering, which might occur through dimerization, could promote one cleavage site over another. Once cleaved, the different-length tethered ligands may induce or stabilize different conformational states in the transmembrane domains and intracellular loops of PAR1 to facilitate preferential or biased association with one class of G proteins over another.[129, 130] Moreover, enzyme co-receptor proteins such as integrins or local micro-environments and lipid rafts[131] could favor biased cleavage and subsequent activation of pre-coupled[130] sub-sets of receptors.

Most recently, MMP-13 was identified as having PAR1 agonist activity.[103] Using cleavage experiments similar to those performed with MMP-1, the TR26 PAR1 peptide was found to be cleaved by MMP-13 at a slightly different site – S_{42}-F_{43} – one residue

toward the C-terminal side of the thrombin cleavage site. This cleavage site was functionally validated through mutation of amino acid F_{43}, which rendered the receptor insensitive to MMP-13 cleavage.[103] Considering the MMP family contains a conserved active site,[97] it is possible that other MMPs are also capable of cleaving PAR1. Several other MMPs tested for PAR1 cleavage and/or signaling, including MMP-2, -3, -7, and -9, appeared to be unable to activate PAR1,[48, 100] though many other MMPs have yet to be tested for agonist activity against PAR1 or the other PARs.

I.3.3 MMP-PAR Signaling in vascular disease

Atherothrombotic disease remains the leading cause of death in the United States, Europe, and Western nations.[132, 133] Despite successful percutaneous coronary interventions (PCIs), 20% of patients still experience a recurrent major adverse cardiac event within three years of treatment.[134] Furthermore, more than 60% of adverse events and nearly half of all deaths are a consequence of the initial culprit lesion, suggesting that destructive vascular remodeling continues even in the face of lesion ablation and widespread use of drug-eluting stents (DESs).[134]

I.3.3.1 MMP-PAR1 signaling in platelet thrombosis and atherosclerosis

Platelets express several metalloproteases including MMP-1, MMP-2, MMP-3, and MMP-14 on their surfaces.[106, 135, 136] Pioneering studies conducted almost 40 years ago showed that human platelets harbored enzymatic activity capable of degrading fibrillar collagen.[137] The platelet-derived collagenase activity was later identified as MMP-1, which was released upon exposure of platelets to thrombin.[106] More recently, it was discovered that collagen-stimulated platelet activation also results in the conversion of proMMP-1 to active MMP-1, which is capable of directly cleaving PAR1 on the platelet

surface.[48] MMP1-PAR1 signaling in platelets leads to activation of $G_{12/13}$-Rho, p38 MAPK pathways, and platelet shape change. Furthermore, the collagen-MMP1-PAR1 pathway mediates platelet aggregation and clot retraction, which is inhibited by PAR1 antagonists, but not thrombin inhibitors.[48] These results suggest that the collagen-MMP1-PAR1 signaling axis is an activator of both early and late platelet signaling events independent of thrombin.

In addition to the role of MMP-1 in PAR1-dependent platelet activation, the matrix-degrading functions of MMP-1 are also critical contributors to normal and patho-physiology.[110] Specifically, there is increasing interest in the diagnostic value of plasma MMP-1 in patients with acute coronary syndrome and its surge after PCI and stenting.[138] Plasma MMP-1 is also significantly increased in diabetic patients and those with high intimal/medial ratios in their carotid artery plaques.[139] Although patho-anatomic studies of human atherosclerotic lesions suggest that large plaques cause ischemic symptoms, the key contributing factor to the morbidity and mortality associated with atherosclerosis is excessive platelet thrombus formation on exposed collagen surfaces following acute plaque rupture.[46] The contribution of MMP-1 during atherogenesis can thus be considered two-fold: destabilization of the collagenous structure of plaques, and a pro-coagulant function caused by its effect on platelets.

Not surprisingly, MMP-1 expression is increased in atherosclerotic plaques.[104, 110, 140] Furthermore, MMP-1 has been shown to be to be expressed by macrophages, SMCs, and endothelial cells surrounding the fibrous cap, especially in the vulnerable shoulder region of the plaque.[140, 141] Also of interest is the presence of a promoter polymorphism in MMP-1 that results in increased expression that has strong associations with arterial plaque burden[142] and myocardial infarction risk.[143]

Similarly, PAR1 expression is also increased in the plaque body,[56] suggesting that the activating enzyme (MMP-1) and receptor (PAR1) are in close proximity during

plaque remodeling; however, the direct relationship between MMP-1 and PAR1 in the atherosclerotic plaque has yet to be shown.

I.3.3.2 MMP-PAR1 signaling in endothelial dysfunction

Sepsis and septic shock represent a cohort of disease states in which dysregulation of the vasculature is a key pathologic feature. The coincident activation of pro-inflammatory mediators contributes to endothelial barrier disruption and subsequent hypotension, hypovolemia, and disseminated intravascular coagulation.[144, 145] Endothelial PAR1 may also be a major mediator of acute inflammatory-coagulation responses and is a potential target in disease states characterized by endothelial dysfunction including abnormal hypercoagulability and sepsis/systemic inflammatory response syndrome.[34, 146, 147] Thrombin activation of PAR1 causes Rho-dependent cytoskeletal rearrangements in endothelial cells and induces cell contraction and rounding.[148, 149] Endothelial cell contraction destabilizes cell-cell contacts, causing an increase in vascular permeability. This facilitates the passage of molecules and leukocytes from the blood into the sub-endothelial compartment and exposure of tissue factor and collagen, which can trigger disseminated intravascular coagulation (DIC). Despite the ability of thrombin to trigger PAR1-dependent activation of endothelial cell contraction, PAR1 signaling confers both beneficial and deleterious effects on sepsis progression and outcomes depending on the timing and the severity of the disease state.[34, 150]

It has recently been shown that MMP1-PAR1 signaling also plays an important role in endothelial barrier function and sepsis outcomes.[101] Sepsis patients had a significant 18-fold increase in mean plasma proMMP-1 levels at time of enrollment relative to healthy controls. For septic patients, elevated proMMP-1 levels significantly correlated with worsening survival outcomes at days 7 and 28 (p=0.006).[101] In mouse

models of sepsis, mouse Mmp-1a was released from the endothelium into the circulation. Both Mmp-1a and MMP-1 triggered PAR1-dependent disruption of barrier function via Rho pathways. Inhibition of MMP-1 in the early stages of sepsis significantly improved the survival of WT and *Par2*$^{-/-}$ mice but had no effect in *Par1*$^{-/-}$ mice.[101] Similar results have been observed with thrombin inhibition in endotoxemia models utilizing WT and *Par2*$^{-/-}$ mice.[150] Administration of exogenous human MMP-1 caused endothelial barrier dysfunction and increased lung vascular permeability in WT but not *Par1*$^{-/-}$ mice.[101] Conversely, sepsis- and LPS-induced vascular leakage could be attenuated by inhibition of MMP-1 activity. Inhibition of MMP-1 also reduced DIC and markedly suppressed the cytokine storm, which was lost in *Par1*$^{-/-}$ mice. The timing of the effects of inhibition of MMP-1 activity on lung vascular permeability, systemic cytokines, and DIC correlated well with survival outcomes in mice.[101] These findings suggest that endothelial MMP1-PAR1 plays an unexpectedly important role in the lethal sequelae of sepsis, and that MMP-1 could be a useful predictive biomarker for outcomes in patients newly diagnosed with sepsis.

I.3.3.3 MMP-PAR1 inhibition in the vasculature

Activation of platelet thrombosis in patients with acute coronary syndromes often occurs under high shear-stress conditions on subendothelial surfaces enriched with collagen fibrils.[46] As previously discussed, spiking human whole blood with PAR1 inhibitors did not affect primary adhesion of platelets to immobilized collagen fibrils under arterial shear.[48] The subsequent growth rate of platelet aggregate "strings," however, was significantly attenuated by an MMP-1 inhibitor, FN-439, or PAR1 inhibitors. Blockade of the MMP1-PAR1 pathway with the MMP-1 inhibitor FN-439 also greatly curtailed arterial thrombosis in a guinea pig model of ferric chloride injury, which caused denudation of

the artery and exposure of type I collagen and other subendothelial matrix proteins.[48] These *in vitro* and *in vivo* data suggest that the collagen-MMP1-PAR1 pathway may be a point of early intervention in preventing arterial thrombosis.

Considering the complex role of MMPs in vascular remodeling, especially in intimal thickening following balloon angioplasty and stenting,[151, 152] the first MMP inhibitor (MMPi) clinical trials in the cardiovascular field were designed to prevent restenosis. Additional evidence from animal models suggested that genetic deletion of MMPs reduced neointimal formation, further supporting the rationale for using MMPis in restenosis prevention.[153, 154] Although MMP inhibition was shown to be successful at inhibiting smooth muscle cell migration,[155] *in vivo* studies have produced mixed results in restenosis models.[156-158] The BRILLIANT-EU studies examined whether DESs coated with batimastat, a broad-spectrum MMPi, would inhibit in-stent restenosis in patients without effects on re-endothelialization.[159, 160] The study concluded that batimastat-coated stents proved safe in larger populations (n=550), but there was no net benefit at primary (major adverse cardiac events) or secondary (binary restenosis, sub-acute thrombosis, angiography) endpoints.[158] Aside from their antibiotic effects, doxycycline and its derivatives have been shown to have broad spectrum MMPi activity.[158, 161-163] A prospective study in 2004[164] (MIDAS) examined the effect of sub-antimicrobial doses of doxycycline in reducing the incidence of plaque rupture in acute coronary syndrome. Doxycycline treated groups showed a 46% reduction in C-reactive protein levels and a 50% reduction in MMP-9 activity; however, there was no difference between treatment and placebo groups for the major cardiovascular endpoints such as MI and death.[164] These *in vivo* studies suggest that inhibiting various MMPs may have beneficial effects; however, further development of MMPis with high specificity for the intended MMP target may improve clinical outcomes.

I.4 Smooth muscle cells in cardiovascular disease and arterial stenosis

SMCs are the major contributing cell type to neointima formation in in-stent restenosis, but also contribute to atherosclerotic lesion development and destructive architectural remodeling in hypertension. Overall restenosis rates following bare-metal stenting range from 10 to 30%, with DESs reducing the incidence to below 10%.[165] In-stent restenosis occurs as a result of vascular SMC de-differentiation and subsequent migration from the medial layer through the damaged endothelium, where they deposit and proliferate to form a neointima. Therefore, understanding the mechanisms driving SMC phenotypic switching remains an important area of research.

I.4.1 Phenotypic switching

Vascular smooth muscle cells line the endothelial layer and contribute to the architecture and function of intact blood vessels. The major function of SMCs in the vessel wall is vascular contraction, which controls vessel tone and luminal diameter, thus regulating blood flow and pressure.[166] Unlike most adult tissues and cells, SMCs exhibit remarkable plasticity in the developed adult.[167] Following exposure to environmental cues after vascular injury, resident SMCs are able to undergo transient and reversible phenotypic modulation in which they change from a differentiated *contractile* cell to a de-differentiated *synthetic* one (**Figure 1.5**). Phenotypic changes occur in a variety of pathological states including atherosclerosis, in-stent restenosis, hypertension, asthma, and cancer.[167] Here we focus mainly on vascular restenosis models, which highlight SMC migration to, and proliferation in, the neointima.

The core changes that must occur in order for a change in phenotype are both molecular and behavioral, and include increased migration, proliferation, and matrix production, in coordination with down-regulation of contractile proteins.[167] Geary and

colleagues[168] conducted a study comparing gene expression profiles in the neointimal cells between primates receiving sham surgery or an aortic graft SMC. One hundred forty-seven genes were differentially expressed between the two cohorts, and most of the genes affected resulted in down-regulation compared to the normal aorta. Only 13 genes were increased over the normal tissue, and the vast majority were involved with ECM production.[168] These results highlight the importance of matrix and matrix-associated proteins in the process of phenotype determination.

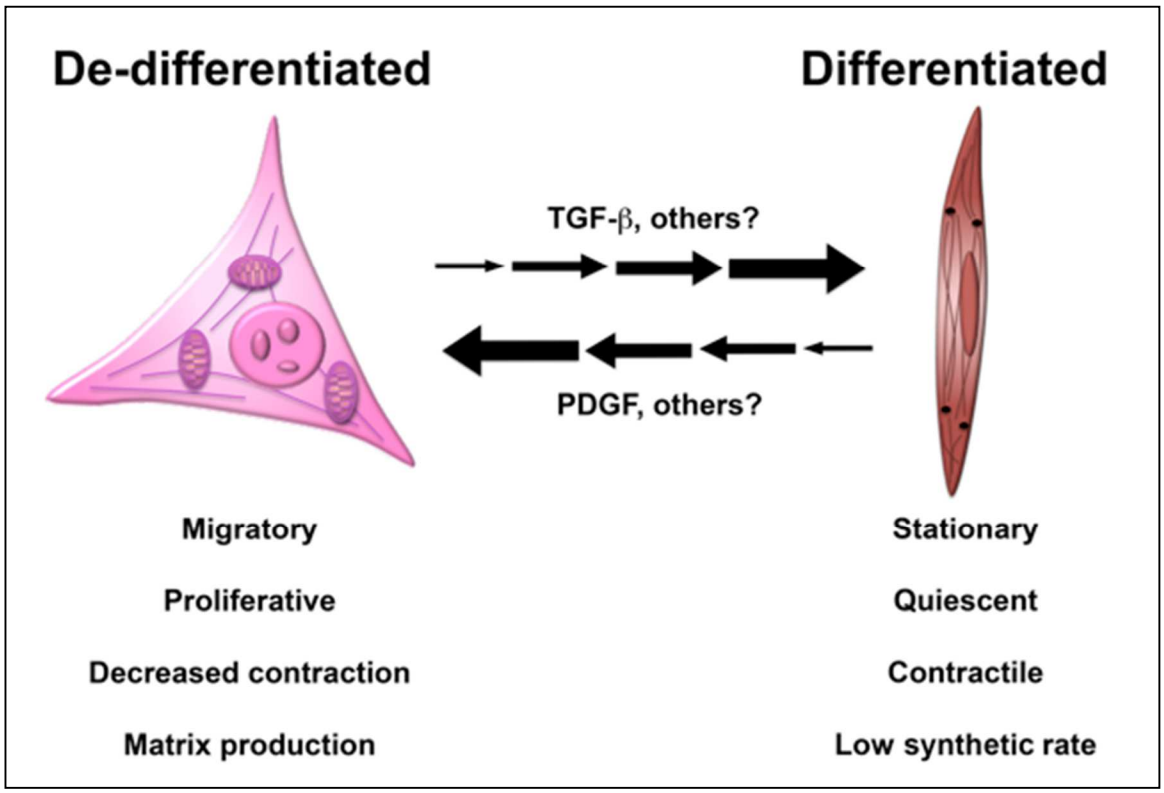

Figure 1.5. Illustration of SMC phenotypic switching. Schematic showing SMC phenotypic switching. The de-differentiated (or contractile) phenotype is shown on the left, and the differentiated (or synthetic) phenotype is shown on the right. The important defining features of each phenotype are discussed below.

The exact mechanisms through which SMCs modify their phenotypes is not fully understood, although several studies have shown that platelet-derived growth factor (PDGF) is a potent stimulator of the synthetic phenotype *in vitro*. SMCs treated with PDGF show increased proliferation and migration, and down-regulate expression of myocardin, the major transcriptional co-activator of SMC-specific genes (**Figure 1.5**).[169] Despite the numerous observations that PDGF is able to stimulate SMC phenotypic switching *in vitro*, no conclusive studies have been able to determine whether this signaling cascade is relevant in complex *in vivo* disease models. Pdgf and Pdgfr (PDGF receptor) knock-out mice die perinatally from severe hemorrhaging due to improperly formed blood vessels, suggesting that PDGF plays a critical role in SMC migration during development, but it's difficult to determine its role in fully mature, injured vessels.[170, 171]

In contrast to PDGF, transforming growth factor-β (TGF-β) has been implicated in the differentiation of SMCs (**Figure 1.5**). TGF-β, in concert with Smads, results in increased expression of myocardin-responsive genes. Additionally, TGF-β signaling has indirect effects through activation of p38 and RhoA, which suppress proliferation and activate contractile pathways.[169] Definitive *in vivo* studies have not confirmed whether the effects of PDGF or TGF-β represent the prominent signaling pathways that determine SMC phenotype.

I.4.2 Current therapeutics

There are currently two approved therapeutics to manage and prevent in-stent restenosis: rapamycin (and its derivatives), and paclitaxel. Both agents are used in DESs and have been clinically beneficial in reducing the rate of in-stent stenosis in

patients that have undergone PCI. Rapamycin (Sirolimus) is an inhibitor of the mammalian target of rapamycin (mTOR) pathway. mTOR exists as two distinct intracellular complexes, mTORC1 and mTORC2, each of which has unique cellular functions. mTORC1 phosphorylates p70 S6 kinase and 4E-binding protein-1 leading to increased translation of a number of mRNAs involved in cell-cycle regulation, such as MYC and cyclin D1.[172] mTORC2 works in complex to phosphorylate AKT at residue S473 to inhibit apoptosis and promote cell survival.[172] Rapamycin is a macrolide antibiotic that is often used for its potent immunosuppressant effects. After rapamycin complexes with an immunophilin, it specifically inhibits mTORC1 but also inhibits cell cycle progression by inducing expression of p27, a cyclin-dependent kinase inhibitor.[173] In vascular SMCs, rapamycin has been shown to activate TGF-β signaling, which is known to promote a contractile phenotype.[173] Furthermore, it increases SMC sensitivity to TNF-α driven apoptosis, thus inhibiting cellular growth and proliferation.[173] Newer derivatives of rapamycin, such as Everolimus, which have improved pharmacodynamic and kinetic properties, have been shown to be both efficacious and safe at doses lower than those used with rapamycin.[173]

Paclitaxel is a microtubule inhibitor that was first isolated from the Western yew tree in the early 1970s. Unlike the vinca alkaloids, paclitaxel (and other taxol-related agents) promotes hyperstability of microtubules, resulting in a dysfunctional tubulin assembly and disassembly equilibrium.[165] Furthermore, mitotic spindle formation is disrupted, resulting in M-phase arrest and eventual apoptosis. For this reason, paclitaxel has had wide application, not only in the cardiovascular field, but also as a chemotherapeutic. Specifically, paclitaxel has been shown to inhibit vascular SMC proliferation and migration both *in vitro* and *in vivo.*[165]

Randomized, prospective clinical trials were conducted to determine whether rapamycin or paclitaxel DESs were superior in reducing in-stent restenosis. Meta-analyses suggest that rapamycin-eluting stents show significant reductions in angiographic restenosis and loss of lumen diameter, as well as lower rates of target lesion revascularization. Interestingly, there was no difference in the rate of in-stent thrombosis, although the rapamycin groups trended towards fewer major adverse cardiac events.[174, 175]

I.5 Non-alcoholic Fatty Liver Disease (NAFLD) and Steatohepatitis (NASH)

I.5.1 Natural history and pathophysiology

Non-alcoholic fatty liver disease (NAFLD) is a frequent sequelae of obesity and insulin resistance. Approximately 20-30% of Western populations experience NAFLD, and up to 25% of these patients will progress to a more serious condition: non-alcoholic steatohepatitis (NASH).[176] NASH is characterized by the presence of steatosis, inflammation, and fibrosis in the liver parenchyma. Patients who have progressed to NASH are at higher risk of developing cirrhosis, hepatocellular carcinoma, and end-stage liver failure.[177] Metabolic Syndrome, which is a constellation of features including central obesity, hyperlipidemia, insulin resistance, and hypertension, is also heavily associated with NAFLD/NASH. Studies report between 43-71% of NASH patients also suffer from concurrent Metabolic Syndrome.[178]

Similar to carcinogenesis, a "two-hit" hypothesis has been proposed for the generation of NASH, in which certain patients are unable to cope with the influx of free fatty acids (FFAs) into the liver and consequently develop a more serious disease (**Figure 1.6**).[179] In both cases, insulin resistance is a precipitating event, which results in excessive lipolysis in peripheral fat stores. In fact, many consider NAFLD and NASH to be the hepatic manifestations of type 2 diabetes (**Figure 1.7**). The result is increased numbers of FFAs trafficked to the liver. Patients who do not properly incorporate the FFAs into triglycerides develop steatosis (NAFLD) as the "first hit." In essence, steatosis occurs when the rate of import or synthesis of FFAs by the hepatocytes exceeds the rate of export or catabolism. NASH develops as a consequence of direct liver toxicity and increased susceptibility to "second hits" such as reactive oxygen species (ROS), viral

infections, and increased inflammation (**Figure 1.6**). Cirrhosis develops as a response by the liver to repair the damaged tissue.[176, 179]

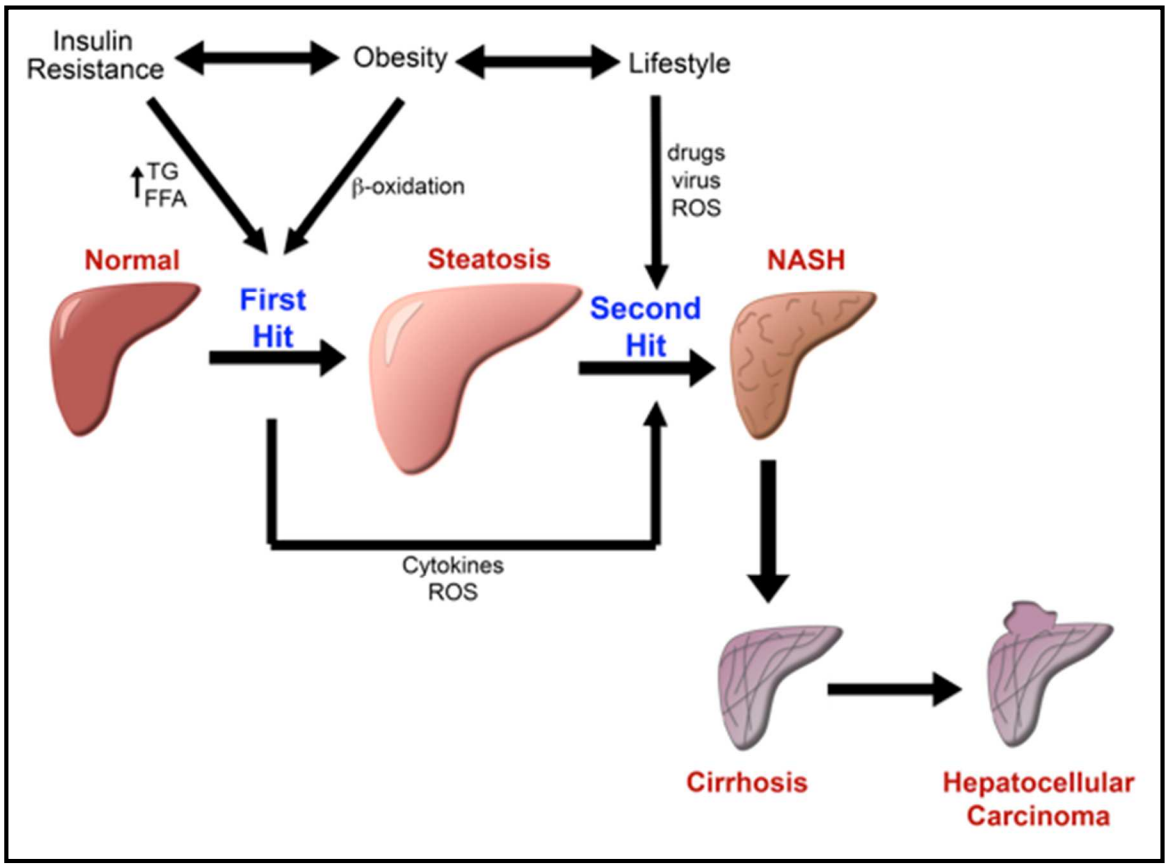

Figure 1.6. Two-hit model of NASH progression. NASH is thought to develop through a two-hit model similar to cancer progression. The initial hit occurs due to increased FFAs, triglycerides (TGs), and β-oxidation as a result of obesity and insulin resistance. The first hit results in simple steatosis of the liver. The second hit results from additional liver injury due to ROS, cytokines, drugs, viruses, *etc.* that can be a result of the inflammatory response to the steatosis or an exogenous insult. Once NASH has developed, fibrotic progression leads to cirrhosis, which can also result in formation of hepatocellular carcinoma.

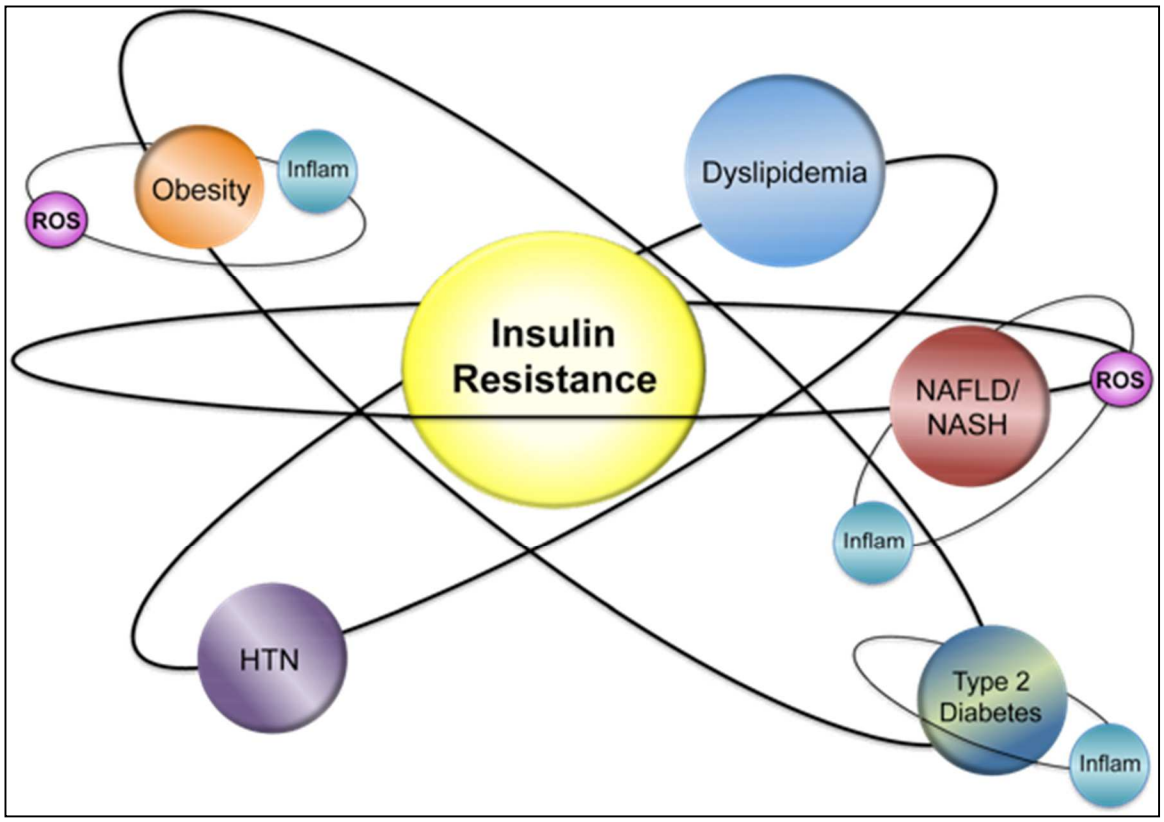

Figure 1.7. The importance of insulin resistance in NAFLD/NASH. Insulin resistance is thought to be a precipitating factor in the development of NAFLD/NASH. Other co-morbidities such as metabolic syndrome (obesity, hypertension (HTN), dys/hyperlipidemia, and type 2 diabetes) all contribute to the central feature of insulin resistance. Each co-morbidity represents a number of individual pathologic features, of which reactive oxygen species (ROS) and inflammation (cytokines, inflammatory cells: inflam) are shown. (Adapted from Marchesini *et al*., 2007) [178]

NAFLD/NASH is generally diagnosed as an abnormal elevation of liver enzymes on routine chemistry panel. The diagnosis is often confirmed with ultrasound imaging.[180] Livery biopsy is the only method for obtaining a precise diagnosis and for determining the severity of disease.[180] A histological scoring system, NASH activity score (NAS), has been developed to determine the stage of disease and takes into account the extent of steatosis, lobular inflammation, and hepatocyte injury.

I.5.2 Hepatic stellate cells

Hepatic stellate cells (HSCs) are specialized pericytes in the liver located in the space of Disse, between the hepatocytes and endothelium lining the sinusoids.[181] HSCs adopt a dendritic morphology and are the primary non-parenchymal cell in the liver. The developmental origin of HSCs remains controversial due to their expression of both mesenchymal and neuronal markers. Although HSCs were initially identified anatomically as fat-storing or sensing cells of the liver, their normal physiologic role is in fact the storage of vitamin A (retinol). HSCs store nearly 80% of the body's retinol, which serves as a useful marker experimentally.[181] Given the location of HSCs, it is not surprising that they also regulate sinusoidal blood flow through contraction and relaxation. In addition, HSCs maintain the proper ECM composition in the space of Disse by secreting the appropriate ECM proteins and MMPs.[181]

Following liver damage, HSCs exit their quiescent stage and undergo activation resulting in increased proliferation, matrix production, and contractility.[181] Morphologically, HSCs increase the size of their rough endoplasmic reticulum, down-regulate vitamin A storage, and express smooth muscle actin, which has become pathognomonic for HSC activation.[181] In addition to molecular and behavioral changes to the HSCs themselves, activation results in the production of a number of pro-

inflammatory cytokines such as IL-6, IL-8, and MCP-1 that exacerbate the fibrotic response.[181] Activated HSCs are the primary cells responsible for collagen deposition and fibrosis in the injured liver, which suggests their activation is causal and not in response to liver fibrosis.[69, 176, 181] In addition to direct ECM deposition, HSCs also up-regulate the production and release of tissue inhibitors of MMPs (TIMPs) which contribute to net liver fibrosis.

HSCs are activated as a consequence of an inflamed microenvironment in the liver due to excessive fat deposition and generation of ROS. Currently, the most potent inducers of HSC activation include TGF-β and PDGF, although a number of other factors have also been shown to stimulate HSC activation (leptin, TNF-α, adiponectin, IL-1 β, IL-6).[176, 181]

I.5.3 Current therapeutics

NAFLD is often a benign disease that does not require pharmacologic intervention, although more severe cases and those that have progressed to NASH are at risk for developing cirrhosis or hepatocellular carcinoma. A number of therapeutic inhibitors have been tested for efficacy in NAFLD/NASH. This section will summarize current clinical trials for agents used to treat NAFLD/NASH.

I.5.3.1 Thiazolidinediones

Insulin resistance has been universally accepted as the major instigator of the "first hit" in the development of NAFLD and NASH; therefore, insulin sensitizers have been proposed as potential treatments for this group of diseases. Thiazolidinediones (TZDs) are PPAR-γ agonists that promote glucose tolerance and insulin sensitivity. TZDs function though activation of PPAR-γ, which binds DNA along with the retinoid X receptor

and modifies gene transcription of a number of downstream targets. Pioglitazone is the most widely prescribed drug in this class, and clinical trials in patients without diabetes resulted in decreases in NAS scores, serum alanine aminotransferase (ALT) levels, hepatocyte injury, and fibrosis.[182, 183] Two meta-analyses have been performed to assess the efficacy of pioglitazone treatment on NAFLD/NASH outcomes; both suggest that TZDs improve liver histological assessment, although there was no significant decrease in fibrosis score.[180]

I.5.3.2 ***Metformin***

Metformin is first-line therapy for obese patients with a recent diagnosis of type 2 diabetes. Similar to the rationale behind the use of TZDs, it was proposed that management of insulin resistance could be a potential therapeutic avenue in NAFLD/NASH. The mechanism of action involves the activation of AMP-activated protein kinase (AMPK), which inhibits expression of genes involved in hepatic gluconeogenesis and increases translocation of the GLUT4 receptor to the membrane surface to increase glucose uptake in the periphery. Clinical trials utilizing metformin in diagnosed NAFLD patient populations have not resulted in definitive recommendations for its use. In most cases, patients using metformin had decreased aminotransferase levels but no histological benefit.[180] In studies controlled to a clinician-prescribed diet, metformin did not show any significant improvements over diet alone,[184] although combined diet and metformin treatment did result in some improvement in aminotransferase levels.[185] In summary, metformin administration does not offer substantial gains in treatment of the histological features of NAFLD, particularly in patients without pre-existing glucose intolerance.[180]

I.5.3.3 ***Statins***

As previously discussed, Metabolic Syndrome is a notorious risk factor for NAFLD and NASH. Hypercholesterolemia is a cardinal feature of Metabolic Syndrome; therefore, it was suggested that HMG co-reductase inhibitors (statins) would potentially benefit this subset of patients. Currently, only small pilot studies have been conducted regarding the effects of statins in patients with NAFLD and NASH, with mixed results. Some studies reported no statistical differences in statin-treated groups compared to placebo, whereas others showed decreases in aminotransferase levels following treatment.[180] Currently, the American Association for the Study of Liver Diseases does not recommend statins in the treatment of NASH.

I.5.3.4 ***Pentoxifylline***

Pentoxifylline is a non-specific phosphodiesterase inhibitor that reduces the synthesis of TNF-α. Elevated TNF-α in the liver parenchyma is thought to contribute to a pro-inflammatory phenotype followed by fibrosis and cirrhosis progression.[180] A meta-analysis of six pilot studies showed a significant decrease in aminotransferase levels,[186] although direct randomized, placebo-controlled clinical trials have not be initiated.

I.5.3.5 ***n-3 Polyunsaturated fatty acids***

N-3 polyunsaturated fatty acid (n-3 PUFA) deficiency has been associated with fatty liver and Metabolic Syndrome.[180] Normally, n-3 PUFA complexes with PPAR-α to regulate lipid metabolism in hepatocytes. Relative deficiencies in n-3 PUFA result in increased hepatic uptake of FFAs, decreased fatty acid oxidation in the liver, reduced production of fatty acid transport proteins, and increased expression of lipogenic genes.[187]

Clinical trials have shown improvements in serum ALT levels, ultrasonic reductions in fatty liver, and serum triglyceride levels.[180] Surprisingly, n-3 PUFA has resulted in the most consistent beneficial clinical trial data. Doses as low as 1g/day produced clinical improvements in patients, and suggest great potential as a widespread therapeutic.[180] At this time, additional large-scale clinical trials are necessary to determine the true efficacy of n-3 PUFA.

I.5.3.6 Orlistat

As weight loss remains the gold-standard for the treatment of NAFLD and NASH, there is renewed interest in adjunct therapies that help patients reduce total body weight. Orlistat, a lipstatin derivative, is used to block intestinal lipases, leading to decreased fat absorption by the gut. In conjunction with a reduced-calorie diet, patients taking orlistat showed increased weight loss over patients relying on reduced-calorie diet alone.[188] [180] A randomized, double-blind, placebo-controlled trial showed a reduction in serum ALT levels in patients given orlistat, although the diet-alone placebo group also saw reductions in ALT. There was, however, a significant decrease in liver steatosis (as measured by ultrasound) in the orlistat-treated group only.[189] Additional studies have shown decreased steatosis and serum aminotransferases, but stratification of the data shows that the observed decreases are always associated with a greater than 5% weight loss. Therefore, it is likely that orlistat's effect on NAFLD and NASH is a direct result of the concomitant weight loss, and not an independent effect.[180]

I.5.3.7 Antioxidants

Increased oxidative stress as a result of the generation of ROS has been shown play a critical role in the progression of NAFLD and NASH (**Figures 1.6 and 1.7**). It was

postulated that antioxidant therapy may benefit patients in the early stages of steatosis. Vitamin E, vitamin C, betaine, glutathione, and *N*-acetylcysteine have all been investigated as potential therapeutics for NASH.[180] Overall, studies using these agents were unimpressive and suffered from inconsistent experimental design. Of the agents used, vitamin E has shown the most promise by reducing serum ALT levels and histological features of NASH.[183] There is, however, concern regarding the safety of high-dose vitamin E use; a meta-analysis of doses larger than 400 IU/day showed an increase in all-cause mortality and prostate cancer rates.[180]

I.5.4 Methionine-choline deficient mouse models of NASH

The methionine/choline deficient (MCD) diet is a widely accepted method of recapitulating NASH-like symptoms in rodents. Studies by Kirsh et al[152] compared the effects of a MCD diet on both male and female rats and mice, and found that male C57BL/6 mice best approximated the histological features of human NASH syndrome.[190, 191]

The mechanism of steatosis in this model is a result of the need for methionine and choline in hepatic β-oxidation and the production of very low-density lipoproteins (VLDLs). Influx of FFAs into the liver stimulates their conversion into triglycerides in the ER lumen of the hepatocytes. There, the VLDL is assembled to include a core of lipid (mostly triglycerides) surrounded by phospholipids, cholesterol, cholesterol esters, and apolipoprotiens.[192] Since both methionine and choline are critical for nascent phospholipid synthesis, dietary restriction of the two results in triglyceride accumulation in the liver. Additionally, choline deficiency inhibits VLDL secretion by hepatocytes.[190] The consequence of aberrant VLDL synthesis and secretion is accumulation of fatty acids in the liver, resulting in the “first hit” of steatosis. Animals on the MCD diet show

increased oxidative stress and inflammatory cytokines, both of which can act as the "second hit" over time.[190]

Animals on the MCD diet mimic a number of the features of clinical features of NASH, including increased serum ALT, steatosis (by day 10), lobular inflammation and hepatocyte ballooning (by day 10), and fibrosis (8-10 weeks).[190] The major disadvantage of MCD diet in animal models is that mice on the diet lack a number of the metabolic changes seen in humans. Mice on MCD diet show significant weight loss, low fasting blood sugar, and low serum insulin and leptin levels, which is in stark contrast to the human disease.[190]

I.5.5 PAR2 in NASH

Mast cell infiltrates have been observed in the liver following injury in both humans and animal models.[193, 194] Levels in cirrhotic livers have been estimated to be roughly 9-fold higher than in normal liver.[171] Furthermore, activated HSCs produce and secrete stem cell factor (c-kit ligand) which has been shown to be a potent chemo-attractant for mast cells.[195] Following stimulation, mast cells release the contents of their granules into the extracellular space. The PAR2 protease agonist, tryptase, is a major component of mast cell granules, and therefore is a potential activator of PAR2 in the injured liver. Although many attribute activation of PAR2 in the injured liver to the availability of mast cell tryptase, definitive *in vivo* experiments have not determined the precise activating protease during liver injury.

Both PAR1 and PAR2 expression increases upon activation of rat HSCs. PAR2 activation on HSCs results in MAPK-dependent increases in proliferation and collagen production.[194] Recent studies utilizing *Par2* knockout mice showed decreased liver fibrosis, collagen gene expression, and hydroxyproline content in experimental models

of liver fibrosis.[70] Additionally, activation of PAR2 on human HSCs resulted in increased proliferation and collagen production, consistent with their role in hepatic fibrosis.[70] In a high-fat diet-induced model of liver steatosis, both *tissue-factor (TF)* and *Par2* knockout mice showed reduced fatty infiltrates in the liver, independent of hematopoietic/inflammatory cell signaling.[196] These data indicate that PAR2 activation in the liver, particularly on HSCs, contributes to the detrimental liver fibrosis.

Chapter 2. Non-canonical MMP1-PAR1 signaling triggers vascular smooth muscle cell de-differentiation and arterial stenosis

II. Chapter 2. Non-canonical MMP1-PAR1 signaling triggers vascular smooth muscle cell de-differentiation and arterial stenosis

II.1 Abstract

Vascular injury that results in proliferation and de-differentiation of vascular smooth muscle cells (SMCs) is an important contributor to restenosis following percutaneous coronary interventions (PCI). Protease-activated receptor-1 (PAR1) has been shown to play a role in vascular repair processes; however, little is known about its function or the relative roles of the upstream proteases thrombin and matrix metalloprotease-1 (MMP-1) in triggering PAR1-mediated arterial restenosis. The goal of this study was to determine whether non-canonical MMP-1 signaling through PAR1 would contribute to aberrant vascular repair processes in SMC de-differentiation and models of arterial restenosis. A mouse carotid arterial wire-injury model was used for studies of neointima hyperplasia and arterial stenosis. Mice were treated post-injury for 21 days with either a small molecule inhibitor of MMP-1 or a direct thrombin inhibitor, and compared to vehicle control. Intimal and medial hyperplasia was significantly inhibited by 2.8-fold after daily treatment with the small molecule MMP-1 inhibitor. Conversely, chronic inhibition of thrombin showed no benefit in suppressing the development of arterial stenosis. Thrombin-PAR1 signaling resulted in a super-contractile, differentiated phenotype in SMCs. Non-canonical MMP1-PAR1 signaling resulted in the opposite effect, and led to a de-differentiated phenotype via a different G protein pathway. MMP1-PAR1 signaling significantly stimulated hyperplasia and migration of SMCs, and resulted in down-regulation of SMC contractile genes. These studies elucidate a previously un-described mechanism for the formation of vascular intimal hyperplasia, and suggest a novel

therapeutic strategy to suppress restenosis by targeting non-canonical MMP1-PAR1 signaling in vascular SMCs.

II.2 Introduction

Cardiovascular disease is the leading cause of mortality in the United States, accounting for more than a quarter of all deaths.[133] Following vessel injury in the context of atherosclerotic plaque rupture or iatrogenic intervention, an important component of the repair process is smooth muscle cell (SMC) activation.[167, 197] SMC proliferation, migration, and reversion from a differentiated *contractile* phenotype to a de-differentiated *synthetic* phenotype are crucial contributors to the pathology associated with maladaptive remodeling.[167, 197] SMC de-differentiation results in overall changes to vascular structure, which are initially adaptive but later become injurious. Despite our understanding of the plasticity and differentiation capacity of SMCs, the signaling cascades triggering phenotypic modulation remain poorly understood.

Any enduring change in vessel architecture requires matrix remodeling, the majority of which is accomplished by matrix metalloproteases (MMPs). MMPs are a family of zinc-dependent endopeptidases whose canonical function is the breakdown of extracellular matrix. Recently, MMPs have proven to be critical contributors to basic cell physiology through cleavage of soluble, matrix-, and membrane-bound ligands.[113-115] The role of MMPs in cardiovascular disease is highlighted by the fact that SMCs constitutively express certain MMPs and TIMPS (tissue inhibitors of MMPs), and focal increases in MMPs have been well described in diseased arteries.[96, 104, 140, 198] Furthermore, clinical studies have shown increased MMP plasma levels in patients following vascular injury and atherosclerotic plaque rupture.[199, 200]

Specifically, MMP-1 has emerged as an important player in cardiovascular disease.[96, 140, 141, 199] MMP-1 is the primary collagenase responsible for the breakdown of collagen types I, II, and III.[92, 96] Furthermore, MMP-1 has been shown to cleave and activate PAR1.[48, 100] PAR1 is a G protein-coupled receptor that is activated through proteolytic cleavage by circulating and interstitial proteases, including thrombin,

activated protein C, and now MMP-1.[7, 100, 201, 202] MMP-1 cleaves PAR1 at a distinct site from the classical agonist, thrombin, prompting the theory that the two differentially signal through PAR1.[48] Despite ample evidence that MMP-1 plays a role in atherosclerotic lesion development and post-angioplasty restenosis,[96, 140, 198] the unique roles of MMP-1- versus thrombin-triggered PAR1 activation in SMC physiology have yet to be explored.

Here we present evidence for PAR1-driven biased agonism between thrombin and MMP-1. We demonstrate that MMP1-cleaved PAR1 functions as a potent inducer of SMC proliferation and migration, but also leads to decreased expression of contractile genes; three cardinal features of SMC de-differentiation. Furthermore, we establish that thrombin-PAR1 signaling in SMCs is primarily coupled to G_i-dependent signaling pathways, unlike MMP1-PAR, which favors non-G_i coupled signaling cascades. Finally, we show that systemic inhibition of MMP-1 following vascular damage inhibits vessel restenosis in animal models of vascular injury, putting forth a new strategy for targeted PAR1 inhibition that does not rely on receptor antagonists.

II.3 Methods

Carotid artery wire-injury model

All animal procedures were approved by the Tufts Medical Center IACUC committee. Fourteen to sixteen week old male C57BL/6 mice were anesthetized with an isoflurane nebulizer and nose-cone. The neck region of the animal was shaved with electric clippers and the area was sterilized using 3 alternating passes of iodine and ethanol swabs. Using sterile instruments a 1.5 cm midline incision was made and the skin and subcutaneous tissue was gently pushed aside using blunt dissection. Retractors were placed inside the neck of the animal to expose the trachea and carotid bundles on each side. The left side was further dissected to isolate the left common, internal and external carotids. A 6-0 suture was used to tie off the external carotid, and vascular clips were placed on the internal and common carotids. A small puncture was made with ocular scissors in the external carotid, at which time a small flexible surgical wire was inserted caudally into the external carotid until it entered the common carotid. The wire was carefully inserted and removed 10 times the entire length of the exposed common carotid (up to the vascular clip). The wire was removed and the vessel incision was tied off with a 6-0 suture. The animal was then closed with 6-0 nylon sutures and given 0.05 mg/kg buprenorphine for post-operative pain control. If animals were in a treatment group, they were treated with the appropriate dose of drug or vehicle at this time. Animals were allowed to recover from anesthesia in individual cages placed on warmed heating pads. Once animals were recovered they were monitored every few hours for the first day, and daily from that point on. At the end of 21 days, animals were anesthetized using isoflurane and the chest was opened and retracted. The animal was perfused with 10% buffered formalin through insertion of a 25 gauge needle attached to a pressurized perfusion bag into the left ventricle of the heart. The animal was perfused

for approximately 1 minute at which point both the left and right common carotid arteries were removed and placed in 10% buffered formalin.

Morphometry

Images for H&E stained carotid arteries were captured using a Nikon Eclipse 80i microscope and a Spot 7.4 Slider camera (Diagnostic Instruments Inc) at both 16x and 40x magnifications. Four images from sequential sections were then analyzed for medial plus intimal thickness using ImageJ software by measuring um length, using a known scale bar, in 4 equally distributed quadrants. All 4 lengths were averaged per carotid artery. Contralateral un-injured carotid arteries were used as controls. A one-way ANOVA followed by Student-Newman-Keuls post-test was performed using Kaleidograph software on natural log transformed medial plus intimal lengths. * $p< 0.05$; ** $p< 0.01$.

DQ-Collagen and S-2238 cleavage assays.

Collagenase activity was measured using DQ-collagen (Molecular Probes) as previously described.[100] Briefly, 5 nM activated MMP-1, MMP-8, and MMP-13 were dilution in 1X reaction buffer (50 mM Tris-HCl, 150 mM NaCl, 5 mM $CaCl_2$, 0.2 mM sodium azide, pH 7.6) and used to cleave 20 μg of DQ collagen for 30 min at room temperature in triplicate in a 96-well plate. FN-439 (5 μM) and 1,10 phenanthroline (100 μM) were diluted in 1x reaction buffer and directly added to the wells. Fluorescence was measured with at absorption of 495 nm and an emission at 515 nm on a Promega GloMax Multi Microplate Multimode reader. Thrombin protease activity was monitored by S-2238 cleavage (Chromogenix) as previously described.[203] Thrombin (0.01–10 nM) was diluted in Tris buffer (50 mM Tris-HCl, 175 mM NaCl, 0.5 mg/mL BSA, pH 7.9) with or without bivlairudin (0.5-50 μM) to a final volume of 180 μL. 20 μL of S-2238 (2 mM) was added

to each well and the reaction was allowed to proceed at room temperature for 30 min. The absorbance was measured at 405 nm on a SpectraMax 340 (Molecular Devices).

Cell Culture

Immortalized smooth muscle cell lines (AO391, CD314) were a generous gift from Wendy Bauer in the Molecular Cardiology Research Institute (MCRI) at Tufts Medical Center. AO391 cells were derived from a human aorta, whereas CD314 cells were harvested from human carotid arteries. Both cell lines were immortalized with retroviral transduction of E6 and E7 genes from human papilloma virus. Immortalized cells were maintained in DMEM supplemented with 10% FBS and 1% penicillin/streptomycin in 5% CO_2 at 37 °C. Primary HCA (human coronary artery) cells were purchased from Invitrogen and maintained in Medium 231 supplemented with smooth muscle growth supplement (SMGS; GIBCO) in 5% CO_2 at 37 °C. Primary cells were assayed only between passages 4-8.

Immunohistochemistry

Human atherosclerotic arteries were obtained with Tufts Medical Center IRB approval from archived blocks in the Tufts Medical Center Department of Pathology in collaboration with Dr. Golrokh Javid. Samples were sectioned and stained with antibodies (1:200) directed at smooth muscle actin (SMA), MMP-1, or PAR1. Slides were initially de-paraffinized and rehydrated by the following procedure: 100% xylene (10 min x 2), 100% ethanol (3 min), 95% ethanol (3 min), 75% ethanol (3 min), 50% ethanol (3 min), rinse with PBS. Antigen retrieval was performed in 10 mM sodium citrate (pH 6) by microwaving on low for 5 minutes; repeat 3 times. Slides were subsequently blocked in 0.3% hydrogen peroxide in PBS for 15 min at room temperature, followed by incubation for 1 hour at room temperature with 2% bovine

serum albumin (BSA)/0.5% Triton X-100 in PBS. Slides were washed with 2% BSA/PBS and incubated overnight at 4° C with primary antibody (1:200). Slides were washed 3 times with Tris buffered saline with 1% Tween (TBST) x 5 min. Slides were then incubated with a biotinylated secondary antibody (1:400) for 1 h at room temperature, followed by washing with TBST. Samples were then incubated for 30 min at room temperature with HRP-conjugated streptavidin, followed by washing with TBST. Slides were developed with DBA reagent for approximately 30 s to 1 min, followed by counterstaining with Mayer's hematoxylin.

Flow Cytometry

Immortalized and primary SMCs were harvested by lifting with 5 mM EDTA/PBS and placed in PBS/1% FBS. Cells were then labeled for 1 h at 4° C with a PAR1 rabbit polyclonal antibody (1:200) targeted against the epitope: SFLLRNPNDKYEPFC. Cells were then incubated with FITC-conjugated secondary antibody (1:1000) for 1 h at 4° C (in dark). Cells were fixed by adding 1% formaldehyde, and PAR1 expression was assayed relative to a FITC conjugated isotype control on a BD FACS Canto II cytometer. Results were analyzed using FlowJo Software (Tree Star).

PAR1 cleavage assay

CD314 cells were lifted with 5 nM EDTA/PBS and resuspended in PBS/1% FBS. Cells were then treated with vehicle, 5 nM MMP-1, or 5 nM MMP-1 + 5 μM FN-439 for 30 min at 37° C. Cells were immediately fixed with 1% formaldehyde/PBS/1% FBS, followed by staining for 1 h at 4° C (in dark) with a FITC-conjugated Span12 antibody (1:400), whose epitope spans both the MMP-1 and thrombin cleavage sites in PAR1. Mean fluorescence was measured on a BD FACS Canto II cytometer, and results were analyzed using FlowJo Software.

Intracellular Calcium Flux

Cells were lifted with 5 mM EDTA/PBS and labeled with Fura-2AM (1:4000) in PIPES or Hank's Buffered Saline Solution (HBSS). Cells were incubated at 37° C on a horizontal rocker for 30 min. Samples were then washed with PIPES or HBSS and re-suspended in 4-5 mL of the respective buffer (PIPES or HBSS). Calcium flux was then measured following the addition of agonists (thrombin, MMP-1, TFLLRN, SFLLRN, etc.) by the ratio of excitation intensity at 340/380 nm on a LS 50B Luminescence Spectrometer. The antagonist RWJ-56110 (5 μM) was added 3 min prior to the addition of agonist. Pertussis toxin (200 ng/mL) was added to cells 16 h prior to lifting.

Trans-well migration assays

Fifteen thousand cells were plated in the top well of 8 μm pore trans-well plates (Corning) in full 10% FBS/DMEM media. Cells were allow to adhere to the membrane for 4-6 hours before media was changed to 0.1% FBS/DMEM in the top well. Lower chambers were filled with 0.1% FBS/DMEM with and without chemo-attractants or full 10% FBS/DMEM as a positive control. Cells were allowed to migrate at 37 °C for 16 h. Membranes were washed 3X with PBS and non-migrated cells were removed from the top side of the membrane with a cotton swab. Membranes were subsequently stained with the Hema 3 stain set (Protocol) and allowed to dry completely at room temperature. Membranes were mounted using Resolve high viscosity mounting medium (Richard-Allan Scientific), and nine fields (16X) were counted to extrapolate the number of migrated cells.

Scratch Assay

For wound healing (scratch) assays, CD314 cells were grown to confluency in 6-well plates and then scratched in a cross-wise pattern 4 times/well with a P1000 pipet tip. Photos were taken at time 0, at which point treatment was added to each well (5 nM thrombin or MMP-1 +/- 5 μM RWJ-56110). Cells were allowed to reconstitute the scratched region for 16 h, at which point additional photographs were taken. The mean number of cells migrated was quantified (n=4 fields at 4x) and expressed as mean ± SEM.

PAR1 endocytosis

SMCs were treated with thrombin (5 nM) or MMP-1 (5 nM) at 37 ºC or 4 ºC and cells fixed at various time points with 1% formaldehyde and stained for PAR1 (SFLLRN-Ab). FITC-conjugated secondary antibody was then added and PAR1-surface expression analyzed with a FACS Canto II (Becton-Dickinson). Mean fluorescence intensities were measured using FlowJo software and normalized to untreated samples to obtain percent PAR1 surface expression.

Crystal violet proliferation assay

Ten thousand cells were plated in six-plicate in 96 well plates in 0.1% FBS/DMEM. Cells were then treated with agonists (5 nM thrombin, 5 nM MMP-1) with and without 5 μM RWJ-56110 for 3 days. For assays utilizing peptide agonists, 30 or 300 μM were used as indicated. After 3 days cells were washed twice with PBS and fixed and stained for 5 minutes at room temperature with gently agitation in 0.5% crystal violet (w/v) in methanol. Plates were washed in doubly distilled water and allowed to dry at room temperature overnight. The following day, the crystal violet was resuspended in 100% methanol solution for 30 min at room temperature with gentle shaking. The absorbance

was then read at 595 nm in a SpectroMax 340 plate reader (Molecular Devices). Results were expressed as mean absorbance plus or minus the standard error.

Rho-GTP activation

For RhoA activation, confluent CD314 cells were treated with thrombin (5 nM) or MMP1 (5 nM) with or without RWJ-56110 (5 μM) for 15 min. The cells were lysed and Rho-GTP was precipitated from cell lysates with glutathione S-transferase (GST)-rhotekin-reduced glutathione-agarose beads as described.[101] Rho-GTP was then quantified by immunoblot analysis with monoclonal antibody to RhoA (1: 400; 26C4,Santa Cruz). A portion of the SMC lysates was reserved and analyzed by immunoblot for total Rho and rhotekin as loading controls.

Western blot

Cells were grown to confluency in 10 cm tissue culture plates in 10% FBS/DMEM supplemented with 1% penicillin/streptomycin. The plates were then serum starved in 0.1% FBS/DMEM for 60 hours, replacing media every 16 h. Antagonists (200 ng/mL pertussis toxin, 5 μM RWJ-56110, 5 μM BAPTA-AM, 5 μM U73122) were added to cells 30 min prior to agonist treatment. To stimulate ERK phosphorylation, cells were treated with 5 nM thrombin or MMP-1 for 15 minutes at room temperature. Cells were then lysed in 300 μL of T-PER lysis buffer using a rubber spatula at 4 °C. Lysates were spun at 14,000 rpm at 4 °C, and supernatant was removed. Lysates were quantified for total protein content using a Bradford assay or nanodrop. Thirty micrograms of total protein was run on 10% polyacrylamide SDS-gels, after which point protein was transferred to nitrocellulose membranes. Membranes were blocked for 1 h at room temperature in 5% non-fat dry milk in Tris-buffered saline/1% Tween (TBST) after which point they were probed for phospho-ERK1/2 (p42/44) at a dilution of 1:1000 in TBST for 1 h at room

temperature with gentle agitation. Membranes were washed 3x5 min in TBST and HRP-conjugated secondary antibody was used at a 1:5000 dilution for 1 h at room temperature. Membranes were was 3x5 min in TBST and developed using ECL reagent (Pierce). Membranes were then stripped with 62 mM Tris/2- β -mercaptoethanol (2-BME) for 1 hour at 56 °C. Membranes were then re-probed with total ERK antibody (1:1000) and β -tubulin (1:5000) at room temperature for 1 h.

Reverse transcriptase quantitative PCR (RT-qPCR)

Total RNA was extracted using the RNeasy mini kit (Qiagen) and 1-2 μg of RNA was reverse transcribed into cDNA using Moloney murine leukemia virus (MMLV) reverse transcriptase as described below. Random oligomers (10-15 bases) (Oligo dT; Invitrogen) were annealed at 72 °C for 10 min, followed by 40 cycles of: 25 °C for 15 min, 37 °C for 60 min, 95 °C for 5 min, 4 °C for 5 min. Quantitative PCR was conducted in 25 μL volumes with 12.5 μL SYBR Green master mix (Invitrogen) and 1.25 μL of both forward and reverse primers (5 μM). All reactions were performed in triplicate and run on a DNA Engine Opticon 2, Continuous Fluorescence Detector (MJ Research). qPCR program consisted for 40 cycles of the following: 95 °C for 15 s, 55 °C for 20 s, and 72 °C for 15 s. Primer sequences are listed in Table 2.1.

Table 2.1 RT-qPCR primers

Gene	Gene ID	Accession No.	Primer Pairs (5' ➔ 3')
Myocardin	MYOCD	NM_001146312.1	F- *TGCACAGAACTCAGGAGCACACG* R- *TGGGCTCCAGAGAAGGGCGG*
SM-22	TAGLN	NM_001001522.1	F- *CCAAGGAGCTTTCCCCAGACATGG* R- *TTGGACTGCACTTCGCGGCT*
Calponin	CNN1	NM_001299.4	F- *GGCCAGCATGGCGAAGACGAA* R- *CCCGGCTCGAATTTCCGCTCC*
Fibronectin	FN1	NM_212482.1	F- *TCATCCCAGAGGTGCCCCAACTC* R- *GTCCACCTCAGGCCGATGCTTG*

II.4 Results

II.4.1 MMP-1 inhibition reduces neointima formation in animal models of restenosis

Despite the well-documented contribution of PAR1 to platelet aggregation and acute arterial thrombosis, it is not clear whether PAR1 on other cell types in the blood vessel wall (*e.g.*, SMCs) promotes or mitigates the hyperplastic response to arterial injury in the chronic timeframe. Studies utilizing genetic deletion of PAR1 demonstrate no net positive benefit in preventing medial thickening,[62] and actually report increased intimal growth in mouse models of arterial injury;[128] however, pharmacologic inhibitors of PAR1[59, 204] or blocking antibodies[205] inhibited neointimal hyperplasia in rats. Given the observed paradoxical nature of PAR1 in response to vascular injury, we hypothesized that PAR1 may exhibit functional biased agonism with respect to the activating protease (see Section I.3.2). This hypothesis is supported by evidence showing that MMP-1 cleaves and activates PAR1 at a distinct site from thrombin, two residues towards the amino terminus (**Figure 1.2**).[48] This cleavage results in a tethered ligand two amino acids longer than the thrombin-generated ligand, which could potentially alter the ligand-receptor interactions and lead to distinct signaling outputs. Since both thrombin[206] and MMP-1[207] are increased in the injured vasculature, we chose to interrogate the distinct contributions of MMP1-PAR1 versus thrombin-PAR1 signaling following vessel injury.

Mouse carotid arteries were injured (n=14 per group) with a vascular wire[208] and animals were treated daily for 21 d with either FN-439, a small molecule inhibitor that is selective for MMP-1, or bivalirudin, a direct thrombin inhibitor indicated as an anticoagulant during PCI (**Figure 2.1**).[203] FN-439 inhibited >92% of MMP-1 collagenase activity, 6% of MMP-8 activity and 36% of MMP-13 activity, and had no inhibitory effects against thrombin (**Figure 2.2a-c**). Conversely, bivalirudin blocked thrombin-dependent cleavage at all concentrations tested (0.5-50 μM) and had no effect on MMP-1

collagenase activity (**Figure 2.2a-c**). Importantly, neither drug affected SMC viability (**Figure 2.2d**). At the 21 day endpoint, vehicle-treated animals had 4-fold increases in mean medial and intimal thickness and marked neointima formation following wire injury as compared to contra-lateral uninjured carotids (**Figure 2.1a-c**). Daily treatment with the MMP-1 inhibitor, FN-439, gave a significant 2.4-fold protective effect against neointimal hyperplasia, whereas treatment with the thrombin inhibitor, bivalirudin, had no discernable effect as compared to untreated animals (**Figure 2.2a-c**). These results indicate that unlike direct thrombin inhibition, blockade of MMP-1 activity significantly decreases arterial neointima formation and stenosis following wire injury in mice.

These data indicate that MMP-1 versus thrombin may play different roles in regulating vascular neointima formation. Given that SMCs are the primary cell type responsible for human in-stent restenosis,[173] we confirmed that our model recapitulates the human disease. Using immunofluorescence on vehicle treated animals we found that SMCs were the major constituent of the media and neointima in our model (**Figure 2.3a-c).** Furthermore, we also looked at the prevalence of smooth muscle actin (SMA) positive cells in human atherosclerotic plaques and found prominent staining in the proliferative fibrous cap, an area of known remodeling and MMP-1 expression (**Figure 2.3d-e**).[141] We then explored the possibility that MMP-1 and PAR1 are juxtaposed in the remodeling vessel, and that MMP1-PAR1 signaling could contribute to the observed detrimental vascular remodeling. Not surprisingly, both human and mouse MMP-1 and PAR1 are in close proximity in the injured blood vessel, and co-localize with SMA+ SMCs (**Figure 2.3**).

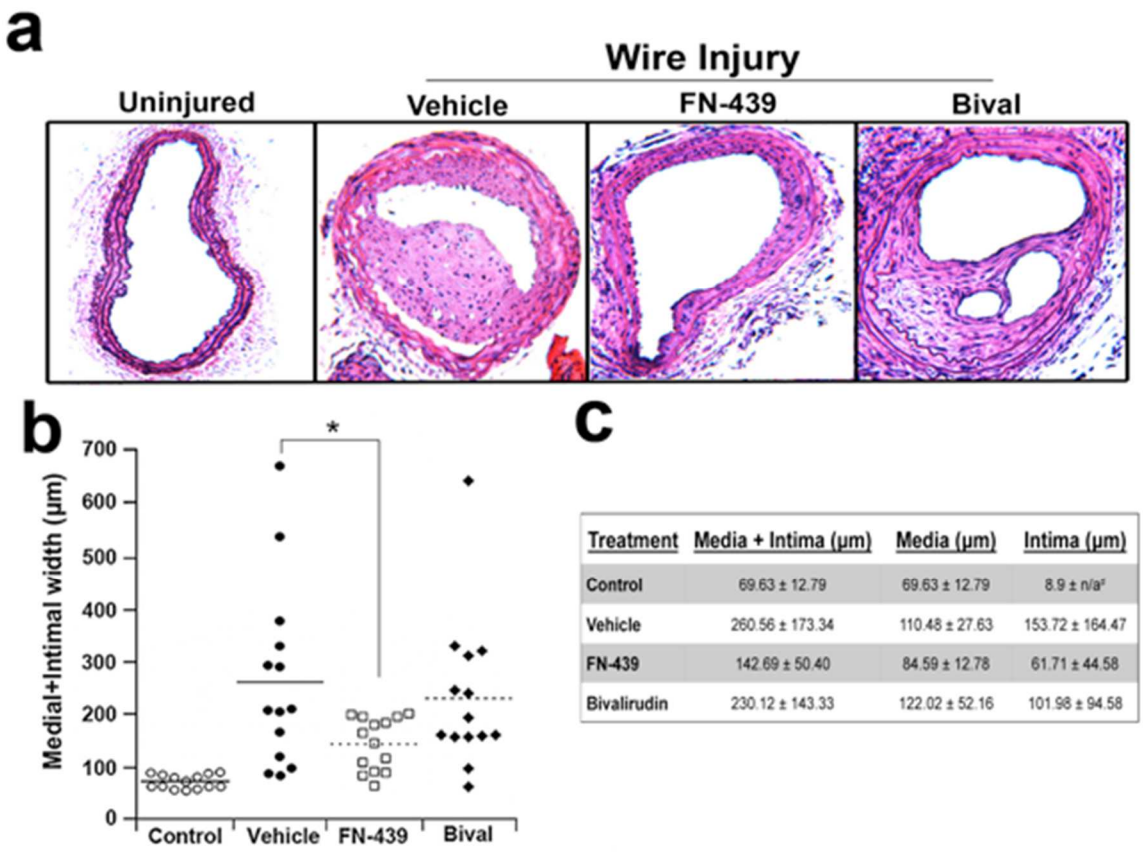

Treatment	Media + Intima (µm)	Media (µm)	Intima (µm)
Control	69.63 ± 12.79	69.63 ± 12.79	8.9 ± n/a[#]
Vehicle	260.56 ± 173.34	110.48 ± 27.63	153.72 ± 164.47
FN-439	142.69 ± 50.40	84.59 ± 12.78	61.71 ± 44.58
Bivalirudin	230.12 ± 143.33	122.02 ± 52.16	101.98 ± 94.58

Figure 2.1. **MMP-1 inhibition reduces medial and intimal lesion thickness following carotid artery wire-injury in mice. (a)** Representative photomicrographs (16x) of carotid arteries from the right uninjured contralateral artery or the left injured artery from male C57BL6 mice treated with daily subcutaneous injections of vehicle (20% DMSO), 5 mg/kg FN-439, or 10 mg/kg bivalirudin (Bival) for 21 days (n=14). **(b)** Medial plus intimal thickness based on a µm scale bar of injured carotid arteries harvested from mice in (A). Each data point represents four averaged (quadrants) measurements from each mouse artery. Horizontal lines indicate mean medial plus intimal thickness in microns. The mean medial thickness (horizontal lines) for each treatment cohort was calculated from cross sections of the arteries as described above in the methods section.**(c)** Individual medial and intimal thickness for control, vehicle, FN-439, and bivalirudin treated groups. #: 8.9 microns represents endothelial thickness, and thus the lowest limit of detection. *, $p < 0.05$ by ANOVA.

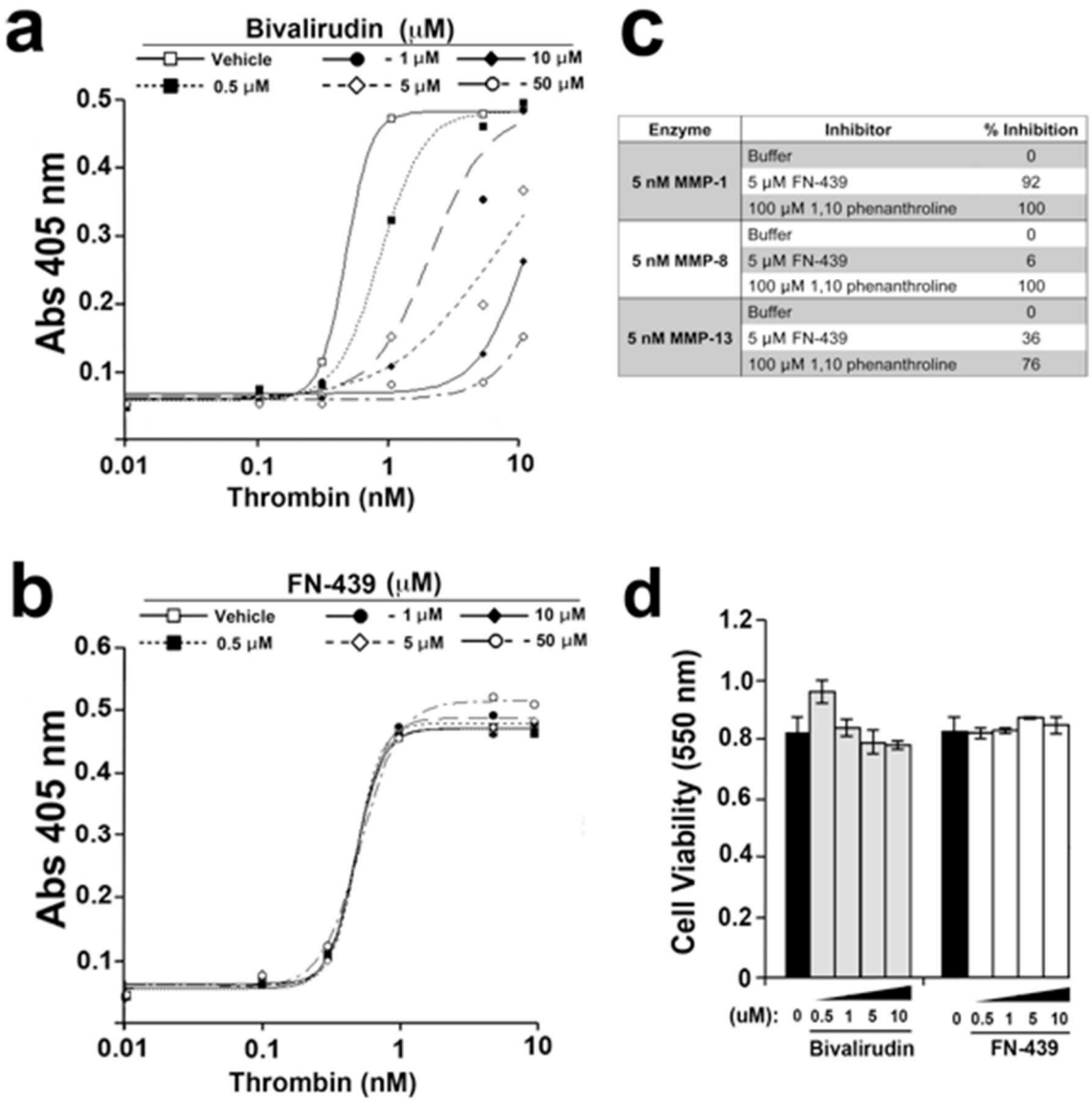

Enzyme	Inhibitor	% Inhibition
5 nM MMP-1	Buffer	0
	5 μM FN-439	92
	100 μM 1,10 phenanthroline	100
5 nM MMP-8	Buffer	0
	5 μM FN-439	6
	100 μM 1,10 phenanthroline	100
5 nM MMP-13	Buffer	0
	5 μM FN-439	36
	100 μM 1,10 phenanthroline	76

Figure 2.2 Bivalirudin and FN-439 selectivity. (a,b) Inhibition of thrombin enzymatic activity (hydrolysis of S2238 over 30 min, 25 °C)[203] by 0.5-50 μM FN-439. **(c),** Percent inhibition by 5 μM FN-439 on the collagenase activity (hydrolysis of FITC-DQ-collagen over 30 min, 25 °C)[100] of the 3 collagenases (5 nM MMP-1, MMP-8 and MMP-13) vs. 100 μM Zn-chelator, 1,10 phenanthroline. Percent inhibition of the enzymatic activity of 1 nM thrombin by 5 μM FN-439 or 5 μM bivalirudin as done in A. **(d)** MTT viability of SMCs treated with 0.5-10 μM bivalirudin and FN-439.

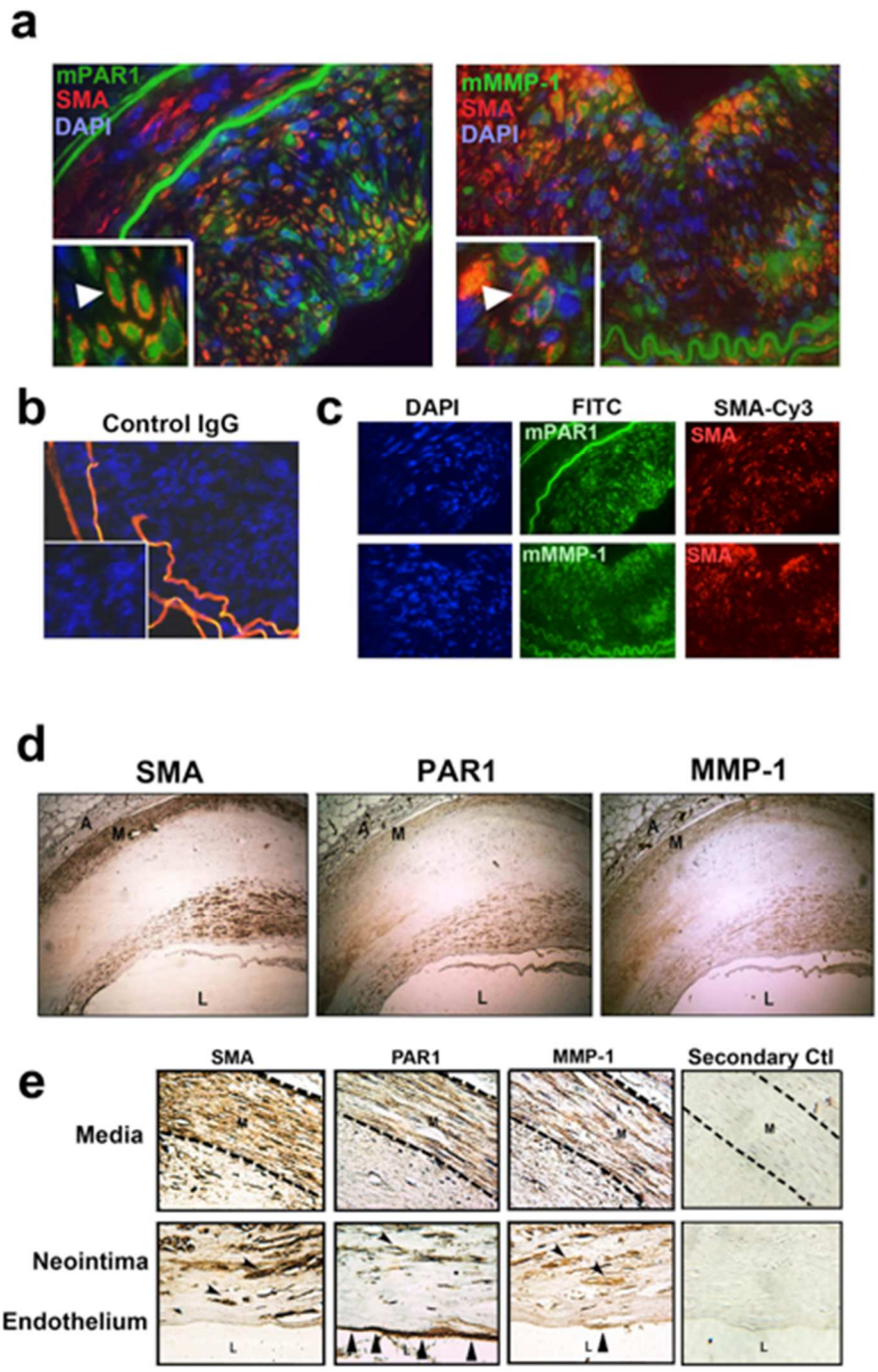

Figure 2.3 PAR1 and MMP-1 localize to SMCs in vascular lesions. (a), Merged immunofluorescence of representative sections from wire-injured carotid arteries of vehicle-treated mice from (A) stained for smooth muscle actin (SMA), mouse Par1 (FITC), and Mmp-1a (FITC). Cell nuclei were counterstained (blue) with DAPI. Inset boxes in lower left corner represent magnified regions prominent co-localization in the neointima (white triangles). Autofluorescence of the elastic lamina can be seen as distinct green bands. **(b-c)** Representative photomicrograph of wire-injured mouse carotid arteries (vehicle) showing background staining of combined FITC- and Cy3-conjugated IgG control antibodies and individual non-merged stains of DAPI, mPAR1, MMP-1a, and SMA expression. **(d),** Immunohistochemistry of sections from human atherosclerotic lesions showing co-localization of SMA with MMP-1 and PAR1. A: adventitia, M: media, L: lumen. **(e)** IHC of MMP-1, PAR1, and SMA depicting co-localization in the media, neointima, and endothelium of a human atherosclerotic plaque. Arrow-heads point to areas of localization in the neointima. Triangles show staining in the endothelium

Our data indicate that MMP-1 antagonism inhibits SMC-driven neointima formation in mice, the converse of thrombin antagonism. We hypothesized that PAR1 is differentially activated by MMP-1 and thrombin, and that MMP1-driven cleavage and activation promotes SMC de-differentiation and neointimal growth. In contrast, thrombin-PAR1 activation protects the vasculature by maintaining a contractile phenotype and promoting hemostasis. Our model was used to drive experimental design and define the contributions of MMP1-PAR1 versus thrombin-PAR1 signaling to SMC behavior and the key features used to define SMC de-differentiation: migration, contraction, and proliferation.

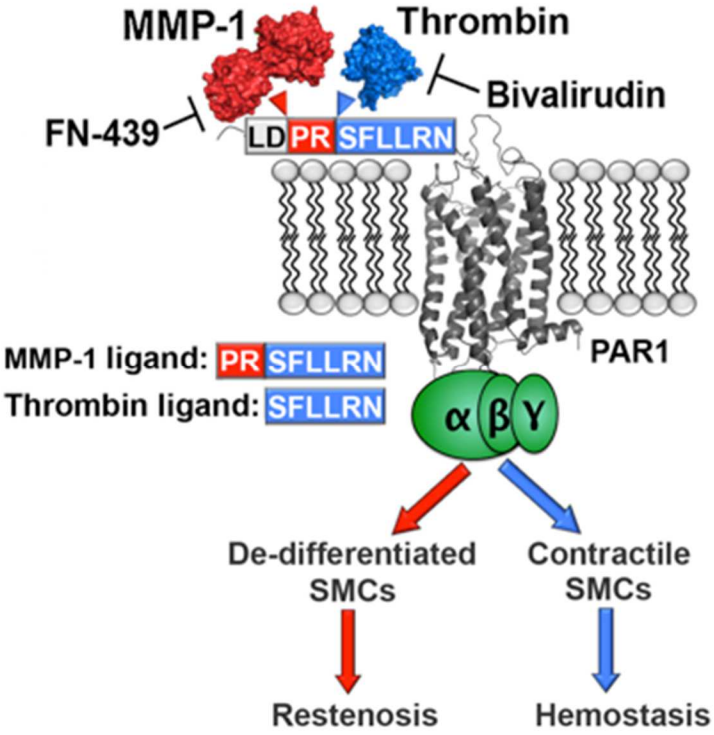

Figure 2.4. Model of PAR1 activation by MMP-1 and thrombin in SMCs. Proposed mechanism of divergent signaling and outcomes resulting from PAR1 activation by MMP-1 versus thrombin at two different cleavage sites in arterial injury and restenosis.

II.4.2 MMP-1 cleaves and activates PAR1 on SMCs

We predicted that PAR1 on SMCs exhibits biased agonism in response to MMP-1 and thrombin, which leads to either detrimental remodeling or preservation of hemostasis. Although thrombin-PAR1 signaling in SMCs has been well documented,[58, 60, 209] MMP-1 driven cleavage of PAR1 on smooth muscle had not been reported. To confirm that MMP-1 was capable of cleaving and activating PAR1 on SMCs, we assayed for PAR1 surface expression in both immortalized (AO391, CD314) and primary (1° HCA) human vascular smooth muscle cell lines by flow cytometry. All SMC lines showed robust PAR1 expression on their cell surface (**Figure 2.5a**). We then tested whether MMP-1 was capable of enzymatically cleaving PAR1 on the surface of SMCs as had been shown in breast cancer cells[100] and platelets[48]. Using an antibody that spans the MMP-1 cleavage site on PAR1 (**Figure 2.4**), and therefore only recognizes intact (uncleaved) receptor, we verified MMP1-mediated PAR1 cleavage on SMCs. CD314 cells incubated with 5 nM MMP-1 had decreased antibody binding, correlating to a loss of epitope and receptor cleavage (**Figure 2.5b**). This effect was blocked by 5 μM of the MMP-1 inhibitor, FN-439, confirming that MMP-1 is a functional agonist for PAR1 on SMCs.

Not all N-terminal cleavages of PAR1 activate receptor signaling (see Section I.2.3.2). To interrogate whether MMP1-driven cleavage triggers a functional signaling cascade in SMCs, we utilized intracellular calcium mobilization as a read-out for PAR1 activation. Equimolar amounts of thrombin and MMP-1 had similar magnitudes of calcium flux in both immortalized and primary SMC lines (**Figure 2.5c**). Additionally, both signals were inhibited by the PAR1-specific small molecule antagonist, RWJ-56110 (RWJ). Together, these results suggest that MMP-1 is capable of cleaving and activating PAR1 on vascular SMCs, which reinforces the hypothesis that MMP-1 is an important PAR1 agonist during vascular injury and repair.

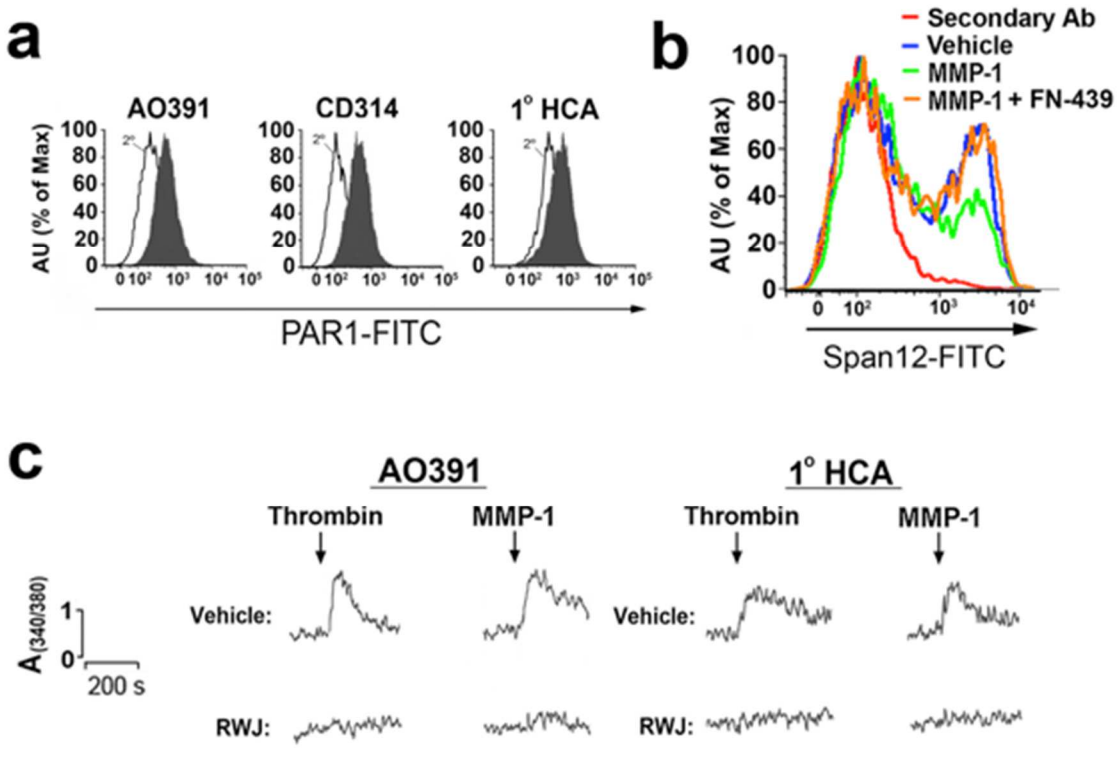

Figure 2.5. MMP-1 cleaves and activates PAR1 on SMCs. (a) PAR1 surface expression (black fill) of 3 SMC lines analyzed by FACS. 2° antibody control is shown as black line with white fill. **(b)** MMP-1 cleavage of PAR1 on CD314 SMCs after 30 min treatment with 5 nM MMP-1 +/- 5 μM FN-439. The Span12 antibody spanning the PAR1 cleavage site was used to recognize full-length receptor. Loss of antibody binding indicates receptor cleavage by MMP-1 (5 nM); 5 μM FN-439 MMP-1 inhibitor. **(c)** Calcium-flux measurements of SMCs following challenge with MMP1 or thrombin (5 nM thrombin or MMP-1). In bottom traces, cells were pre-treated for 3 min with the PAR1 inhibitor 5 μM RWJ-56110 (RWJ) prior to the addition of agonist.

II.4.3 MMP1-PAR1 signaling is a potent chemo-attractant for SMC migration

Acquisition of cell migration and invasion are important and defining features of SMC phenotypic de-differentiation (see Section I.4.1). Synthetic SMCs migrate into the luminal space where they proliferate to create a pathologic neointima.[167] To interrogate the contribution of thrombin-PAR1 versus MMP1-PAR1 signaling to SMC migration, we performed overnight trans-well migration assays with immortalized and primary human SMC lines using either 5 nM thrombin or MMP-1 as a chemo-attractant. Thrombin stimulated modest SMC migration, increasing by approximately 1.25 fold over background (**Figure 2.6a,b**). Surprisingly, MMP-1 functioned as a potent chemo-attractant with statistically significant increases in migration ranging from 2-2.5 fold over vehicle at equimolar concentrations compared to thrombin (**Figure 2.6a,b**). These effects were equivalent to the use of 10% FBS as a chemo-attractant. Blockade of PAR1 with RWJ-56110 completely abolished MMP-1's pro-migratory effects. In alternate assays of cell migration, such as wound-healing scratch assays, we found that MMP-1 stimulated improved closure of the wound-space compared to thrombin, which was blocked by RWJ-56110. (**Figure 2.7**)

Protease-activated receptors offer the unique ability to create synthetic activating peptides that mimic the tethered ligand produced by proteolytic cleavage. [48, 210] Similar to the results observed with thrombin, both thrombin-generated peptides (SFLLRN and TFLLRN) had modest effects on 16 h migration at lower concentrations, and had no effect at higher concentrations (**Figure 2.8a-c**). Conversely, the MMP-1 generated peptide (PR-SFLLRN), showed a comparable increases in migration at lower concentrations but had markedly increased migration at higher concentrations in all cell lines tested (**Figure 2.8a-c**). Furthermore, we designed a negative control peptide, RP-SFLLRN, in which the first two residues are reversed, resulting in an inactive peptide.[211]

This control peptide had no effect on migration (**Figure 2.8a-c**), suggesting that proper MMP1-induced cleavage is essential for PAR1 signaling.

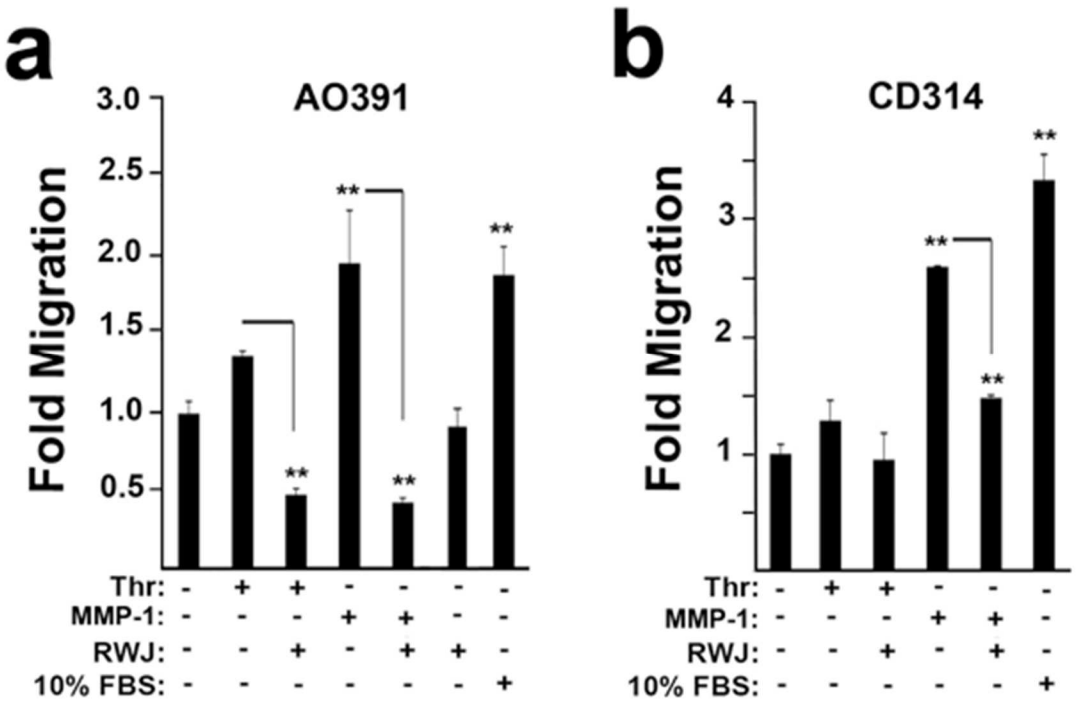

Figure 2.6. MMP-1 is a potent chemo-attractant for PAR1-dependent SMC migration. **(a)** 16 h migration in Boyden chambers of AO391 and **(b)** CD314 SMCs towards either 5 nM thrombin or 5 nM MMP-1, with and without 5 μM RWJ-56110 (RWJ). 10% FBS was used as a positive control. **p<0.01 by ANOVA followed by Student-Newman-Keuls post-test.

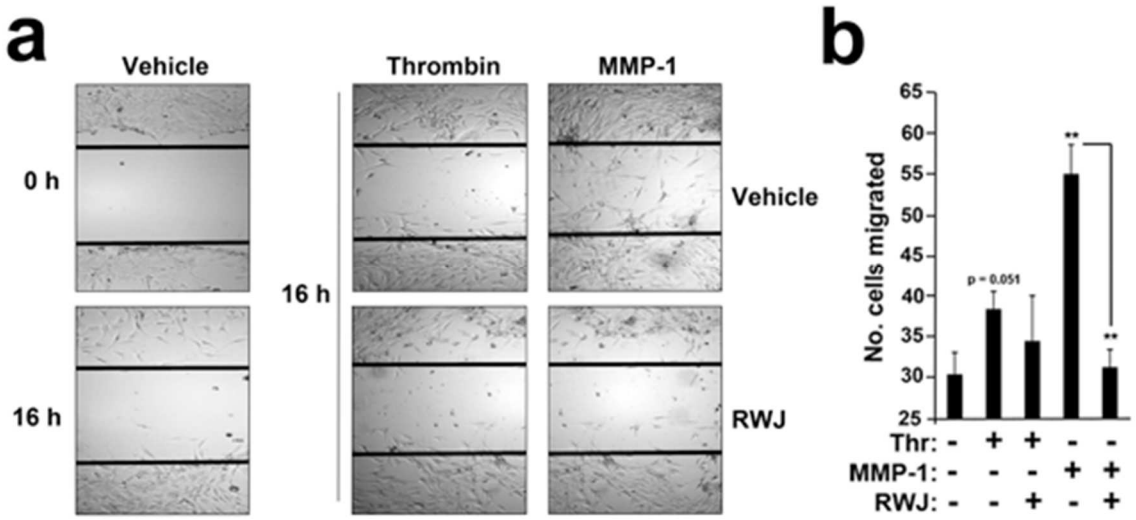

Figure 2.7. MMP-1 induces SMC migration in wound-healing assays. (a) CD314 cells were grown to confluency in 6-well plates and scratched using a sterile P1000 polypropylene pipet tip. The cells were then treated with either 5 nM thrombin or MMP-1 with or without 5 μM RWJ-56110 (RWJ) and allowed to migrate for 16 h. Four micrographs (4x) at time 0 and 16 h were used to compare treated and untreated (PBS buffer (vehicle) wells. **(b)** The mean number of cells migrated in (n=4 fields) are quantified on the right. Data is shown as mean ± SEM. Student's unpaired *t*-test: ** $p<0.01$.

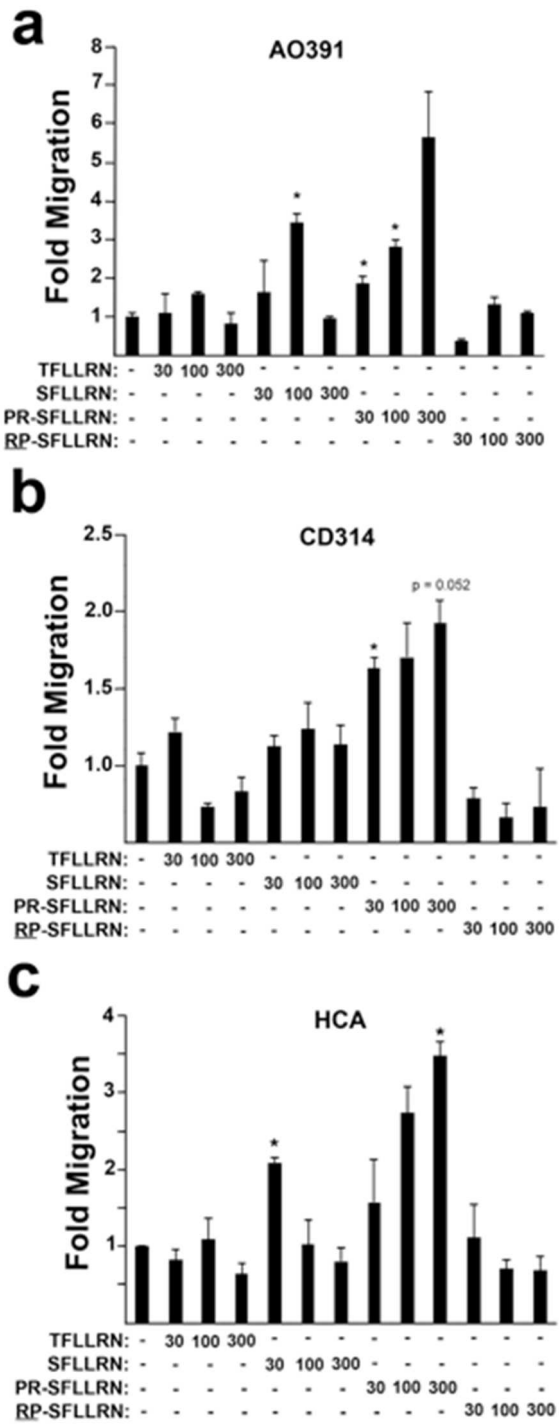

Figure 2.8. MMP-1 derived peptide ligands stimulate PAR1-dependent migration.16 h migration of **(a)** AO391, **(b)** CD314 and **(c)** 1° HCA SMCs towards agonist peptides (Thr: TFLLRN, SFLLRN; MMP-1: PR-SFLLRN; Reversed MMP-1: RP-SFLLRN) at the concentrations indicated (30 -300 μM). *p<0.05 by ANOVA followed by Student-Newman-Keuls post-test.

II.4.4 Desensitization of PAR1 to thrombin and MMP-1

Following activation, PAR1 is rapidly phosphorylated and internalized as the primary means of quenching the signal.[39] As both thrombin and MMP-1 were capable of cleaving and signaling through PAR1 (**Figure 2.5**), we were surprised to observe such dramatic differences in their abilities to function as chemo-attractants for vascular SMCs. In contrast to thrombin-generated peptides which showed negligible or decreased migration at higher concentrations, migration occurred even at high concentrations of the MMP1-ligand (**Figure 2.8**), suggesting that MMP1-PAR1 may have altered kinetics of endocytosis/recycling as a means of prolonging the protease signal.[39] To test this hypothesis we assayed PAR1 surface expression, as a measure of endocytosed receptor, following cleavage by both equimolar amounts of both thrombin and MMP-1. Both enzymes resulted in rapid and efficient internalization of PAR1 by 5 min at 37 °C, however, activation by MMP-1 resulted in faster re-emergence of PAR1, with 100% surface expression returning by 30 min (**Figure 2.9**). Thrombin resulted in a return of only 40% PAR1 surface expression by 30-60 min. Suppression of endocytosis at 4 °C prevented loss of PAR1 surface expression by either protease agonist (**Figure 2.9**). The quicker reappearance of PAR1 after exposure to MMP-1 as compared to thrombin is consistent with the observation that MMP-1 is a more efficient chemo-attractant for SMCs.

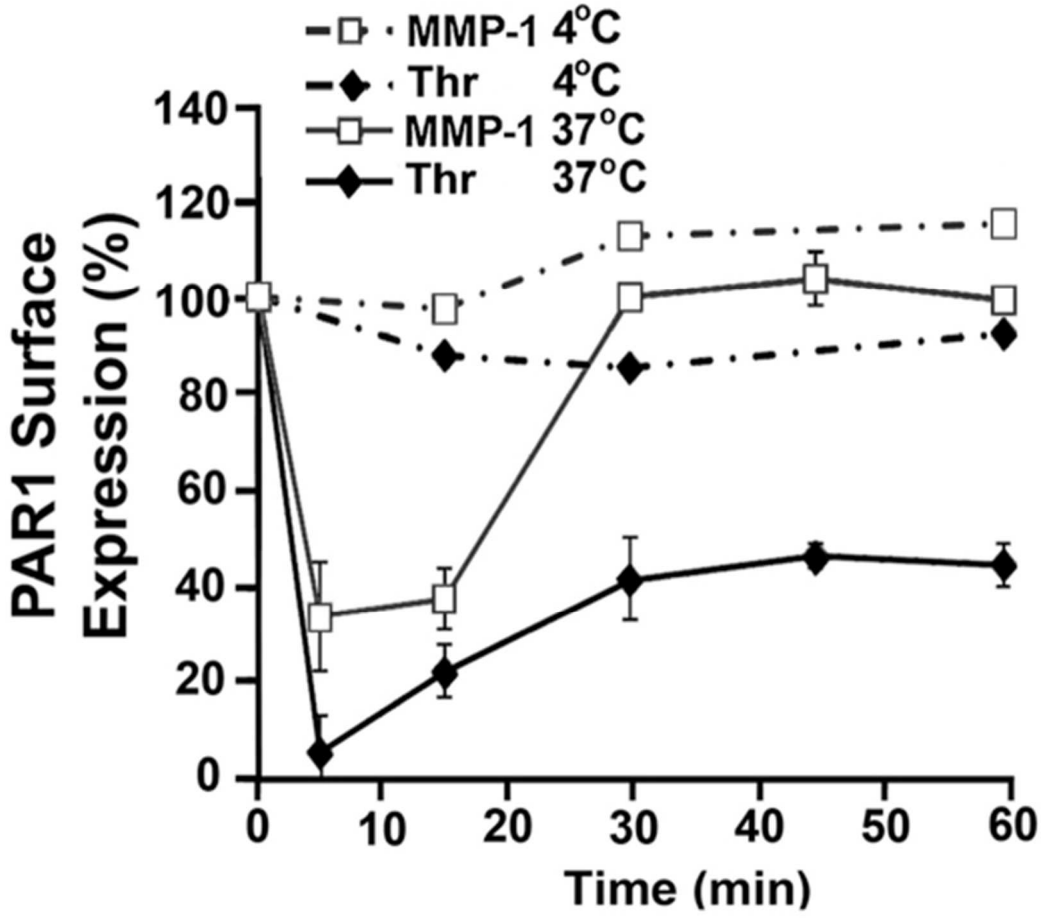

Figure 2.9. PAR1 desensitization following MMP-1 or thrombin cleavage. PAR1 surface expression on CD314 SMCs over 60 min as observed by FACS following treatment with either 5 nM thrombin or 5 nM MMP-1. Experiments were performed at either 37 °C or 4 °C (to inhibit endocytosis).

II.4.5 Thrombin vs. MMP1-stimulated SMC contraction

The ability of SMCs to contract is an intrinsic quality that controls blood vessel tone and subsequently blood flow. Furthermore, physiologic contraction underscores one of the major functional differences between differentiated and de-differentiated SMCs (see Section I.4.1). Because MMP-1 cleaves PAR1 at a unique non-canonical site from thrombin (**Figure 2.4**) we hypothesized that MMP-1 and thrombin differentially regulate SMC contractile function. To determine the efficacy of thrombin versus MMP-1 stimulation on SMC contraction, we assayed myosin light chain (MLC) phosphorylation and smooth muscle (F)-actin polymerization in CD314 SMCs. Thrombin-PAR1 significantly induced phosphorylation of MLC and thrombin-generated peptide agonists stimulated F-actin polymerization in the SMCs (**Figure 2.10a,b**).[212] MMP-1 treatment only modestly increased MLC phosphorylation, similar to the effect of the MMP1-generated peptide on F-actin production (**Figure 2.10a,b**).

Biochemical analysis of phosphorylation of focal adhesion kinase (FAK), which activates downstream proteins involved in cellular shape change and contraction,[212] was also investigated as a marker of SMC contraction. FAK was phosphorylated over 60 min more robustly following stimulation with thrombin as compared to MMP-1 (**Figure 2.10c**). As GPCR-induced cell shape change is mediated through the $G_{12/13}$ family of G-proteins with subsequent activation of RhoA-GTP,[34] we tested whether thrombin and MMP-1 were capable of activating this pathway. Thrombin increased PAR1-RhoA activation to a greater extent than MMP-1; both effects were blocked by RWJ-56110 (**Figure 2.10d**). Together, these data suggest that thrombin is capable of stimulating more robust contraction of SMCs through PAR1 as compared to MMP-1.

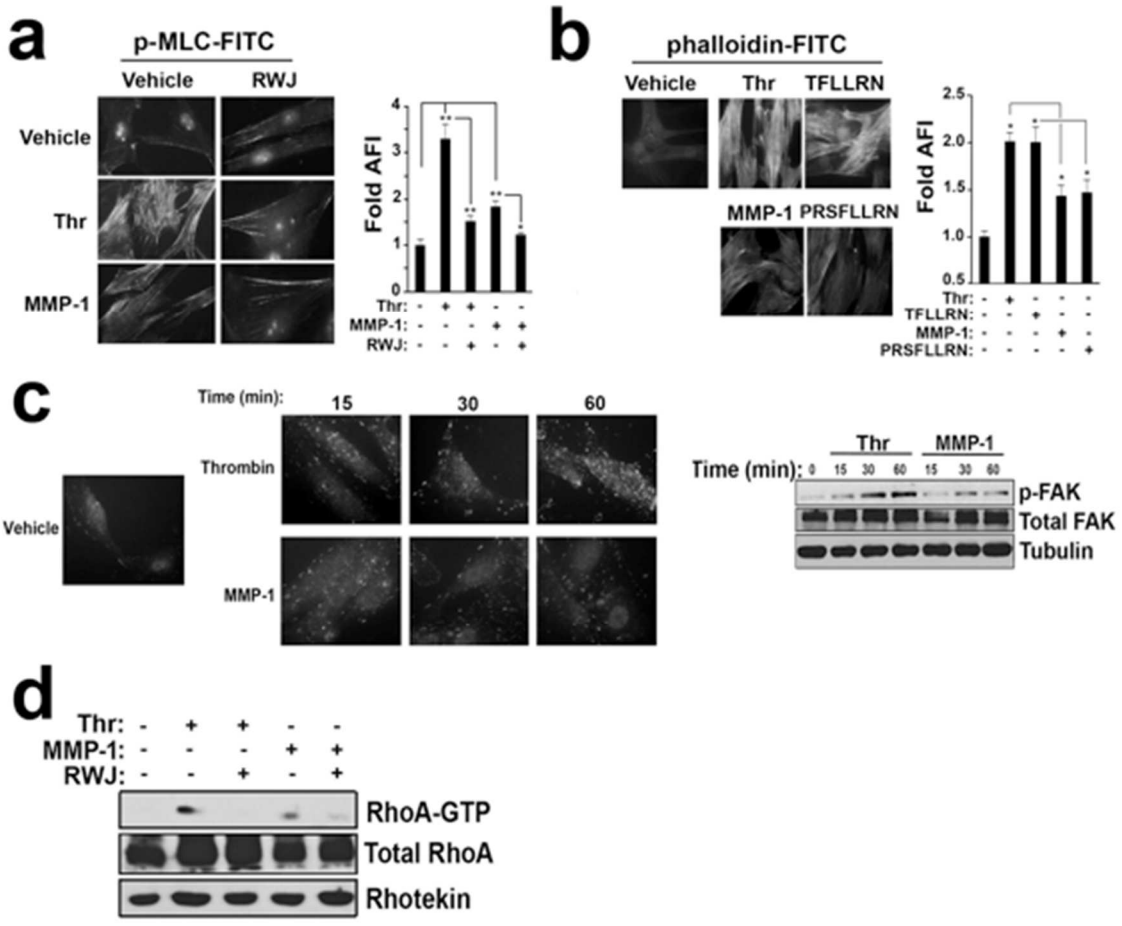

Figure 2.10. Thrombin-PAR1 activates SMC contraction. (a) Immunofluorescence of FITC-phospho-MLC in CD314 cells treated for 15 min with either 5 nM thrombin or 5 nM MMP-1, with and without 5 μM RWJ-56110 (RWJ). Quantification of mean green fluorescence intensity of 6 fields is shown on right. DAPI was used as a nuclear counter stain. **(b)** Immunofluorescence of FITC-phalloidin in CD314 cells treated for 5 min with either 5 nM thrombin or 5 nM MMP-1, with and without 5 μM RWJ-56110 (RWJ). Quantification of mean green fluorescence intensity of 6 fields is shown on right. DAPI was used as a nuclear counter stain. **(c)** Immunofluorescence and Western blot analysis of phospho-FAK (Tyr397) following stimulation with either 5 nM thrombin or 5 nM MMP-1 at the time points indicated. **(d)** Western blot analysis of RhoA bound to GTP 15 min following stimulation with either 5 nM thrombin or 5 nM MMP-1, with and without 5 μM RWJ-56110 (RWJ) pre-treatment for 15 min. *p<0.05; ** p<0.01 by ANOVA followed by Student-Newman-Keuls post-test.

II.4.6 Molecular Phenotypic modulation of SMCs by thrombin and MMP-1

SMC contraction represents rapid physiologic signaling in cells. To determine how thrombin or MMP-1 could affect to long-term maintenance of a contractile phenotype, we performed RT-qPCR for contractile markers[166] on primary SMCs treated with thrombin or MMP-1, with and without RWJ-56110 for 24 hours. Primary cells were utilized for this assay because there early passage number more closely mimics a naive SMC-state outside the blood vessel wall. Thrombin treatment resulted in a 3-10 fold increased expression of differentiation/contractile markers of SMCs including myocardin,[213] SM-22,[166, 167] and calponin[166, 167] which was suppressed by the PAR1 inhibitor, RWJ-56110 (**Figure 2.11**). Myocardin is the major transcriptional co-activator responsible for expression of the SMC gene box[213] and is both necessary and sufficient for a differentiated smooth muscle phenotype. Both SM-22 and calponin are crucial members of the contractile apparatus, and represent SMC specific gene products[166, 167]. In contrast, MMP-1 treatment markedly suppressed (3-17 fold) contractile gene expression and myocardin, which was reversed by the PAR1 inhibitor (**Figure 2.11**). Fibronectin, a component of the secreted extracellular matrix important for maintenance of a differentiated phenotype,[214] was unaffected by thrombin, but substantially decreased by MMP-1. These data indicate that activation of PAR1 by thrombin promotes a contractile/differentiated phenotype, whereas activation of PAR1 by MMP-1 triggers a de-differentiated phenotype, which may contribute to the observed detrimental phenotypic modulation of SMCs associated with restenosis.

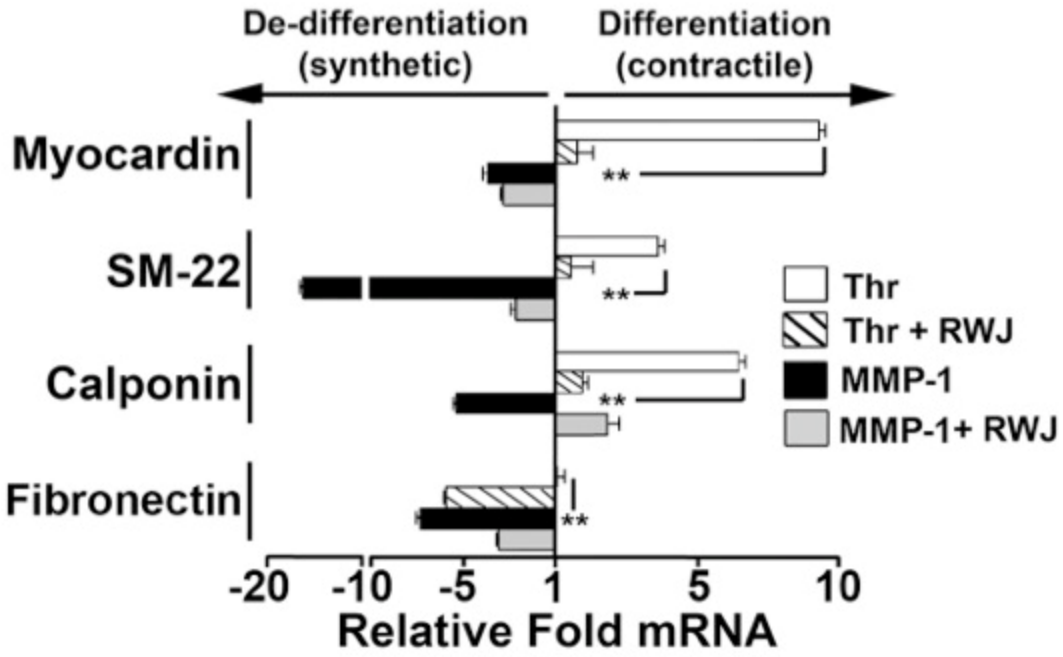

Figure 2.11. MMP1-PAR1 drives SMC de-differentiation. RT-qPCR in 1° HCA cells of myocardin, SM-22, calponin, and fibronectin following 24 h treatment with either 5 nM thrombin or 5 nM MMP-1, with and without 5 μM RWJ-56110 (RWJ). Data are expressed as relative fold changes of triplicate over untreated samples normalized to GAPDH. ** $p<0.005$, by ANOVA with Bonferroni post-test correction.

II.4.7 Thrombin-PAR1 vs. MMP1-PAR1 signaling in SMC proliferation

Another critical feature of de-differentiated SMCs is their ability to re-enter the cell cycle and proliferate to repair the injured site.[167, 197, 215] Over-persistence of the hyperplastic phenotype of SMCs can eventually narrow the vessel lumen resulting in a stenotic lesion. We found that both MMP-1 and thrombin stimulated PAR1-dependent proliferation of cultured and primary SMCs to a similar extent (**Figure 2.12**). The thrombin (TFLLRN) and MMP-1 (PR-SFLLRN)-generated peptide ligands recapitulated the proliferative effects on SMCs observed with either thrombin or MMP-1 (**Figure 2.12a,b**). Thrombin stimulated ERK phosphorylation in SMCs was blocked by the PAR1 inhibitor (**Figure 2.12e**); MMP-1 stimulation of phospho-ERK was blocked by both the MMP-1 inhibitor, FN-439, and the PAR1 inhibitor, RWJ-56110 (**Figure 2.12e**).

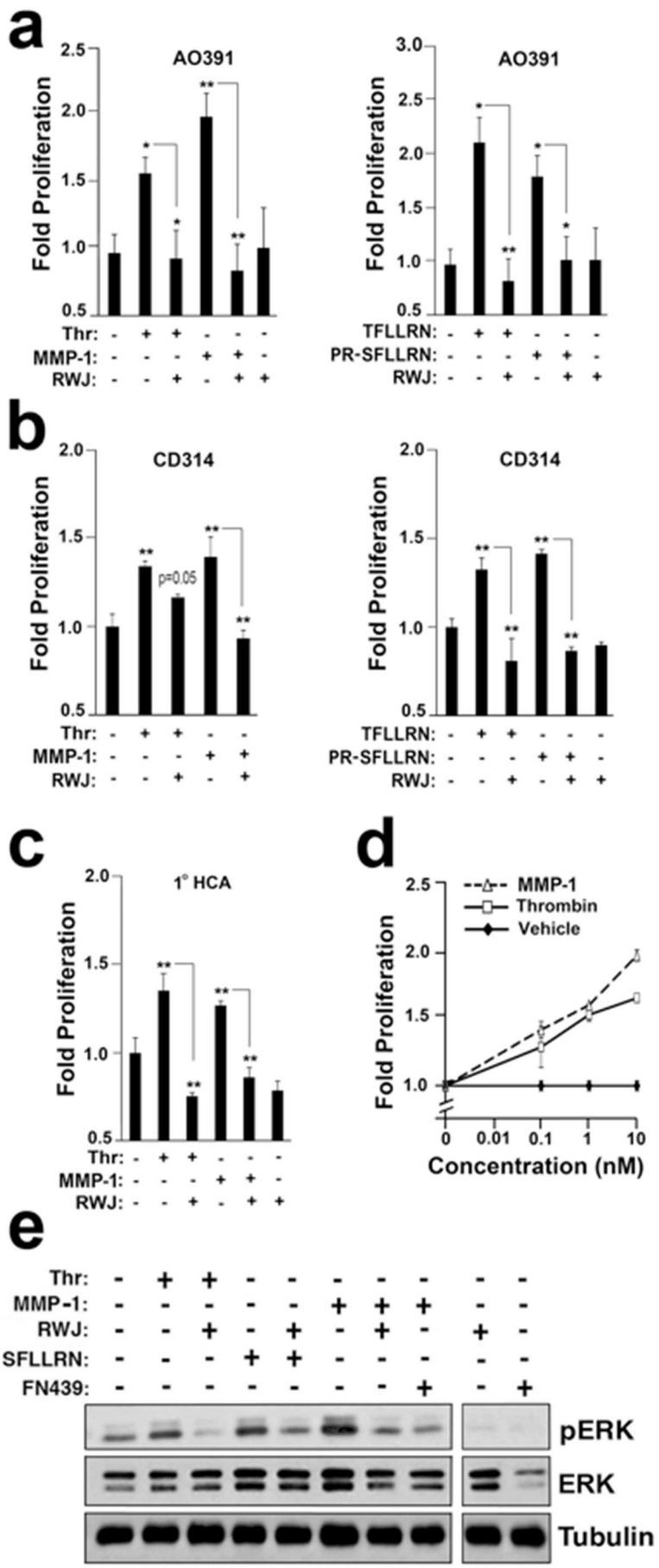
a
AO391
Fold Proliferation
Thr:
MMP-1:
RWJ:
AO391
TFLLRN:
PR-SFLLRN:
RWJ:
b
CD314
p=0.05
CD314
c
1° HCA
d
MMP-1
Thrombin
Vehicle
Concentration (nM)
e
Thr:
MMP-1:
RWJ:
SFLLRN:
FN439:
pERK
ERK
Tubulin

Figure 2.12. MMP-1 and thrombin stimulate SMC proliferation. (a-c) Fold change in proliferation (DNA-crystal violet staining, A_{595} nm) after three days of treatment with 5 nM thrombin, 5 nM MMP-1, 300 μM TFLLRN, or 300 μM PR-SFLLRN, with or without 5 μM RWJ-56110 (RWJ) in **(a)** AO391, **(b)** CD314, and **(c)**1° HCA cell lines. **(d)** Proliferative dose-response curves in SMCs to thrombin and MMP-1 over the concentrations (nM) indicated. **(e)** ERK1/2 phosphorylation in CD314 cells 15 min after treatment with either 5 nM thrombin, 5 nM MMP-1, or 30 μM SFLLRN in the presence or absence of 5 μM RWJ-56110 (RWJ) or 5 μM FN-439. *p<0.05; ** p<0.01 by ANOVA followed by Student-Newman-Keuls post-test.

II.4.8 G-protein coupling of thrombin-PAR1 vs. MMP1-PAR1

PAR1 exhibits promiscuous G-protein coupling with three of the four Gα families: G_i, $G_{12/13}$, and G_q. Following our observations that MMP-1 and thrombin produced different functional outcomes in SMCs, we first ascertained whether the G_i-inhibitor, pertussis toxin (PTx), could affect intracellular calcium mobilization in SMCs. Thrombin-stimulated calcium flux was completely inhibited by the addition of PTx, whereas the MMP-1 signal was only partially suppressed (**Figure 2.13a**). Thrombin-PAR1 induced proliferation was inhibited by PTx, whereas MMP1-PAR1 induced proliferation was not (**Figure 2.13b**). Moreover, PTx blocked thrombin-stimulated ERK-phosphorylation, but instead enhanced MMP1-ERK phosphorylation (**Figure 2.13c,d**). The βγ subunits coupled to PAR1-G_i are potent activators of PLC-β and calcium dependent pathways (**Figure 2.14**).[216] Accordingly, inhibitors of PLC-β and calcium, U73122 and BAPTA-AM, respectively, suppressed ERK phosphorylation induced by thrombin, but conversely increased MMP1-induced activation of phospho-ERK (**Figure 2.14a**). These results demonstrate that thrombin-PAR1 activates mitogen-activated protein kinase pathways and proliferation through G_i, whereas MMP1-PAR1 utilizes a non-G_i pathway in SMCs.

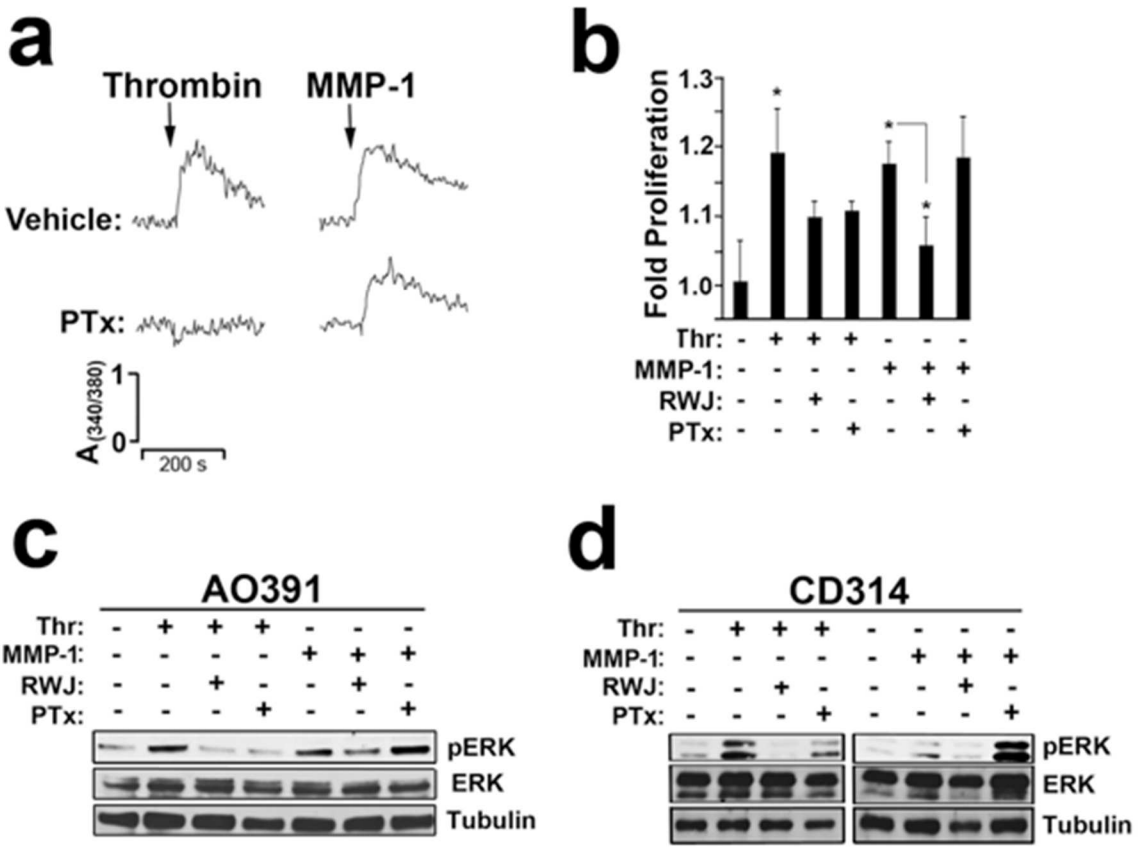

Figure 2.13. Thrombin and MMP-1 differentially signal through PAR1-G_i pathways in SMC proliferation. (a) Representative calcium traces of AO391 cells treated with either 5 nM thrombin or 5 nM MMP-1. Cells were pretreated with 200 ng/mL PTx (pertussis toxin) for 16 h. **(b)** 24 h proliferation of CD314 cells treated with either 5 nM thrombin or 5 nM MMP-1, with and without 200 ng/mL PTx. All proliferation assays are representative graphs expressing average fold changes from 6 individual replicates per treatment. ERK1/2 phosphorylation in **(c)** AO391 and **(d)** CD314 cells 15 min following treatment with either 5 nM thrombin or 5 nM MMP-1 in the presence of 5 μM RWJ-56110 (RWJ) or 200 ng/mL pertussis toxin (PTx). * $p<0.05$, by ANOVA followed by Student-Newman-Keuls post-test.

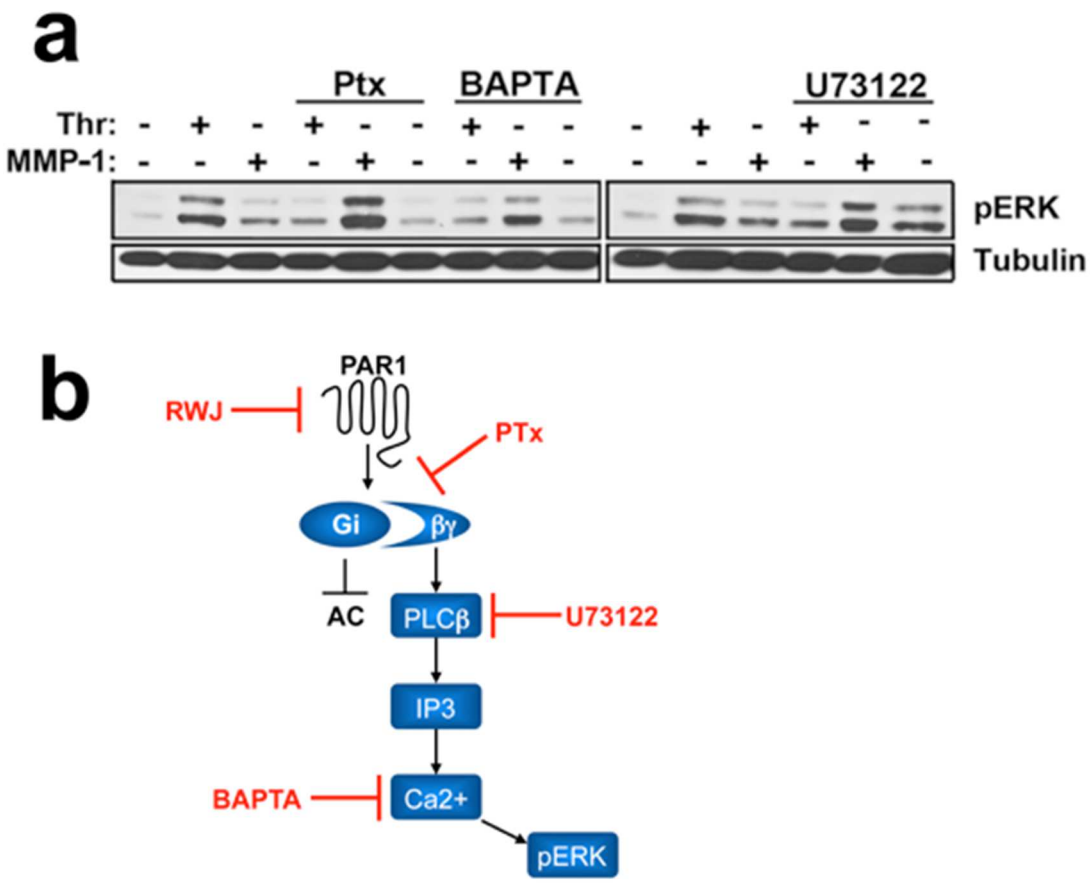

Figure 2.14. Thrombin-PAR1 signaling in SMCs couples to a G_i-PLCβ-Ca^{2+} pathway. (a) ERK1/2 phosphorylation in CD314 cells 15 min following treatment with either 5 nM thrombin or 5 nM MMP-1 in the presence or absence of 200 ng/mL pertussis toxin (PTx), 5 μM BAPTA-AM (BAPTA), or 5 μM U73122. **(b)** Schematic of pathway inhibitors used in ERK assays from (a).

II.5 Discussion

Matrix metalloprotease-1 has long been implicated in the pro-inflammatory and tissue-remodeling events leading to cleavage of collagen in the vascular wall and promotion of vulnerable atherosclerotic plaque formation.[104, 140, 198] Recently, there has been an increasing awareness of the potential clinical utility of measuring circulating MMP-1 levels for risk-stratification in acute coronary syndrome patients undergoing coronary intervention and stenting.[217, 218] MMP-1 is also significantly elevated in patients with high intimal/medial ratios in their carotid artery plaques.[139] Here, we describe a previously unknown vascular remodeling mechanism by which MMP1-PAR1 drives arterial stenosis following injury of carotid arteries, and leads to intimal hyperplasia and de-differentiation of SMCs. Activated PAR1 exhibited metalloprotease-specific signaling patterns distinct from thrombin activation, known as biased agonism, that produced divergent functional outputs by the SMCs. Inhibition of MMP-1 activity with the small molecule FN-439 led to significantly reduced neointimal formation following wire-injury of carotid arteries in mice. Inhibition of thrombin showed no benefit. Thrombin-PAR1 signaling caused rapid contraction of SMCs and resulted in a contractile, differentiated phenotype. MMP1-PAR1 resulted in the opposite effect and led to a de-differentiated phenotype, via a different G protein pathway.

De-differentiation of SMCs results in the transformation from a quiescent, contractile cell to a proliferative and migratory one, lacking an organized contractile apparatus.[167] The pathologic role of phenotypic modulation of SMCs in cardiovascular disease has been well established,[167] and current therapeutic strategies, including drug eluting stents, are aimed at targeting SMC de-differentiation.[219] Considering the role of MMPs in vascular matrix remodeling, especially in intimal thickening following balloon angioplasty and stenting,[151, 152] broad-spectrum MMP inhibitors have been evaluated in

clinical trials for the prevention of restenosis following PCI.[158] The BRILLIANT-EU study examined whether stents coated with the broad-spectrum MMP inhibitor batimastat, would suppress restenosis without effects on re-endothelialization. The study concluded that batimastat-coated stents proved safe in larger populations (n=550), although there was no significant benefit at primary (major adverse cardiac events) or secondary (binary restenosis, sub-acute thrombosis, angiography) endpoints.[158]

Downstream inhibition of PAR1 has had beneficial effects in animal models of restenosis,[220] but orally-active PAR1 inhibitors such as vorapaxar,[221] can have adverse effects on hemostasis.[222] Direct thrombin and Xa inhibitors have shown promise in the treatment of atrial fibrillation and venous thromboembolism,[223] but similar to PAR1 inhibitors, there is a dose-dependent increased risk for bleeding and they have not been thoroughly evaluated in phase III clinical trials for patients with acute coronary syndrome.[223] Moreover, clinical studies with thrombin inhibitors have not demonstrated a beneficial effect in preventing restenosis of culprit lesions post-PCI.[224-226] Inhibition of the upstream protease, MMP-1, may provide the advantage of specifically impacting PAR1 signaling cascades that promote phenotypic switching and restenosis, without affecting thrombin-PAR1 driven hemostasis. Development of more selective MMP inhibitors, especially ones directed against MMP-1, may be useful for upstream blockade of this MMP1-PAR1 restenotic pathway in PCI patients.

In addition to MMP-1, MMP-13 was recently identified as having PAR1 agonist activity in cardiomyocytes leading to cardiac hypertrophy and heart failure.[103] MMP-13 was found to cleave PAR1 at a slightly different site from both MMP-1 and thrombin, one residue toward the C-terminal side of the thrombin cleavage site.[103] It is currently unclear whether MMP13-PAR1 signaling plays a similar role to MMP-1 in SMC-driven vascular remodeling, but it further underlines the emerging importance of metalloprotease-PAR signaling in the regulation of pathological repair processes in cardiovascular diseases.

In conclusion, we provide evidence for a MMP1-PAR1 signaling axis that promotes SMC de-differentiation, resulting in increased cell proliferation and migration, while down-regulating expression of proteins that are critical for SMC contraction. Conversely, thrombin-PAR1 signaling led to a differentiated, contractile phenotype, consistent with notion that thrombin-PAR1 promotes hemostasis rather than restenosis. Upstream inhibition of MMP-1 may provide the advantage of selectively antagonizing a non-canonical PAR1 signaling cascade that promotes restenosis without adversely affecting thrombin-PAR1 hemostasis.

Chapter 3. A PAR2-antagonist pepducin reduces steatosis and hepatic inflammation in models of non-alcoholic fatty liver disease and steatohepatitis.

III. Chapter 3. A PAR2-antagonist pepducin reduces steatosis and hepatic inflammation in models of non-alcoholic fatty liver disease and steatohepatitis

III.1 Abstract

The prevalence of obesity and type 2 diabetes in Western populations has led to the emergence of non-alcoholic fatty liver disease (NAFLD) as the leading cause of chronic liver disease, recently surpassing viral hepatitis. Studies have shown that protease-activated receptor-2 (PAR2) contributes to hepatic stellate cell (HSC) activation in the liver, and subsequent hepatocyte injury, collagen deposition, and inflammation. We hypothesized that inhibition of PAR2, with a cell-penetrating pepducin antagonist, could ameliorate the histologic and systemic symptoms of NAFLD and its more severe form, steatohepatitis (NASH). Using a diet-induced model of NAFLD, we report that a PAR2 antagonist, PZ-235, significantly reduced vesicular fat deposits by approximately fifty percent. Lobular inflammation was also reduced in pepducin treated animals. We observed a decline in both the individual and total NASH activity scores (NAS) for PZ-235 treated mice, which corresponded to decreased histologic disease-progression. In pepducin treated mice there was a trend towards reduced serum alanine aminotransferase (ALT) levels and liver triglycerides. These results indicate that PAR2 is a valid therapeutic target for the treatment of NAFLD/NASH.

III.2 Introduction

NAFLD is the most prevalent chronic liver disorder in the United States. It is estimated that upwards of 46% of Americans have diagnosable NAFLD, and the incidence predictably tracks with obesity.[180, 227] NAFLD is defined as triglyceride accumulation in hepatocytes without a positive history of excessive alcohol consumption or other liver injury (e.g. viral hepatitis).[227] Progression of NAFLD can lead to a more severe disease (NASH) characterized by hepatocyte injury, inflammation, and fibrosis. The major risk factors predisposing to NAFLD, and by extension NASH, are obesity and insulin resistance, although Metabolic Syndrome consisting of the combination of abdominal obesity, hyperlipidemia, hypertension, and insulin resistance, is also a prominent risk factor. Considering the striking relationship between insulin resistance, obesity, and NAFLD, it is often considered the hepatic manifestation of type 2 diabetes.[228]

The activation and differentiation of hepatic stellate cells (HSCs) plays a prominent role in the progression of NAFLD/NASH. HSCs are specialized pericytes that normally store the majority of the body's vitamin A, but become activated following liver injury. The influx of free fatty acids into the liver is a potent activator of HSCS, and a hallmark of NAFLD/NASH. Upon activation, HSCs up-regulate expression of smooth muscle actin (SMA), and modify their matrix and cytokine secretion. Release of pro-inflammatory cytokines, including IL-1, IL-6, and MCP-1, along with increased deposition of collagen, incite architectural and inflammatory changes that lead to liver fibrosis.[181]

PAR2 belongs to a family of G protein coupled receptors that are activated by proteolytic cleavage of the N-terminus resulting in the formation of a tethered ligand that subsequently activates G-protein signaling.[1] Unlike other members of the PAR family, PAR2 is unresponsive to thrombin cleavage. Instead, it is fully activated by trypsin and trypsin-like proteases (e.g. mast cell tryptase). [24]

PAR2 is widely expressed throughout the gastrointestinal system, including gut epithelium, intestinal smooth muscle cells, pancreatic acinar cells, enteric neurons, and liver Kuppfer cells and HSCs. [1,24] Furthermore, HSC activation results in increased PAR2 surface expression, and which then stimulates HSC proliferation and collagen synthesis.[194] Recently, Knight et al[70] have shown that *Par2*$^{-/-}$ mice have decreased collagen deposition and HSC activation in experimental mouse models of liver fibrosis. Given the significance of PAR2 in these studies, we hypothesized that inhibition of PAR2 in models of NAFLD/NASH could protect against disease progression.

In this study, we provide evidence that a cell-penetrating PAR2-antagonist pepducin, PZ-235, reduces steatosis and hepatic inflammation in a methionine-choline deficient diet-induced model of NAFLD/NASH. Additionally, we also show that delayed treatment with PZ-235 diminishes serum alanine aminotransferase (ALT) levels and pathological hepatocyte ballooning to levels comparable to *Par2*$^{-/-}$ mice. Finally, we show that PZ-235 inhibits PAR2-dependent HSC intracellular calcium mobilization, MAP-kinase activation, and cytokine release. Together, these data put forth a new strategy for targeted PAR2 inhibition for non-alcoholic fatty liver syndromes.

III.3 Methods

MCD mouse model

All animal models were approved by the Tufts Medical Center IACUC committee. Eleven-week old male C57BL/6 mice were purchased from Charles River Laboratories and placed on an *ad libitum* methionine-choline deficient (MCD) diet (Harlan # TD.90262) or either a control diet with methionine and choline added back (Harlan # TD.99366) or regular chow (Harlan #8604). The mice remained on MCD diet for either 2 or 3 weeks. Treatment animals were injected daily with subcutaneous injections of either vehicle (5% DMSO) or 10 mg/kg PZ-235 for 14 days starting at day 0 (2 week cohorts) or day 7 (3 week cohort). At the end of the experiment, animals were anesthetized with isoflurane and a mid-line incision was made exposing both the chest and abdominal cavities. The chest cavity was exposed and retracted in order to insert a 25 gauge needle into the left ventricle where approximately 500 μL of blood was removed for serum analysis. The animals were then perfused for approximately 1 minute with PBS using a pressured pump. The liver was then dissected away from the abdominal organs and placed in PBS. Livers were dried and weighed immediately following excision. The largest lobe was placed in 10% buffered formalin for histological analysis. The remainder of the liver was flash frozen in liquid nitrogen for RNA, protein, and ELISAs. Blood was allowed to coagulate at room temperature for 2 hours, after which time it was centrifuged at 4000 rpm for 5 min to isolate serum.

Immunohistochemistry

Livers were fixed in 10% buffered formalin then embedded in paraffin blocks. Sequential sections were cut and stained with H&E and or smooth muscle actin (SMA).

Alanine aminotransferase assay

Alanine aminotransferase was assayed by EIA from mouse serum according to the manufacturer's instructions (Sigma). Briefly, 10- 20 μL of serum was used to measure the generation of pyruvate through a coupled enzyme assay. Samples were performed in duplicate at 37 °C with a standard curve, and absorbance was monitored over time at 570 nm. Total units/liter (U/L) were extrapolated from absorbance data. One unit of ALT activity was defined as the amount of enzyme that generates 1.0 mmole of pyruvate per minute at 37 °C.

Liver triglyceride assays

Flash frozen livers were weighed and crushed with a mortar and pestle. Liver triglycerides were measured by EIA according to the manufacturer's instructions (Cayman Chemicals). Briefly, samples were lysed in Standard Diluent (1X) and diluted 1:5. Ten microliters of the 1:5 dilution were used to measure the generation of glycerol at room temperature. Absorbance was monitored at 540 nm, and measured 15 min after initiation of the assay. Milligrams of triglyceride were conveyed as mgs per gram of liver tissue.

Cell Culture

LX-2 cells were a generous gift from Dr. Scott Friedman at the Mt. Sinai. School of Medicine , New York, NY. LX-2 cells maintained in M199 supplemented with 5% FCS in 5% CO_2 at 37 °C.

Intracellular Calcium flux

LX-2 were lifted with 5 mM EDTA/PBS and labeled with Fura-2AM (1:4000) in Kreb's Ringers Bicarbonate (KRB) buffer. Cells were incubated at 37 °C on a horizontal rocker for 30 min. Samples were then washed with KRB buffer and re-suspended in 4-5 mL of KRB. Calcium flux was then measured following the addition of agonists (100 μM SLIGRL, 1 nM trypsin) by the ratio of excitation intensity at 340/380 nm on a LS 50B Luminescence Spectrometer. The antagonist PZ-235 (30 μM) was added 3 min prior to the addition of agonist.

ERK phosphorylation

LX-2 cells were grown to confluency in 10 cm tissue culture plates in 5% FCS/M199 medium. PZ-235 (3 μM) was added to cells 15 min prior to agonist treatment. To stimulate ERK phosphorylation, cells were treated with 30 μM SLIGRL or 1 nM trypsin for 15 minutes at room temperature. Cells were then lysed as previously described.[63] Briefly, plates were lysed in 300 μL of T-PER lysis buffer using a rubber spatula at 4 °C. Lysates were spun at 14,000 rpm at 4 °C, and supernatant was removed. Lysates were quantified for total protein content using Bradford reagent or a nanodrop. Thirty micrograms of total protein was run on 10% polyacrylamide SDS-gels, after which point protein was transferred to nitrocellulose membranes. Membranes were blocked for 1 h at room temperature in 5% non-fat dry milk in TBST after which point they were probed for phospho-ERK1/2 (p42/44) at a dilution of 1:1000 in TBST for 1 h at room temperature with gentle agitation. Membranes were washed 3x5 min in TBST and HRP-conjugated secondary antibody was used at a 1:5000 dilution for 1 h at room temperature. Membranes were was 3x5 min in TBST and developed using ECL reagent (Pierce). Membranes were then stripped with 62 mM Tris/2- β -mercaptoethanol (2-BME) for 1

hour at 56 °C. Membranes were then re-probed with total ERK antibody (1:1000) and β-tubulin (1:5000) at room temperature for 1 h.

MCP-1 ELISA

LX-2 cells were plated in 6-well plates with 1 mL of M199 medium supplemented with 5%FCS. The cells were then incubated with 100 μM SLIGRL or 1nM trypsin, with and without 1 μM PZ-235, for 24 h. The conditioned media was then harvested and assayed for MCP-1 protein levels by ELISA (Quantikine). MCP-1 ELISA was performed according to manufacturer's instructions. Briefly, a sandwich ELISA was performed using MCP-1 antibody coated plates. Fifty microliters of conditioned media (un-concentrated) was bound to the plates. A second MCP-1 antibody was then used to detect the bound form. Levels of MCP-1 are expressed as pg/mL.

III.4 Results

III.4.1 PZ-235 reduces fatty liver in mouse models of NAFLD/NASH

NAFLD is the most common liver disease in the United States, with a prevalence ranging between 10% and 46%.[180, 227] It has previously been shown that excessive activation of liver-associated PAR2 contributes to HSC activation and fibrosis..[69, 70] To determine whether pharmacologic inhibition of PAR2 could potentially benefit NAFLD/NASH patients, we put 11 week old male C57BL/6 mice on a methionine-choline deficient (MCD) diet for 2 weeks. MCD diets are a well accepted model for the development of liver steatosis and progression to NASH in mice.[190] Animals were given daily sub-cutaneous injections of either vehicle (5% DMSO) or 10 mg/kg PZ-235 for the duration of the experiment (14 d) (**Figure 3.1a**). At completion of the experiment we observed a trend towards decreased gross liver size and serum alanine aminotransferase (ALT) levels in the PZ-235 treated group despite comparable total body weights (**Figure 3.1b-e**). Histological examination demonstrated roughly 50% decreased vesicular fat deposits (**Figure 3.2a,b**). Analysis of liver triglyceride levels trended towards an approximate 30% decrease in PZ-235 treated livers over vehicle alone (**Figure 3.2c**).

The NASH Activity Score (NAS) is a histological assessment used to grade and diagnose NASH in patients. The three histologic features include, steatosis, lobular inflammation, and hepatocyte ballooning (**Figure 3.3,top**). Use of the NAS system to score both the vehicle and PZ-235 treated livers showed decreases in all 3 categories for pepducin treated mice. The largest reductions were seen on both steatosis and lobular inflammation (**Figure 3.3**). NAS scores between 4-8 are considered positive, while anything below 4 is not NASH. PZ-235 treatment reduced the overall NAS score from 4.1 to 3 in two-weeks (**Figure 3.3**). These data suggest that PAR2 antagonism with

PZ-235 protects against liver steatosis, inflammatory infiltrates, and hepatocyte injury in diet-induced models of NASH.

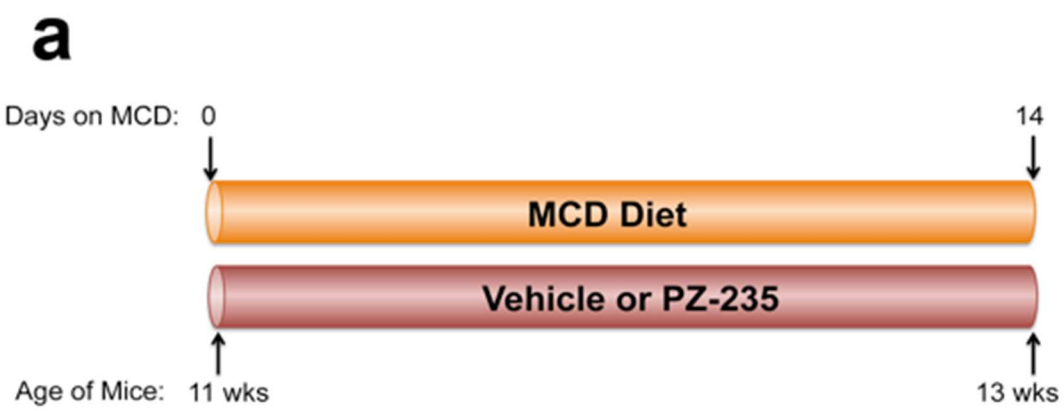

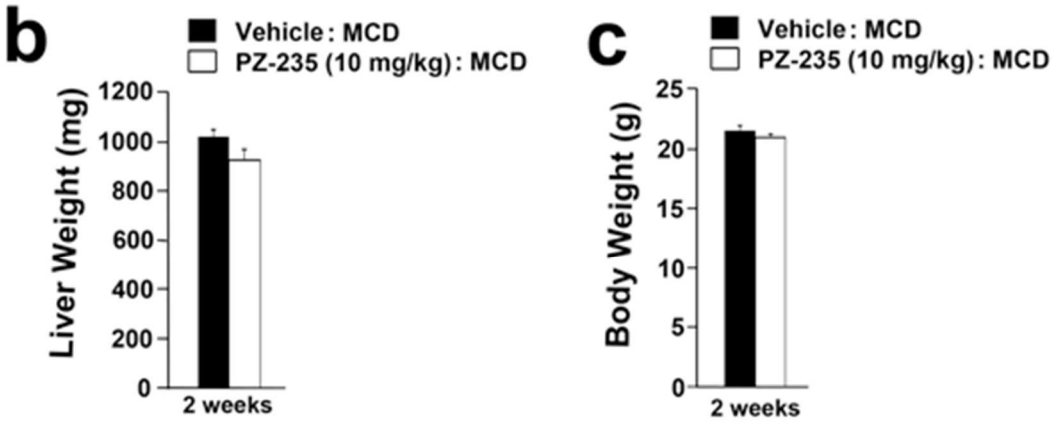

d

2 Weeks	Average Starting Body Weight (g)	Average Ending Body Weight (g)	Average Liver Weight (mg)	Average Liver/ Body Weight %
Untreated: normal chow	23.6 ± 0.6	24.1 ± 0.6	1248.6 ± 141	5.19 ± 0.26
Vehicle: MCD	24.2 ± 0.69	21.3 ± 1.1	1015.5 ± 107.6	4.7 ± 0.58
PZ-235: MCD	24.1± 1.2	20.9 ± 0.8	926.7 ± 129.7	4.4 ± 0.20

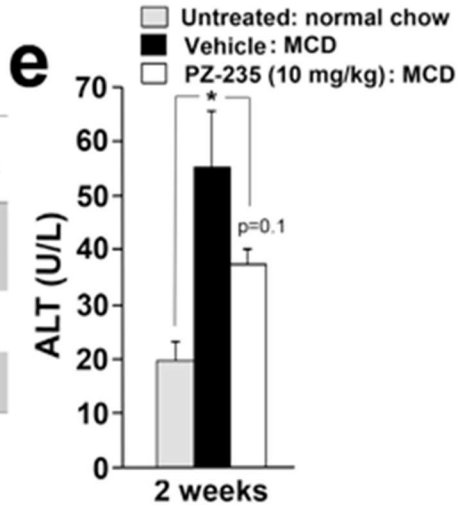

Figure 3.1. Two-week PZ-235 treatment reduces serum ALT levels of mice on MCD diet. (a) Schematic of 14 d animal experiment.**(b)** Average liver weights of vehicle (5% DMSO) and 10 mg/kg PZ-235 treated mice after 14 d on MCD diet. (n=10) **(c)** Average body weights of vehicle and PZ-235 (10 mg/kg) treated mice after 14 d on MCD diet. (n=10) **(d)** Average starting and ending body weights for animals on normal chow and MCD diet over 14 d. Average liver weights and body weight-adjusted liver weights for animals on normal chow and MCD diet over 14 d.(n=10) **(e)** Serum ALT levels in untreated mice on normal chow and vehicle or PZ-235 treated animals on MCD diet for 14 d. (n=5) * $p<0.05$ by Student's *t*-test.

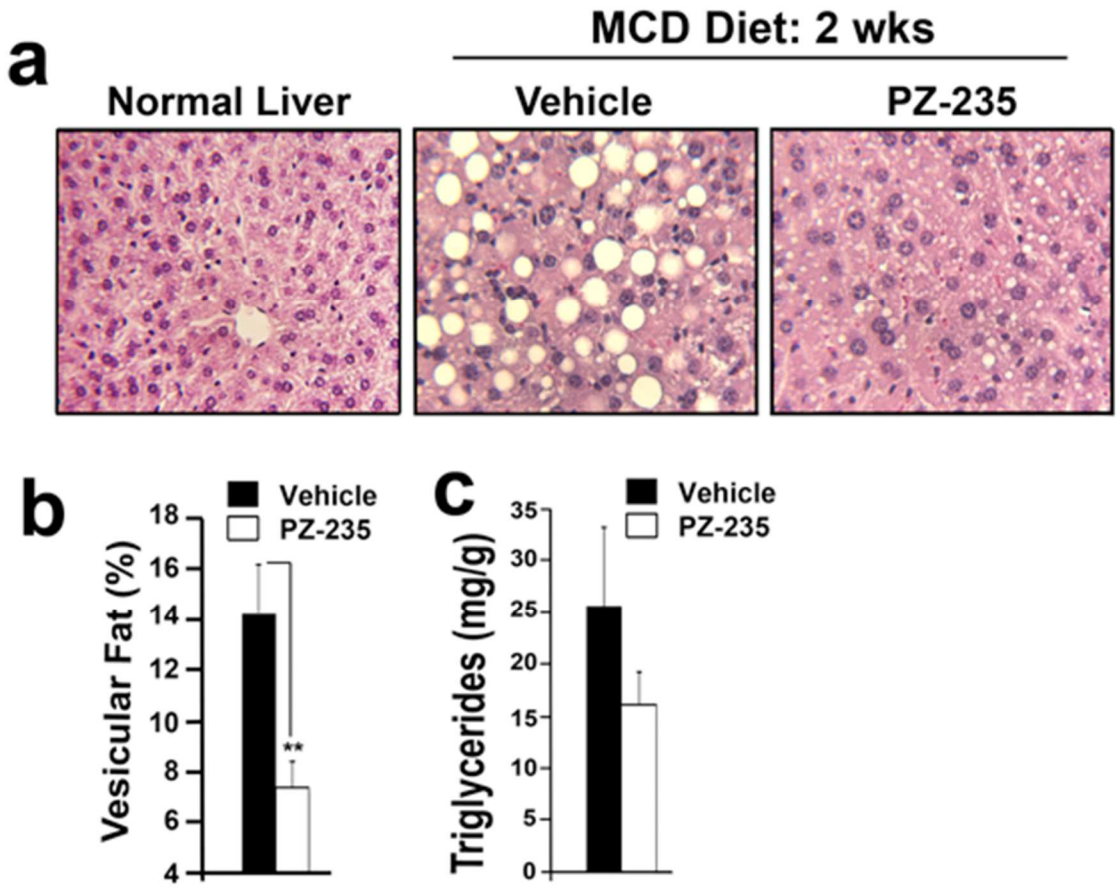

Figure 3.2. Two-week PZ-235 treatment reduces fatty liver NASH models. (a) Representative pictures of livers from normal and 2 week treated vehicle (5% DMSO) and 10 mg/kg PZ-235 mice. 20x magnification. **(b)** Quantification of vesicular fat in livers from vehicle and PZ-235 (10 mg/kg) mice after 14 d on MCD diet. (n=10) **(c)** Liver triglyceride levels per mg of liver in vehicle and PZ-235 (10 mg/kg) treated mice after 14 d on MCD diet. (n=5)

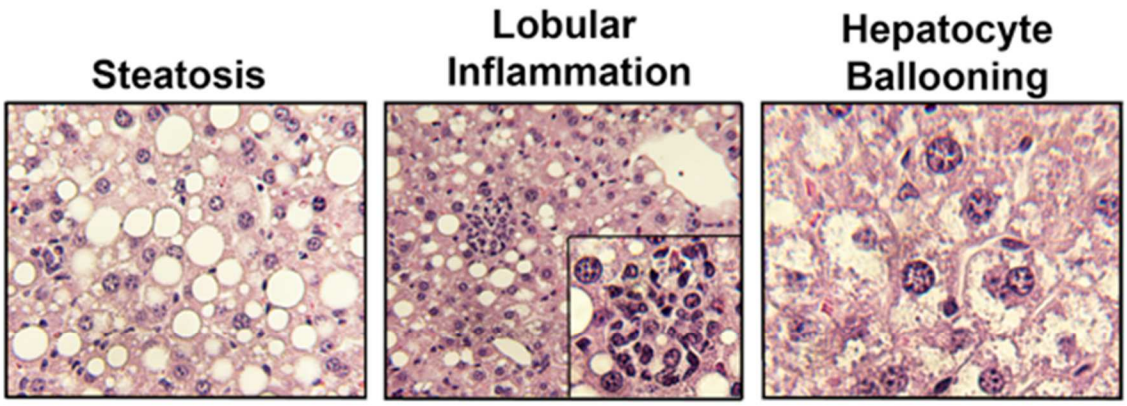

Treatment Group	Steatosis (0-3)	Lobular Inflammation (0-3)	Hepatocyte Ballooning (0-2)	NAS (0-8)
Vehicle: 2 wks	1 ± 1.2	1.4 ± 0.7	1.7 ± 0.5	**4.1 ± 1.9**
PZ-235: 2 wks	0.5 ± 0.7	0.8 ± 0.6$^{\#}$	1.6 ± 0.5	**3 ± 1.0**

Figure 3.3. PZ-235 reduces steatosis and lobular inflammation in mouse models of NAFLD/NASH. (Top) Representative pictures illustrating the 3 criteria for NAS. Inset picture is 40x magnification of inflammatory cells surrounding a central lobule. Arrow-head: inflammatory cluster and examples of hepatocyte ballooning. **(Lower)** Breakdown of the average score ± standard deviation for each NAS category and the cumulative NAS score for mice on MCD diet for 2 weeks with concomitant treatment with either vehicle (5% DMSO) or PZ-235 (10 mg/kg).(n=10) #: p=0.057

III.4.2 PZ-235 partially corrects the histological features of NAFLD/NASH

The overwhelming majority of NAFLD/NASH patients suffer from long-term, pre-existing obesity and type 2 diabetes.[227] Furthermore, the two-hit hypothesis of NASH-development suggests a slow-progression over time (see Section I.5.1; **Figure 1.6**), with patients developing the disease in stages. Given that PZ-235 decreased fat deposition when given simultaneously with the MCD diet, we interrogated whether delayed treatment could reverse the pre-existing liver disease. We performed a similar experiment to Figure 3.1, except mice were placed on MCD diet for 1 week, followed by two weeks of treatment with either vehicle or 10 mg/kg PZ-235 (**Figure 3.4a**). To determine if our effects were truly PAR2-dependent, we also placed *Par2*$^{-/-}$ mice on MCD diet for the extent of the experiment (3 weeks). Delayed treatment resulted in a statistically significant decrease in liver weight, while total body weight remained constant (**Figure 3.4b-d**). Serum ALT levels were roughly 50% higher in vehicle treated animals on 3 weeks of MCD diet compared to those on 2 weeks of diet. Both PZ-235 and *Par2*-deficiency markedly reduced ALT levels after 2 weeks of delayed treatment compared to vehicle control (**Figure 3.4e**). Surprisingly, there was no significant difference between vehicle and PZ-235 treated animals in vesicular fat deposition or liver triglyceride levels (**Figure 3.5a-c**). *Par2*$^{-/-}$ mice are currently being analyzed for fat deposits and liver triglycerides.

Consistent with the observation that PZ-235 had little effect on liver steatosis, 3-week NAS scores showed modest histological improvement with PZ-235 treatment (4 to 3.9) (**Figure 3.6**). The largest effect was seen on hepatocyte ballooning, which is in stark contrast to the initial 2-week experiment showing effects mainly on steatosis and inflammation. *Par2*$^{-/-}$ mice exhibited marginal improvements in overall NAS score over PZ-235 (3.9 to 3.4) (**Figure 3.6**). These data predict that PZ-235 is unable to correct pre-

existing steatosis, but may prove beneficial in reversing hepatocyte injury as evidenced by reduced serum ALT levels (**Figure 3.4e**) and histological hepatocyte ballooning (**Figure 3.6**).

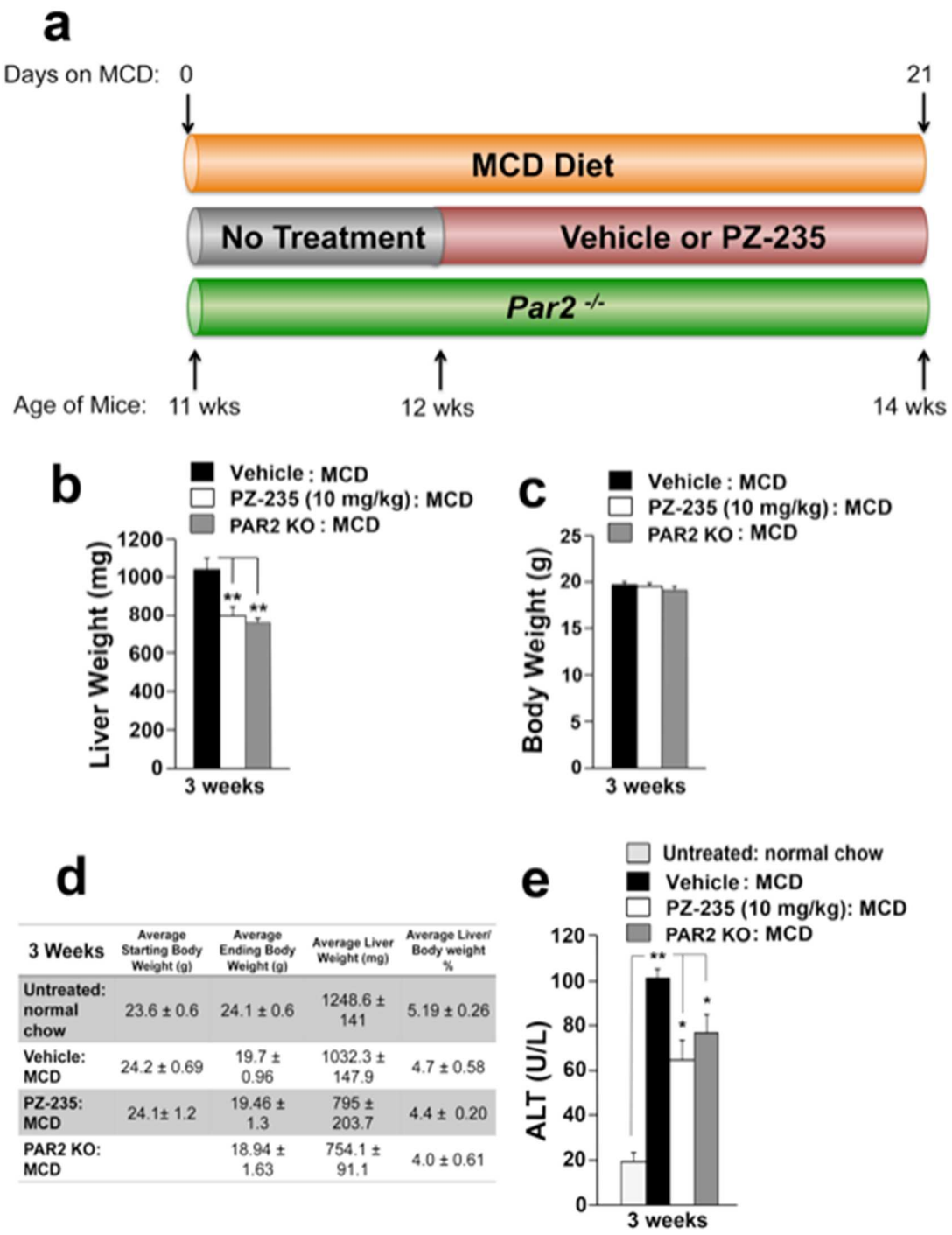

3 Weeks	Average Starting Body Weight (g)	Average Ending Body Weight (g)	Average Liver Weight (mg)	Average Liver/ Body weight %
Untreated: normal chow	23.6 ± 0.6	24.1 ± 0.6	1248.6 ± 141	5.19 ± 0.26
Vehicle: MCD	24.2 ± 0.69	19.7 ± 0.96	1032.3 ± 147.9	4.7 ± 0.58
PZ-235: MCD	24.1± 1.2	19.46 ± 1.3	795 ± 203.7	4.4 ± 0.20
PAR2 KO: MCD		18.94 ± 1.63	754.1 ± 91.1	4.0 ± 0.61

Figure 3.4. PAR2 inhibition or genetic deletion reduces liver weights in mice on MCD diet. (a) Schematic of 21 d (3 week) animal experiment. **(b)** Average liver weights of animals MCD diet for 21 d with 14 d of treatment (vehicle, 10 mg/kg PZ-235) or no treatment (*Par2*$^{-/-}$: PAR2 KO). (n=10) **(c)** Average body weights of animals on MCD diet for 21 d with 14 d of treatment (vehicle, PZ-235) or no treatment. **(d)** Average starting and ending body weights of mice on normal chow and mice on MCD diet for 21 d. Average liver weights and body weight adjusted liver weights.(n=10) **(e)** Serum ALT levels from untreated animals on normal chow or mice on MCD diet for 3 weeks. (n=5) ** $p<0.01$ by Student's *t*-test.

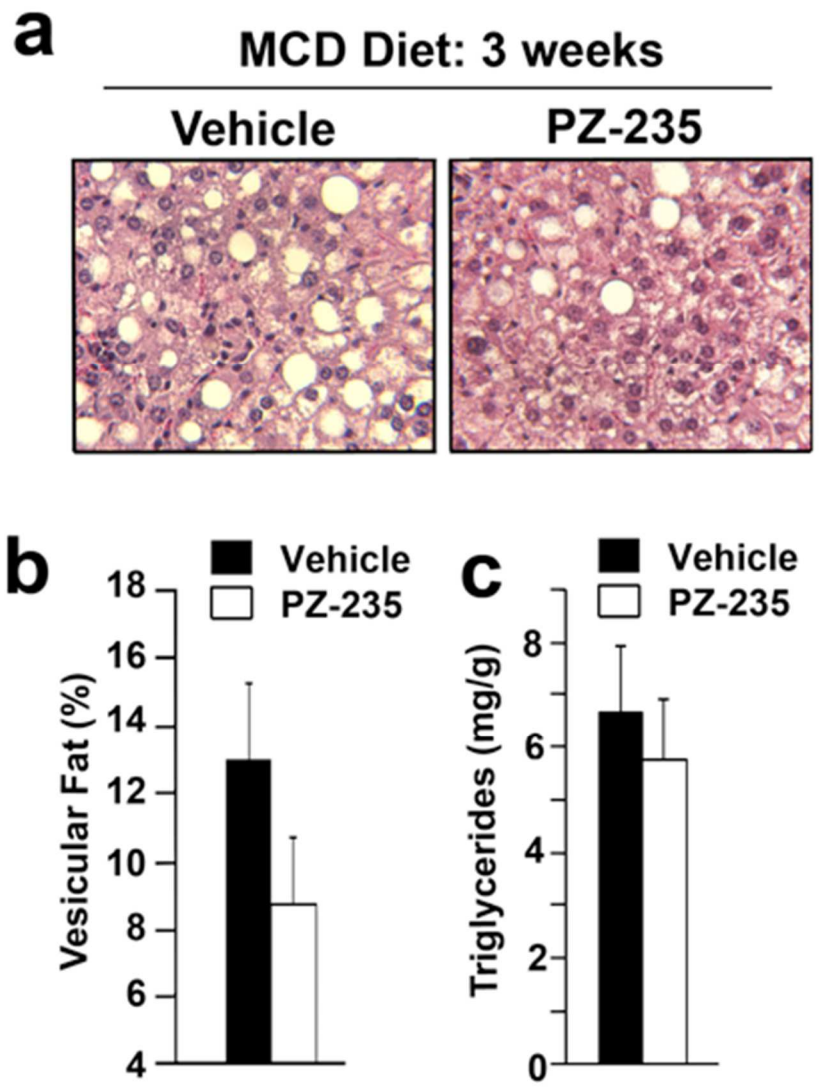

Figure 3.5. Delayed PZ-235 treatment does not reverse steatosis. (a) Representative pictures from vehicle treated (5% DMSO) and PZ-235 treated (10 mg/kg) livers after 3 weeks on MCD diet with 2 weeks of treatment. (n=10). **(b)** Percent of vesicular fat in the liver from vehicle (5% DMSO) and PZ-235 (10 mg/kg) treated animals from (a). **(c)** Liver triglyceride levels in vehicle (5% DMSO) and PZ-235 (10 mg/kg) treated animals from (a).

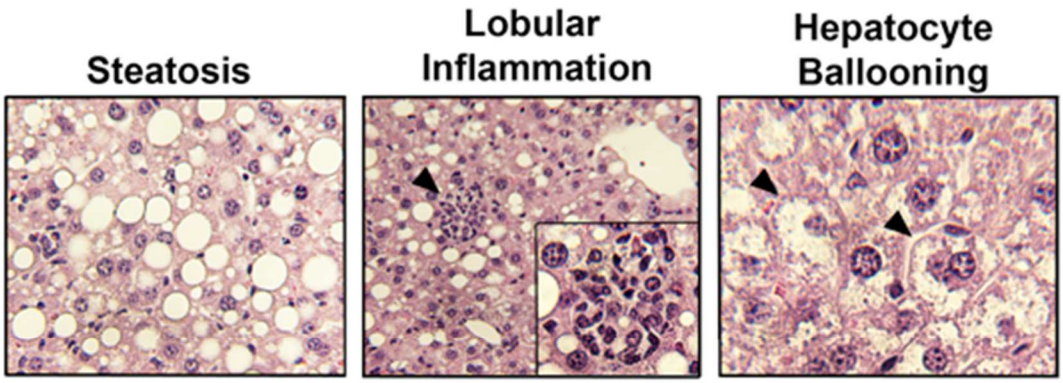

Treatment Group	Steatosis (0-3)	Lobular Inflammation (0-3)	Hepatocyte Ballooning (0-2)	NAS (0-8)
Vehicle: 3 wks	0.8 ± 0.9	1.2 ± 0.4	2 ± 0	**4 ± 1.2**
PZ-235: 3 wks	0.8 ± 0.8	1.5 ± 0.8	1.6 ± 0.5*	**3.9 ± 1.4**
PAR2 KO: 3 wks	1.0 ± 0.9	0.8 ± 0.4*	1.6 ± 0.5*	**3.4 ± 0.9**

Figure 3.6. NAS for PZ-235 versus vehicle treated livers after 3 weeks on MCD diet. Mice were fed MCD diet for 3 weeks, with treatment (vehicle or 10 mg/kg PZ-235) during the last 2 weeks. **(Top)** Representative micrographs of the 3 criteria for the NASH activity score (NAS). Inset picture is 40x magnification of inflammatory cells surrounding a central lobule. Arrow-head: inflammatory cluster and examples of hepatocyte ballooning. **(Bottom)** Average NAS scores ± standard deviation for each category and the average total NAS are listed. (n=10) * : $p<0.05$

III.4.3 PZ-235 inhibits hepatic stellate cell signaling

HSCs are one of the major orchestrating cells in the progression of NAFLD/NASH. Following activation in response to liver injury (*e.g.* steatosis), HSCs dysregulate their matrix production and MMP/TIMP secretion.[181, 194] They also up-regulate smooth muscle actin (SMA) and secrete a number of pro-inflammatory cytokines that enhance the inflammatory response and result in further liver damage. [181] To determine whether PZ-235 affected HSC activation, we first verified that PZ-235 could inhibit PAR2-dependent signaling in HSCs.

Immortalized human HSC cells, LX-2, were used to monitor intracellular calcium flux in response to PAR2 agonists and PZ-235. Cells treated with 100 μM of the PAR2 peptide agonist, SLIGRL, showed increased intracellular calcium mobilization (**Figure 3.7a**). Furthermore, the negative control peptide, in which the first two residues are reversed (LS-IGRL), had no effect on calcium flux (**Figure 3.7a**). Pre-treatment with the PZ-235 completely inhibited the SLIGRL calcium signal (**Figure 3.7a**). PZ-235 inhibition was specific to PAR2, since cells still responded to the PAR1 agonist, thrombin, following PZ-235 pre-treatment (**Figure 3.7a**). These results suggest that PZ-235 is a direct and specific PAR2 antagonist in HSCs.

Since HSC activation results in broad changes to gene transcription and proliferation, we wanted to investigate upstream pathways that are closely linked to these functions, such as MAP-kinase signaling. LX-2 cells were treated with the PAR2 peptide agonist, SLIGRL, or the PAR2 protease agonist, trypsin, with and without PZ-235 and assayed for ERK1/2 phosphorylation (**Figure 3.7b**). Both SLIGRL and trypsin resulted in robust activation of ERK1/2 after 15 min, whereas PZ-235 treatment completely antagonized this effect by both agonists (**Figure 3.7b**). These results suggest

that PZ-235 actively inhibits PAR2-ERK-dependent gene transcription events in LX-2 cells.

Our *in vivo* results suggest that early treatment with PZ-235 reduces lobular infiltrates in the liver (**Figure 3.3**). Since HSCs are known to secrete a number of pro-inflammatory factors following activation, we tested the hypothesis that PZ-235 could inhibit HSC cytokine production. We assayed levels of monocyte chemo-attractant protein-1 (MCP-1/CCL2) in the conditioned media 24 h after PAR2 stimulation on LX-2 cells (**Figure 3.7c**). Both PAR2 agonists (SLIGRL and trypsin) increased MCP-1 production, which was reduced by co-treatment with PZ-235 (**Figure 3.7c**).

Based on previous studies indicating a role for PAR2 in HSC activation, and our results showing that PZ-235 blocked PAR2-dependent HSC signaling, we hypothesized that our *in vivo* effects were a result of decreased stellate cell activation in the PZ-235 treated livers. We analyzed SMA-positive cells per high-powered field in 2-week treated livers from both the vehicle and PZ-235 cohorts (**Figure 3.1a**). Surprisingly, pepducin-treated livers only showed a slight trend towards decreased HSC activation (**Figure 3.8**). Given that HSCs represent up to 20% of the total cell volume of the liver, it is possible that histological characterization is not sensitive enough to detect overall differences between treatment groups. Additional studies in established HSC cell lines or isolation of primary HSCs are needed for future functional and biochemical analysis. These results suggest that although PZ-235 inhibits PAR2 signaling in HSCs and reduces MCP-1 secretion, it does not appear to affect the absolute number of activated stellate cells.

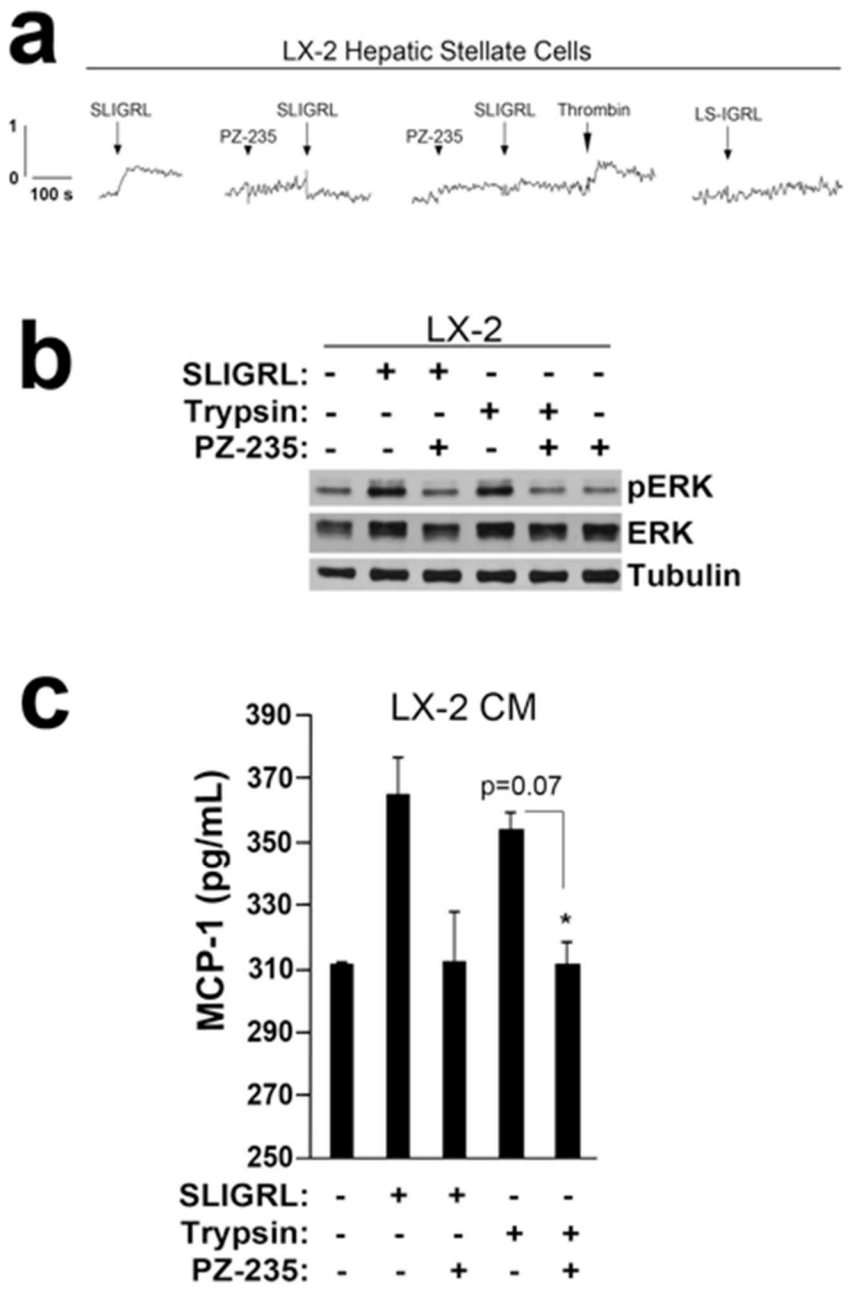

Figure 3.7. PZ-235 inhibits LX-2 stellate cell signaling. (a) Intracellular calcium mobilization in LX-2 cells after the addition of 100 μM SLIGRL (small arrow) with and without 30 μM PZ-235 pretreatment (arrow-head). Subsequent PAR1 activation was shown by the addition of 1 nM thrombin (large arrow). The LS-IGRL control peptide was used at 100 μM. **(b)** ERK1/2 phosphorylation 15 min following stimulation with 100 μM SLIGRL or 1 nM trypsin, with and without 1 μM PZ-235 pre-treatment. Total ERK and tubulin were used as loading controls. **(c)** Levels of MCP-1 in the conditioned media of LX-2 cells following 24 h treatment with 100 μM SLIGRL or 1 nM trypsin, with and without 1 μM PZ-235. *p<0.05 by Student's *t*-test.

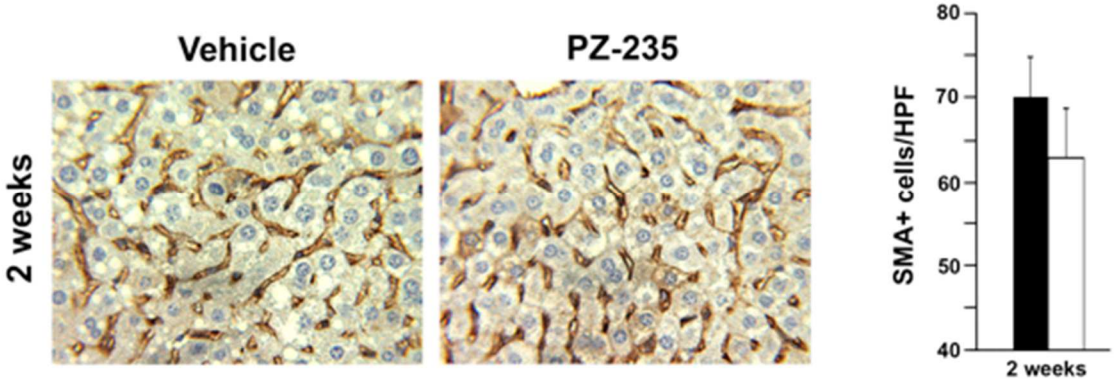

Figure 3.8. Smooth muscle actin (SMA) positive HSCs in vehicle and PZ-235 treated livers. (left) Representative pictures of SMA+ cells in vehicle and PZ-235 (10 mg/kg) treated animals after 2 weeks on MCD diet. **(right)** Quantitation of the number of SMA+ cells per high powered field (HPF: 40X magnification).(n=10)

III.5 Discussion

Non-alcoholic fatty liver disease and its successor, steatohepatitis, impact up to ~40% of the population in the United States.[227] Current therapeutic guidelines recommend weight loss accompanied by diabetes management. Despite overwhelming evidence that weight loss can both halt and reverse the effects of NAFLD, patients often struggle to abide by dietary restrictions.[229, 230]

Here, we report that concomitant treatment with a PAR2 antagonist pepducin, PZ-235, reduces steatosis and inflammation in mouse models of NAFLD/NASH. Additionally, PZ-235 inhibits PAR2-dependent MCP-1 secretion from HSCs. MCP-1 is a potent pro-inflammatory cytokine that recruits leukocytes to areas of injury and is increased in the serum of patients with NASH.[231] Inhibition of MCP-1 secretion by PZ-235 provides a possible mechanism for the decreased lobular inflammation observed *in vivo.* Future studies will look at macrophage infiltration (F4/80 staining) in treated livers and levels of MCP-1, among other inflammatory markers.

Delayed PZ-235 treatment did not significantly affect vesicular fat deposition or liver triglyceride levels, but did show improvements in serum ALT and hepatocyte injury. Based on these results, we propose that PAR2 contributes separately to the two phases of NAFLD/NASH progression. The first phase is the initiation of steatosis and inflammation. If addressed early, these features are reversed with a PZ-235, possibly through reduced HSC cytokine secretion. After the establishment of steatosis, additional liver insults perpetuate hepatocyte injury as the second phase. Treatment with PZ-235 at this juncture only ameliorates the damage done to the hepatocytes and has little effect on fatty deposits and surrounding inflammatory infiltrates.

These data indicate that in addition to its function on HSCs, PAR2 may be playing a distinct role on an alternative cell type (*e.g.* Kuppfer cells [resident hepatic

macrophages], oval cells [hepatic progenitor cells]). Additional studies looking at the effects of PAR2 activation and inhibition on these cell types will provide critical evidence as to the mechanism of PZ-235's effects. Special interest will be paid to the contribution of Kuppfer cells, considering PAR2's role in MCP-1 production. Kuppfer cells are the first responding-cell to hepatocyte injury, and thus represent early stages of liver injury. Recent evidence suggests that TNF-α-producing Kuppfer cells are critical for NASH initiation in animal models.[232] Future studies aimed at understanding the role of PAR2 in this subpopulation of injury-responsive liver cells are warranted.

IV. Chapter 4. Thesis Discussion

IV.1 General Discussion

SMC de-differentiation

Protease-activated receptors have proven critical contributors to numerous disease processes in which aberrant protease signaling drives cellular changes that propagate disease progression. It is clear that PAR1 remains a critical player in the diseased vasculature. We show that despite PAR1's penchant for thrombin-triggered signaling, non-canonical activation by MMP-1 has an unforeseen role in SMC de-differentiation. PAR1 exhibits biased signaling, in that thrombin promotes a differentiated, contractile phenotype, whereas MMP-1 stimulates de-differentiation into a synthetic, pathologic phenotype. Others have shown PAR1 biased agonism in the endothelium.[116, 233] In both cases, cleavage of PAR1 by either MMP-1 or APC at non-canonical sites led to distinct gene expression profiles and cytoprotective effects, respectively. [116, 233] To our knowledge, we are the first to describe PAR1 biased agonism in smooth muscle cells.

The exact mechanism behind PAR1 biased agonism has yet to be elucidated. We have shown that differential G-protein coupling accounts for differences in proliferation, but this may not explain all aspects of the divergent signaling. Alternatively, differences in functional signaling can be grouped into divergence occurring either "outside" or "inside" the cell. Outside effects would include differences in enzyme kinetics between thrombin and MMP-1 or environmental factors that might affect proteolytic cleavage. For example, APC has been shown to have a preference for cleavage of PAR1 associated with lipid rafts,[131] suggesting that the contextual environment of PAR1 influences receptor cleavage. Likewise, receptor dimerization has been known to affect GPCR signaling, particularly PAR signaling.[128] Additionally, the

original dual-conformation theory of GPCR activation has been challenged, and a new multi-conformation theory has emerged which suggests that individual ligands help stabilize distinct active GPCR conformations, leading to distinct pathway activation.[234]

"Inside" effects include pre-assembly with particular G-proteins as well as association with beta-arrestins. Fluorescence resonance energy transfer (FRET) studies have shown the pre-association of PARs with certain G-proteins, prior to proteolytic activation. The implication of these studies warrants the consideration that pre-assembly may be an important contributor to the activation of protease-activated receptors. [235] [236] Additionally, beta-arrestins have been known to act as scaffolding proteins linking the GPCR to effector proteins to influence the down-stream signaling. [237] This function is separate from its role in receptor desensitization, which illustrates the complicated network of signaling cascades that contribute to functional outputs.

Recent evidence suggests that MMP-13 is also capable of cleaving PAR1 at a cryptic site one residue towards the C-terminus of the thrombin cleavage site, which promotes overstimulation of beta-adrenergic receptors. Whether PAR1 also exhibits an activating bias towards MMP-13 is currently unclear, but it emphasizes the importance of non-canonical PAR1 cleavages in disease. Whether or not MMP-13-driven cleavage of PAR1 performs important functions in normal physiology is yet to be determined. It is possible that aberrant expression and exposure to proteases (*e.g.* MMP-13) in the pathological setting pre-disposes to cryptic cleavages. Additional studies are needed to fully understand the normal role of these signaling pathways, if any.

The therapeutic implications of our results suggest that direct PAR1 inhibitors in the treatment of in-stent restenosis are likely to result in net outcomes that are detrimental to the remodeling process. Furthermore, development of specific MMP inhibitors is expected to have an important therapeutic impact on the restenosis field.

Hepatic Steatosis

We have shown that PAR1 signaling influences cellular differentiation and phenotype in the cardiovascular system. Additionally, PAR2 activation also appears to induce differentiation and activation of hepatic stellate cells (HSCs).[70] HSCs are the major producers of collagen in the injured liver. Furthermore, activation also results in production of an array of cytokines that promote a hyper-inflammatory environment that recruits macrophages, neutrophils, and other inflammatory mediators. Using a specific cell penetrating PAR2 antagonist pepducin, PZ-235, we showed a reduction in hepatic fat accumulation, serum ALT levels, and overall NASH activity scores. Furthermore, PZ-235 inhibited PAR2-dependent signaling and MCP-1 secretion immortalized HSCs.

Our results indicate that PAR2 inhibition may protect against the development of steatosis and inflammation of the liver. But, a lingering question remains: what is the PAR2-activating protease in the liver? Studies have shown mast cell influx into the liver following injury, suggesting that mast-cell tryptase is one possibility. Interestingly, a recent report revealed that a broad-spectrum serine protease inhibitor, bovine pancreatic trypsin inhibitor (aprotinin), protected against acute liver injury in carbon tetrachloride-induced models of liver fibrosis, suggesting that perhaps serine proteases are more prevalent throughout the injured liver than previously thought.[238] Furthermore, protease profiling of the liver showed that a disintegrin and metalloprotease with thrombospondin type-1 motif-1 (ADAM TS-1) was up-regulated in human liver fibrosis samples,[239] although ADAM TS-1 cleavage of PAR2 has not been reported.

IV.2 Strengths and Weaknesses

IV.2.1 Chapter 2.

Given the prevalence of cardiovascular disease and percutaneous interventions in Western populations, every effort was taken to incorporate translational approaches in order to recapitulate human disease. Additionally, results were often confirmed in numerous cell lines to avoid cell-line specific results. On that same note, primary cells were used, when available, to closely mimic SMCs from the blood vessel wall.

MMP inhibitors are notorious for cross-reactivity with other metalloprotease family members. To determine that the majority of the effects seen *in vivo* with FN-439 were due to MMP-1 inhibition, we performed DQ-collagenase assays to define the percent inhibition of the other two collagenase family members, MMP-8 and MMP-13. FN-439 had no appreciable effect on MMP-8 activity, and only partially blocked (~36%) MMP-13 activity. We therefore feel confident that our results represent MMP1-PAR1 signaling in the injured vasculature.

The use of animal models can often be a shortcoming when modeling human disease; we utilized the most widely accepted methods currently available. With that said, in-stent restenosis occurs in the context of diseased arteries. Our mouse model injures previously normal carotid arteries, and thus may no represent the full extent of the pre-existing inflammatory state that is present in atherosclerotic vasculature. It is possible that to completely mirror the human disease animals with previously diseased blood vessels (*ApoE*$^{-/-}$) should be employed.

IV.2.2 Chapter 3.

NAFLD/NASH represent a complex spectrum of disease that is difficult to model *in vivo.* Use of the MCD diet has been shown to closely mimic the human disease, and thus was used for our studies. Despite MCD's ability to recreate NAFLD/NASH in mice, it does not fully recapitulate a number of the metabolic and chemokine changes observed in humans.[190] Furthermore, the mice lose up to 30% of their total bodyweight while on the diet, which is in stark contrast to the human NAFLD/NASH population, which is undoubtedly obese. Recent studies have suggested that leptin-deficient mice (*ob/ob*) on MCD show the histological features of NASH while maintaining an overweight phenotype and future studies should consider the use of these animals.[190]

Surprisingly, PAR2 inhibition, both by PZ-235 and genetic deletion, resulted in smaller liver-size following 3 weeks on MCD diet. Methionine-choline deficient diets lead to free fatty acid accumulation and decreased VLDL production and secretion. The MCD diet also leads to cachexia; we observed a 20% decrease in body weight over 3 weeks in all groups. In addition to decreased body weight, we found that the PZ-235 and *Par2*$^{-/-}$ animals had a statistically significant decrease in liver weight compared to body weight, suggesting that they were disproportionately losing more liver mass than vehicle treated animals. It has been reported that MCD diet inhibits ERK1/2 activation in hepatocytes, which sensitizes them to TGF-β induced apoptosis. [240] Given that PZ-235 and *Par2* knockout animals showed decreased liver weights at 3 weeks, it is possible that PAR2 signaling works to antagonize this pathway in hepatocytes and that pharmacologic inhibition or genetic deletion can encourage hepatocyte apoptosis, leading to disproportionate decreases in liver size.

IV.3 Future Directions

We determined that MMP1-PAR1 signaling results in de-differentiation of SMCs and maladaptive vascular remodeling. Additionally, we found that thrombin-PAR1 activation couples to G_i dependent pathways in SMCs. Future studies should focus on the G protein pathways associated with MMP1-PAR1 signaling. Utilization of dominant-negative G protein constructs and blocking antibodies would be useful reagents for these studies. The observation that MMP-13 is capable of cleaving PAR1 on cardiomyocytes provokes the idea that a similar pathway could exist in SMCs. Since FN-439 inhibits approximately 36% of MMP-13 collagenase activity, it is possible that a component of FN-439's effect on neointima formation is due to MMP-13 inhibition. Additional studies should investigate the contribution of MMP13-PAR1 signaling to SMC phenotypic switching and neointima formation.

NAFLD studies are still in progress. Because the effect of PZ-235 on liver steatosis was more pronounced with early treatment, there has been renewed focus to understanding the mechanism of this effect. First, we will be investigating the effect of *Par2*-deficiency in 2-week models of MCD. To investigate the role of PAR2 and PZ-235 treatment in liver fibrosis, we have initiated a carbon tetrachloride-induced fibrosis model in which mice will be treated daily for 8 weeks with either vehicle or PZ-235 (10 mg/kg). Additional studies will attempt to mimic clinical recommendations for dietary modification; mice will be placed on MCD diet for 3 weeks, followed by 2 weeks of regular chow with concurrent treatment with either vehicle or PZ-235 (10 mg/kg).

PZ-235 treatment did not appear to affect hepatic stellate cell activation *in vivo*, despite previous studies suggesting PAR2 activation on HSCs is a contributing factor to disease progression. It is possible that PZ-235 affects PAR2 activation on alternate cell types, including Kuppfer cells (liver macrophages) or oval cells (hepatic progenitor cells).

To understand the mechanism of PZ-235's effect on steatosis, we will be interrogating PAR2 activation on these cell types.

IV.4 Final Remarks

This thesis highlights the important role of protease-activated receptor signaling following vascular and hepatic injury. Emerging evidence suggests that this class of receptors participates in a plethora of disease and physiologic states, and continued research is needed to understand the intricate mechanistic nuances between receptors. Here, we have provided critical evidence to suggest that direct PAR1 inhibitors are unlikely to produce predictable and beneficial effects in patients with in-stent restenosis. Instead, revitalization of research into MMP-specific inhibitor drug development may prove more beneficial.

V. Appendix

V.1 Genetic deletion of *Mmp-1a* reduces atherosclerotic plaque burden in *ApoE*$^{-/-}$ mice on high-fat diet

V.1.1 Rationale

Studies have suggested that the mouse homologue of MMP-1, Mmp-1a, has reduced expression in normal tissues but is up-regulated in overt pathological disease.[241] Previous work from our lab has shown that systemic inhibition of Mmp-1a with FN-439 reduces plaque burden in mouse models of atherosclerosis (G.Koukos; unpublished data). To further investigate the role of Mmp-1a in plaque formation, we obtained *Mmp-1a*$^{-/-}$ mice from the laboratory of Dr. Lopez-Otin and bred them onto an *ApoE*$^{-/-}$ background, which is a well-established model for atherosclerotic plaque formation in animals fed a high fat diet. *Mmp-1a*$^{-/-}$ *,ApoE*$^{-/-}$ double knock-out and *ApoE*$^{-/-}$ knockout animals were placed on a high fat diet for 16 weeks, and the thoracic and abdominal aortas were analyzed for atherosclerotic plaque burden.

V.1.2 Methods

Atherosclerosis mouse model

Both wild-type and *Mmp1a* $^{-/-}$ four-week old male C57BL/6 mice (n=7-8) were placed on high fat (21%) Western diet (HFD:Opensource, #D12079B) for 16 weeks. Animal weights and serum samples were taken weekly while on HFD. At the end of 16 weeks, animals were anesthetized using isoflurane and the chest was opened and retracted. The animal was perfused with PBS through insertion of a 25 gauge needle attached to a pressurized perfusion bag into the left ventricle of the heart. The animal was perfused for approximately 1 minute at which point the aorta was dissected out and fixed in 10%

buffered formalin followed by separation into the thoracic arch and abdominal iliac regions. The arteries were then mounted and splayed for *en face* Oil-red-O staining. Percent lesion area was calculated using ImageJ software.

Oil-red-O en face staining

Formalin fixed aortas were cleaned to removed fat and adventitia. The aorta was then cut open on the ventral side and pinned into place. The aortas were stained for 30 min at room temperature with a 6:4 dilution of oil-red-O (0.2% w/v 2-propanol stock) to water. The samples were then de-stained with 70% ethanol and gentle agitation. Aortas were rinsed with water and images were taken. Images were analyzed using ImageJ software.

Immunofluorescence

Carotid arteries were embedded in OTC medium and flash frozen. Eight-micron sections were cut using a cryostat, and 3 sequential sections were placed on each slide. Slides were subsequently blocked for 1 hour at room temperature with 2% bovine serum albumin (BSA)/0.5% Triton X-100 in PBS. Slides were washed with 2% BSA/PBS and incubated overnight at 4° C with primary antibody (PECAM 1:400; Mmp-1a 1:100). A Mmp-1a blocking peptide was used as a control for specificity. Slides were washed 3 times with Tris buffered saline with 1% Tween (TBST) x 5 min and then incubated with a fluorescent-conjugated secondary antibody (1:400) for 1 h at room temperature in the dark, followed by washing with TBST. Samples were stained with DAPI (1:5000) for 5 min at room temperature. Slides were mounted using vectashield (Vector Labs).

V.1.3 Results

Human atherosclerotic plaques express a variety of MMPs, although MMP-1 expression is prominent in the plaque body and fibrous cap region.[141, 207] To determine if the mouse homologue of MMP-1, Mmp-1a, was also a important feature of murine plaques, we performed immunofluorescence on carotid artery plaques from *ApoE* $^{-/-}$ male mice fed a high-fat diet (HFD) for 16 weeks. Carotid arteries were removed and sectioned for histology. H&E staining showed large occlusive plaques with regions of necrosis and recanalization (**Figure 5.1**). Immunofluorescence staining for Mmp-1a and PECAM (CD31) revealed robust Mmp-1a expression, present in both the plaque body and endothelium (**Figure 5.1**). Wild-type vessels had little Mmp-1a, consistent with reports that it is critically up-regulated primarily in diseased states.

To determine whether Mmp-1a promoted plaque progression, as has been suggested for human plaques, four-week old male C57BL/6 mice on either a *ApoE* $^{-/-}$ or *ApoE*$^{-/-}$ *Mmp1a*$^{-/-}$ were fed a HFD for 16 weeks and plaque burden was scored based on Oil-red-O staining. Oil-red-O staining of both the arch and iliac regions of the aorta showed decreased fat accumulation in the *ApoE*$^{-/-}$*;Mmp1a*$^{-/-}$ animals that approached significance for the iliac region (**Figure 5.2**). Additionally, at the end of 16 weeks we observed no statistical difference in body weight between the two cohorts (**Figure 5.2**). These data suggest a role for Mmp-1a in plaque incidence and progression in mouse models of atherosclerosis. Unpublished work from our lab has also shown that Mmp-1a inhibition with FN-439 reduces plaque burden, and that Mmp-1a is likely working through PAR1 to propagate a number of its effects (G. Koukos, unpublished data).

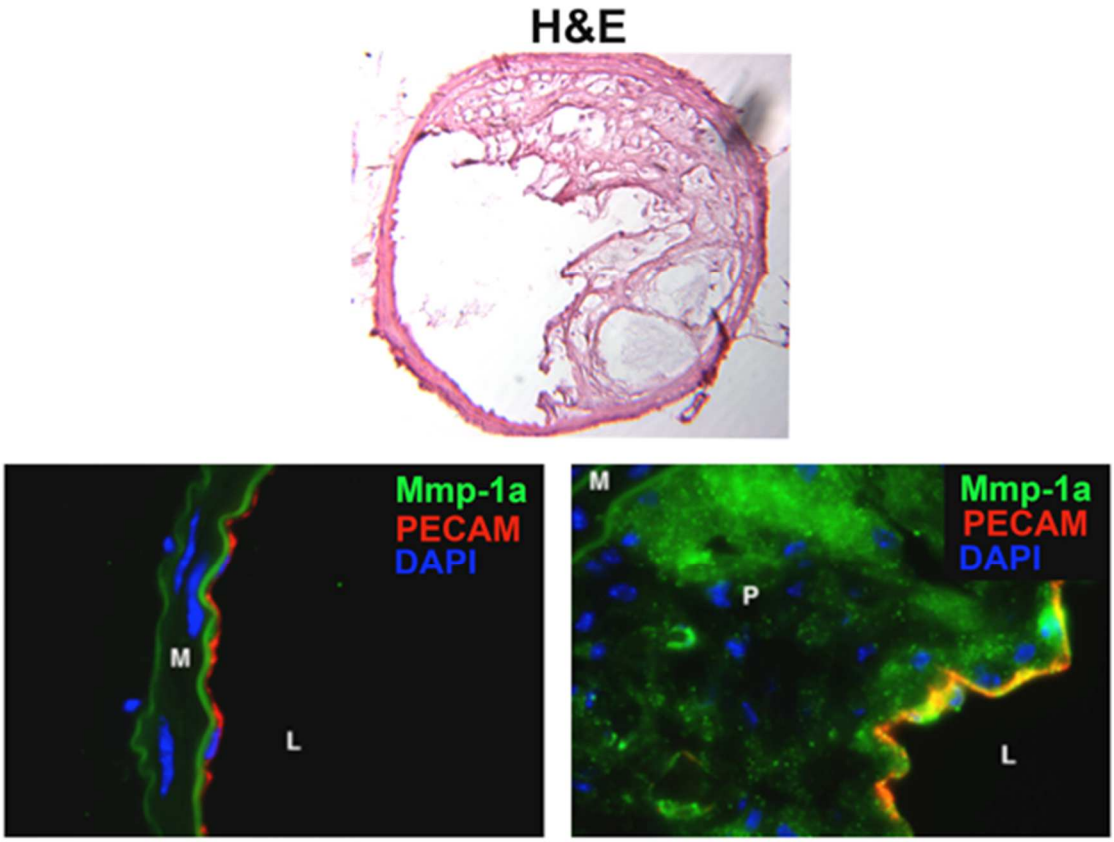

Figure 5.1. Mmp-1a expression in murine atherosclerotic plaques. (Top) Representative H&E stain of a carotid artery from *ApoE*$^{-/-}$ mice placed on HFD for 16 weeks. **(Bottom)** Immunofluorescence of Mmp-1a and PECAM (CD31) in a normal blood vessel (left) and atherosclerotic plaque (right) from *ApoE*$^{-/-}$ mice placed on HFD for 16 weeks. Mmp-1a staining was prominent in the plaque body and endothelium (colocalization with CD31). Lumen: L; media: M; plaque: P. (Done in collaboration with G. Koukos, PhD)

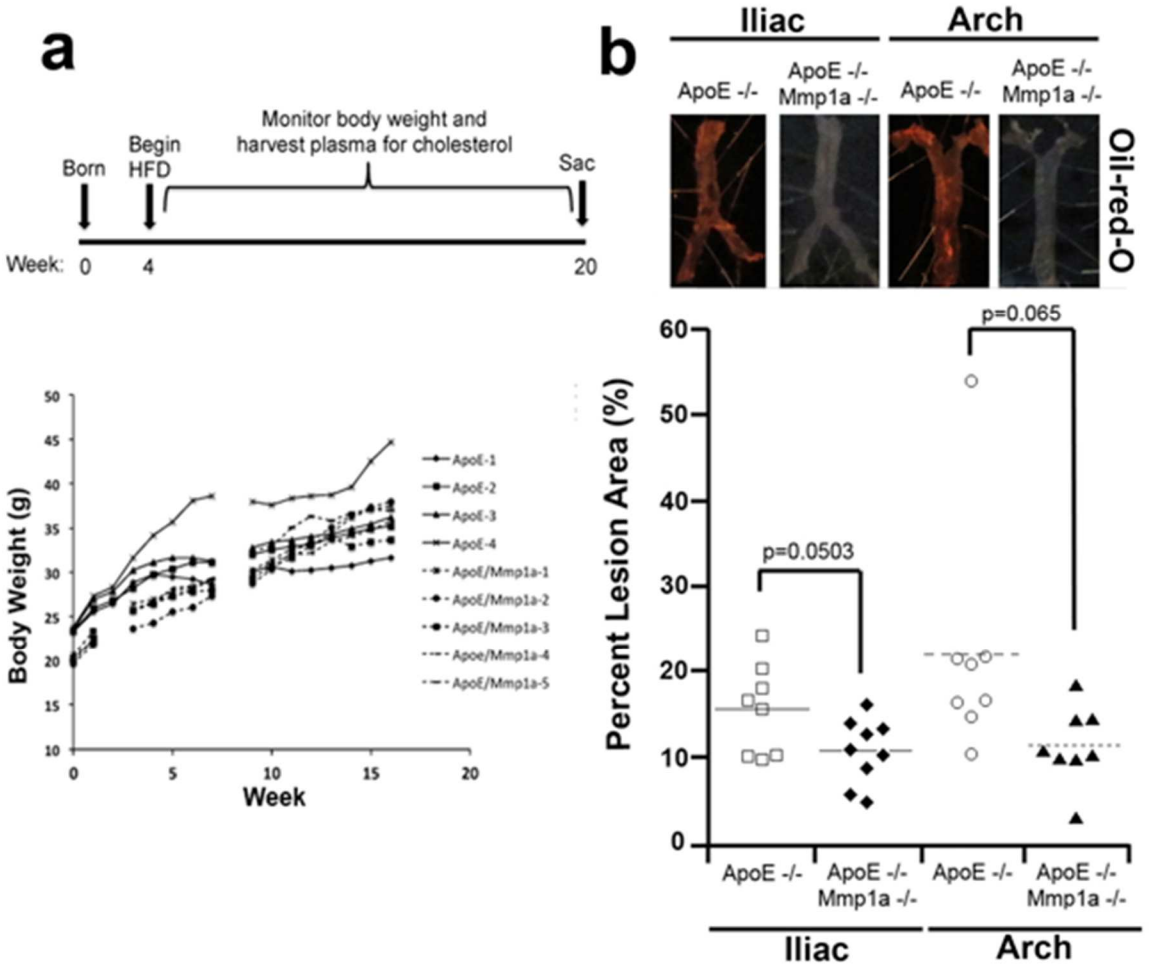

Figure 5.2. *ApoE$^{-/-}$;Mmp-1a$^{-/-}$* mice show a trend towards decreased atherosclerotic plaque burden in mouse models. (A) (Top): Schematic of animal model. (Bottom): Body weights of individual mice on high-fat diet over 16 weeks. **(B)** (Top): Oil-red-O staining from the iliac and arch regions of the aorta. (Bottom): Quantification of plaque burden by percent lesion area over the entire aorta. (n=8) (Done in collaboration with George Koukos, PhD)

V.1.4 Conclusions

Our data suggest that Mmp-1a, the mouse homologue of MMP-1 may play an important role in the development of atherosclerosis. Currently, our data are trending towards significance, especially in regards to the iliac bifurcation, therefore additional animals are needed to fully determine the importance of Mmp-1a in this process. Subsequent mechanistic studies will be performed to understand how genetic deletion of Mmp-1 ameliorates disease progression in mouse models of atherosclerosis.

Murine atherosclerotic plaques are notorious for their failure to rupture without physical disruption.[242] In humans, plaque rupture is often associated with an imbalance of matrix degradation compared to matrix deposition. [242] Furthermore, rupture in humans can lead to myocardial infarction and death, and therefore is the most worrisome feature of atherosclerosis. Our data suggest that murine MMPs, and in this case Mmp-1a, may play an alternate role in plaque development that is independent of its proteolytic function.

V.2 *Par2*, but not *Par1*, knock-out mice have defective collateral formation in models of critical limb ischemia

V.2.1 Rationale

Arteriogenesis, or collateral artery formation, represents a complex network events that results in the formation of new collateral vessels and restoration of perfusion to a previously ischemic area. Two areas of unmet need regarding arteriogenesis are peripheral artery disease (PAD) and extremity combat injury. [243] PAD refers to progressive vessel occlusion as a result of atherosclerotic lesion development. In the United States nearly 5% of people over the age of 40 suffer from PAD, with that number rising to between 15-20% in patients over 70.[244] Roughly 10% of patients present with intermittent claudication, while nearly one third have complete occlusion of a major lower-extremity artery as their presenting symptom.[245] Furthermore, critical limb injuries account for the majority of combat-related casualties, highlighting the importance of mechanistic studies aimed at understanding collateral formation. [243]

We sought to determine whether PAR1 and PAR2 contribute to arteriogenesis and limb reperfusion. We utilized a mouse model of hind limb ischemia (HLI) whereby the femoral artery was severed in the upper thigh to cause an immediate ischemic crisis. We then interrogated perfusion to the injured limb in wild-type, *Par1*$^{-/-}$, and *Par2*$^{-/-}$ mice over time. Our data indicate that Par2, but not Par1, plays a role in collateral formation following critical limb ischemia.

V.2.2 Methods

Cell Culture

An endothelial cell line hybridized to the lung cancer cell line A549 (EAhy549) and two SMC lines (CD314 and RAD542) were maintained in DMEM supplemented with 10% FBS and 1% penicillin/streptomycin in 5% CO_2 (normoxia: 20% O_2) at 37 °C or in a hypoxia chamber 5% CO_2 0.2% O_2 at 37 °C for either 8 or 24 h.

Hind limb ischemia model

Six to eight week old C57BL/6 mice were anesthetized with an isoflurane nebulizer and nose-cone. The left thigh region of the animal was shaved with electric clippers and the area was sterilized using 3 alternating passes of iodine and ethanol swabs. Using sterilized instruments an incision was made in the upper left thigh and the femoral vein, artery and nerve were exposed. Through careful blunt dissection, the femoral sheath was dissected and the artery was isolated. Two 6-0 silk sutures were used to tie off the femoral artery approximately a quarter centimeter apart. The femoral artery was then severed between the sutures. The animal was closed and sutured using 6-0 nylon sutures, and given 0.05 mg/kg buprenorphine for pain management. Animals were allowed to recover from anesthesia in individual cages placed on warmed heating pads. Once animals were recovered they were monitored every few hours for the first day, and daily from that point on. Hind limb perfusion was monitored using a Moor Instruments laser Doppler imager (physically located at St. Elizabeth's Hospital, Brighton, MA). Perfusion was reported as the mean perfusion in the injured versus non-injured paw.

Reverse transcriptase quantitative PCR (RT-qPCR)

Total RNA was extracted using the RNeasy mini kit (Qiagen) and 1-2 μg of RNA was reverse transcribed into cDNA using Moloney murine leukemia virus (MMLV) reverse transcriptase as described below. Random oligomers (10-15 bases) (Oligo dT; Invitrogen) were annealed at 72 °C for 10 min, followed by 40 cycles of: 25 °C for 15 min, 37 °C for 60 min, 95 °C for 5 min, 4 °C for 5 min. Quantitative PCR was conducted in 25 μL volumes with 12.5 μL SYBR Green master mix (Invitrogen) and 1.25 μL of both forward and reverse primers (5 μM). All reactions were performed in triplicate and run on a DNA Engine Opticon 2, Continuous Fluorescence Detector (MJ Research). qPCR program consisted for 40 cycles of the following: 95 °C for 15 s, 55 °C for 20 s, and 72 °C for 15 s. Primers are listed in Table 5.1

Table 5.1 Primers for RT-qPCR

Gene	Gene ID	Accession No.	Primer Pairs (5' ➔ 3')
VEGF-A(5)	VEGFA	NM_001171627.1	F- *AGAGCAAGACAAGAAAATCCC* R- *AACGCGAGTCTGTGTTTTTG*
PAR1	F2R	NM_001992.3	F- *GTTTGGGTCTGAATTGTGTCGC* R- *GGACTGCATGGGATACACCA*
PAR2	F2RL	NM_005242.4	F- *GCACCATCCAAGGAACCAATAG* R- *TTTCCAGTGACGTGGGATGTG*
MMP-1	MMP1	NM_002421.3	F-*TGTCAGGGGAGATCATCGGGACA* R- *CCCCTCCAATACCTGGGCCTGG*

V.2.3 Results

V.2.3.1 Par2, not Par1, knock-out mice have impaired collateral formation

Six to eight-week old female wild-type, *Par1*$^{-/-}$, or *Par2* $^{-/-}$ C57BL/6 mice were observed for collateral formation and reperfusion in models of HLI. Left femoral arteries were ligated and severed as described above. Animals were monitored by laser Doppler flow of the lower limbs starting 24 h following surgery and up to 16 d after. *Par2* $^{-/-}$ animals showed delayed perfusion to the injured limb, compared to the contralateral control paw, which became significant at 16 days (**Figure 5.3a,b**). In contrast, *Par1*$^{-/-}$ mice did not exhibit significant delays in reperfusion, and tracked with their wild-type counterparts for the extent of the experiment (**Figure 5.4a,b**).

V.2.3.2 Increased PAR2 expression under hypoxic conditions

We then investigated whether PAR expression levels were changed under hypoxic conditions in endothelial-derived cells and SMCs. RT-qPCR was performed on cells incubated for either 8 or 24 h in hypoxic conditions. In endothelial-derived EAhy926 cells, expression of the pro-angiogenic factor, VEGF-A was increased, as would be expected, but we also saw significant decreases in both PAR1 and PAR2 expression 24 h (**Figure 5.5**). In contrast, SMCs (RAD542 and CD314) showed up-regulation of PAR2 expression after exposure to hypoxic conditions (**Figure 5.5**). These data indicate that perhaps PAR2 on SMCs is an important factor following ischemic injury.

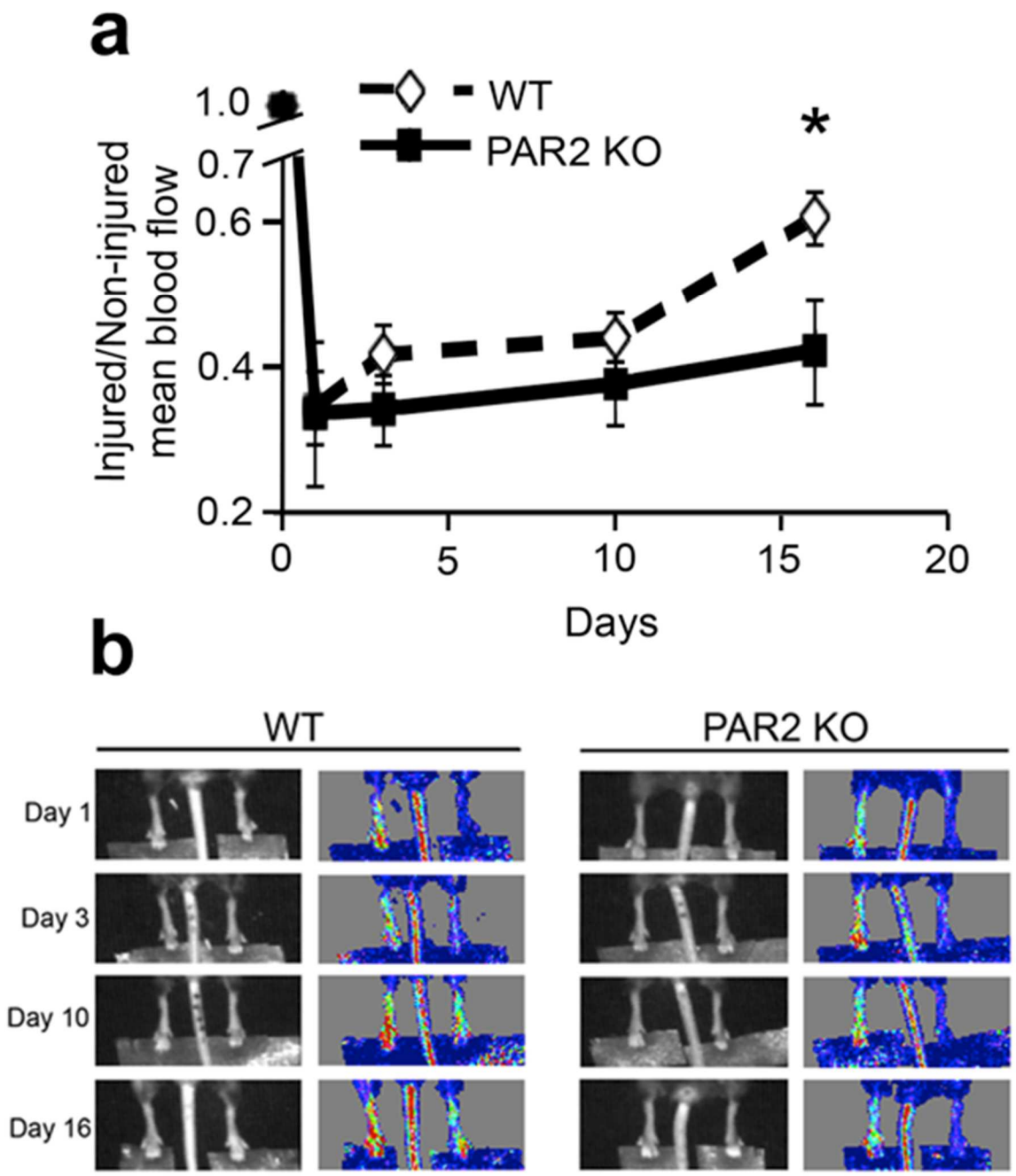

Figure 5.3. *Par2* knock-out mice show significant delays in collateral formation in models of HLI. (a) Ratio of mean blood flow in the injured versus non-injured limb in wild-type (WT) and *Par2*$^{-/-}$ (PAR2 KO) mice (n=10) up to 16 d following femoral artery ligation. **(b)** Representative photographs of hind limb perfusion in wild-type (WT) and *Par2*$^{-/-}$ (PAR2 KO) mice over the course of the experiment from (a). * $p<0.05$ by ANOVA followed by Student-Newman-Keuls post-test.

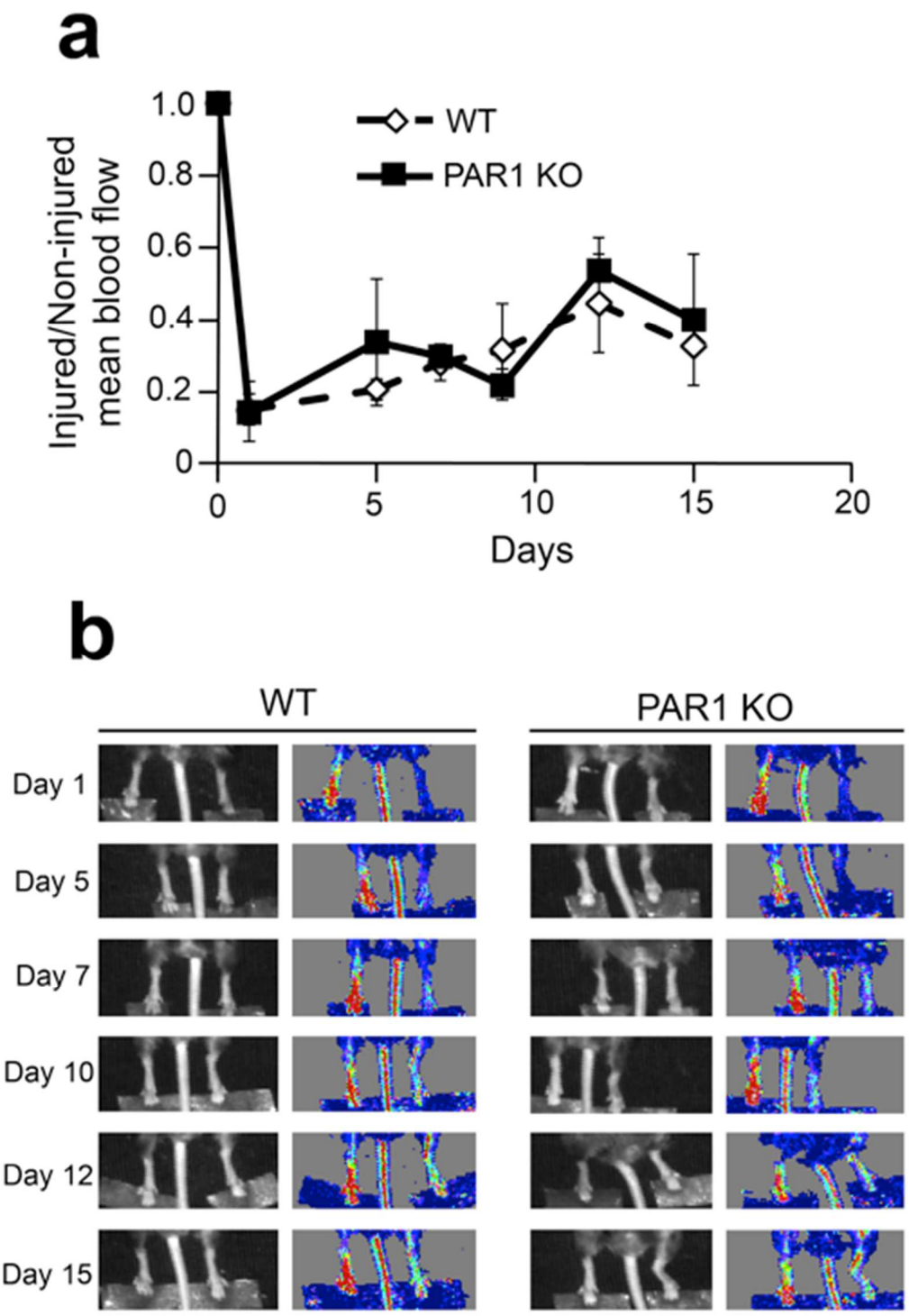

Figure 5.4. *Par1*-deficiency has no effect on collateral formation in models of HLI. **a)** Ratio of mean blood flow in the injured versus non-injured limb in wild-type (WT) and *Par1*$^{-/-}$ (PAR1 KO) mice (n=4-5) up to 15 d following femoral artery ligation. **(b)** Representative photographs of hind limb perfusion in wild-type (WT) and *Par1*$^{-/-}$ (PAR1 KO) mice over the course of the experiment from (a).

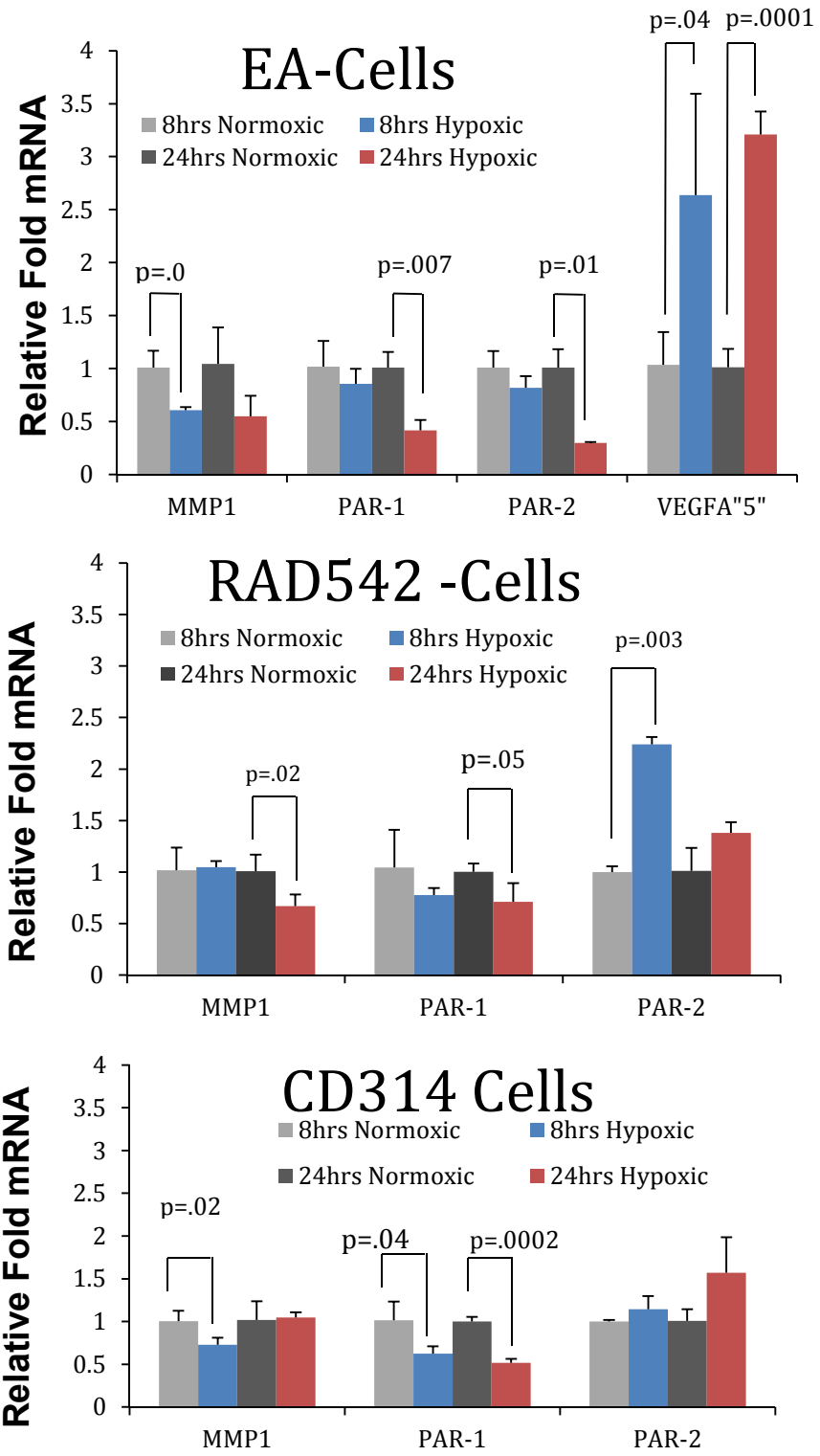

Figure 5.5. RT-qPCR of PAR1 and PAR2 under hypoxic conditions. Relative fold mRNA levels of MMP-1, PAR1, PAR2, and VEGF-A in endothelial (EA) or smooth muscle (RAD542 and CD314) cells grown for either 8 or 24 h in normoxia (20% O_2) or a hypoxia chamber (0.2% O_2). Statistical analysis was performed using ANOVA followed by Student-Newman-Keuls post-test. (Done in collaboration with Andrew Shearer).

V.2.4 Conclusions

Here, we show that Par2, but not Par1, is important for collateral formation following hind limb ischemia in mice. Additionally, increased PAR2 expression on SMCs following hypoxia suggests that SMC-derived PAR2 may contribute to collateral formation *in vivo*. Conversely, PAR1 expression was reduced in all cells following hypoxia, consistent with our observation that *Par1* knock-out mice showed not discernable defect in limb reperfusion out to 15 d. This result is somewhat surprising since *Par1*$^{-/-}$ mice show approximately 50% embryonic lethality, which is corrected by re-expression in endothelial cells, suggesting that loss of Par1 affects endothelial and vascular development.[14] It is possible that surviving *Par1*$^{-/-}$ mice have compensated for this vascular defect and do not accurately represent true *Par1*-deletion in the vasculature. In contrast, *Par2*-deficiency showed a marked reduction in limb reperfusion by day 16. Previous studies have shown that treatment with a PAR2 activating peptide increased capillarity and restored reparative hemodynamics in models of critical limb ischemia.[246] Our results confirm these studies and provide additional evidence to support the critical role of PAR2 in collateral formation.

Future experiments will be aimed at understanding the mechanism of PAR2's effect on collateral formation. Additionally, studies should be undertaken to identify the PAR2-activating protease during critical limb ischemia and reperfusion.

V.3 Thrombin-PAR1 signaling in vascular smooth muscle cells results in increased MMP-1 expression and secretion.

V.3.1 Rationale

We have shown that non-canonical MMP1-PAR1 activation on SMCs is promotes cellular de-differentiation and leads to arterial restenosis (see Chapter 1). Studies have shown that thrombin-PAR1 signaling results in increased MMP expression. Specifically, PAR1 activation in human chondrosarcoma cells increases expression of both MMP-2 and MMP-13.[247] Additionally, thrombin has been shown to induce MMP-9 expression in osteosarcoma cells to promote tumor migration and invasion.[248] To determine if a similar pathway functioned in SMCs, we investigated whether MMP expression was up-regulated following thrombin stimulation. We found that thrombin-triggered activation of PAR1 resulted in increased MMP-1 expression and release from SMCs. Furthermore, secreted MMP-1 functioned in a paracrine (and most likely autocrine) manner to promote PAR1-driven SMC migration.

V.3.2 Methods

Coomassie Staining

CD314 SMCs were treated with 1 nM thrombin or vehicle and conditioned media was harvested at the time points indicated. Forty microliters of conditioned media was run on a 12% SDS-PAGE gel and stained with 0.25% Coomassie brilliant blue G-250 stain (50% methanol/10% acetic acid) for 2 h at room temperature. The gel was then de-stained with 40% methanol/10% acetic acid.

MMP Zymography

CD314 cells were treated with 5 nM thrombin with or without 5 μM RWJ-56110 and conditioned media was harvested at the time points indicated. Forty microliters of conditioned media was then run on a 10% SDS-PAGE gel with 1 mg/mL collagen without the addition of 2-β mercaptoethanol to the sample buffer. The gel was then incubated in re-naturation buffer for 30 min at room temperature. MMP digestion was then allowed to proceed for 2 d at 37 °C in digestion buffer. The gel was then Coomassie stained as described above.

RT-qPCR

Total RNA was extracted using the RNeasy mini kit (Qiagen) and 1-2 μg of RNA was reverse transcribed into cDNA using Moloney murine leukemia virus (MMLV) reverse transcriptase as described below. Random oligomers (10-15 bases) (Oligo dT; Invitrogen) were annealed at 72 °C for 10 min, followed by 40 cycles of: 25 °C for 15 min, 37 °C for 60 min, 95 °C for 5 min, 4 °C for 5 min. Quantitative PCR was conducted in 25 μL volumes with 12.5 μL SYBR Green master mix (Invitrogen) and 1.25 μL of both forward and reverse primers (5 μM). All reactions were performed in triplicate and run on a DNA Engine Opticon 2, Continuous Fluorescence Detector (MJ Research). qPCR program consisted for 40 cycles of the following: 95 °C for 15 s, 55 °C for 20 s, and 72 °C for 15 s. **MMP-1 primers**: Forward-*TGTCAGGGGAGATCATCGGGACA*, Reverse-*CCCCTCCAATACCTGGGCCTGG.*

Immunofluorescence

CD314 cells were plated on poly-L-lysine coated glass coverslips and allowed to adhere overnight. Cells were then serum starved with 0.1%FBS/DMEM for 16 h. Cells were then treated with 5 nM thrombin and incubated at room temperature for 30 min. The

coverslips were then fixed and stained as described above. MMP-1 antibody (linker; 1:200); FITC secondary (1:400), DAPI (1:5000).

Migration

CD314 cells were treated with 5 nM thrombin with or without 5 μM RWJ-56110 for 60 h at which point conditioned media was harvested and used as chemo-attractant. A portion of conditioned media was used for Western blot analysis of secreted MMP-1. For migration, CD314 cells were placed in Boyden chambers with the previously mentioned conditioned media in the lower well. The cells were allowed to migrate for 16 h, when the membranes were stained and counted.

V.3.3 Results

V.3.3.1 Thrombin-stimulation influences SMC protein secretion.

Following initial vessel injury, thrombin is generated due to the exposure of sub-endothelial tissue factor, but is quickly inactivated by anti-thrombin III, although studies have suggested that atherosclerotic plaques may be a reservoir for thrombin in the diseased blood vessel.[249] To understand the interaction between acute thrombin exposure on SMCs we treated CD314 cells with 5 nM thrombin with and without 5 μM RWJ-56110 and harvested conditioned media up to 60 h after treatment (**Figure 5.6**). SMCs treated with thrombin for more than 48 h showed a marked increase in the number of secreted products suggesting that acute thrombin stimulation modifies the SMC secretome (**Figure 5.6**).

V.3.3.2 Thrombin-PAR1 signaling stimulates MMP-1 expression and secretion in SMCs

To determine if thrombin treatment affected expression of MMPs, we performed collagen zymography on conditioned media from SMCs treated with thrombin for 24 to 60 h. SMCs constitutively express MMP-2, which was present at all time points tested (upper bands; **Figure 5.7a**). Surprisingly, there was a dramatic increase in MMP-1 secretion (54 kD doublet), which was blocked by RWJ-56110 pre-treatment (**Figure 5.7a**). This effect was seen at both 48 and 60 h.

We next confirmed increased MMP-1 gene expression in SMCs following thrombin stimulation by RT-qPCR. Both immortalized and primary SMCs treated with thrombin showed increased MMP-1 expression that was sensitive to PAR1 inhibition (**Figure 5.7b**). We then postulated that SMCs treated with thrombin were both increasing expression of MMP-1 and inducing MMP-1 secretion. Immunofluorescence analysis of

intracellular MMP-1 showed a diffuse staining pattern 30 min following thrombin stimulation compared to untreated cells, suggesting that MMP-1 vesicles are trafficked to the cell surface upon PAR1 activation in SMCs (**Figure 5.7c**).

Finally, we determined the functional significance of MMP-1 secretion from SMCs. CD314 cells were treated with 5 nM thrombin, with and without 5 μM RWJ-56110, and conditioned media was harvested 60 h following treatment. The presence of MMP-1 protein in the conditioned media was confirmed by Western blot analysis (**Figure 5.7d**). The conditioned media was then used in the lower well of Boyden chambers as a chemo-attractant for SMCs in 16 h migration assays. As predicted from our results in Chapter 1, SMCs migrated towards the conditioned media harboring the most MMP-1 (**Figure 5.7d**). Conditioned media that had been treated with RWJ-56110 produced less MMP-1 and subsequently resulted in decreased migration.

V.3.4 Conclusions

We have shown that thrombin-PAR1 signaling stimulates MMP-1 expression and secretion in SMCs. Furthermore, the released MMP-1 functions as a potent chemo-attractant for SMCs through a PAR1 dependent pathway, suggesting that MMP1-induced migration functions in both an autocrine and paracrine manner. These data imply that initial vascular injury results in acute thrombin production, which can subsequently lead to increased MMP-1 levels in the injured vessel. Based on our previous work from Chapter 1, this would predict that continued thrombin generation eventually becomes deleterious due to production of MMP-1 and its detrimental effects on SMC phenotype.

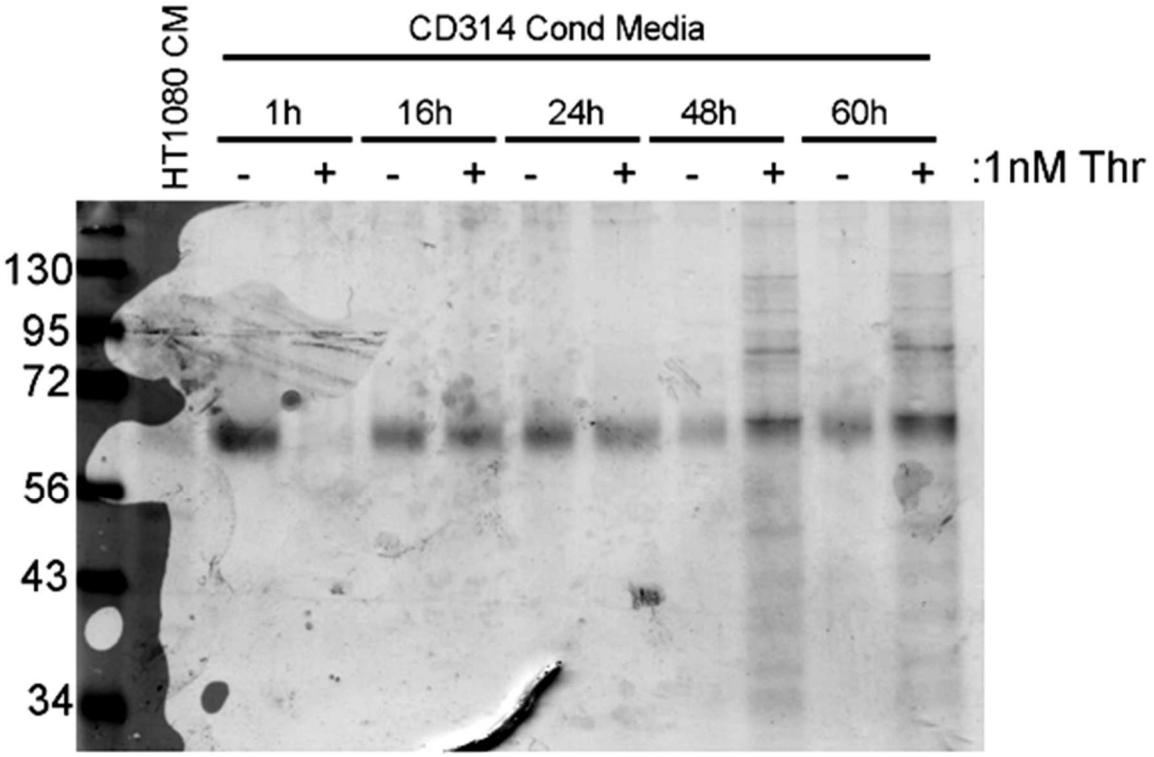

Figure 5.6. Coomassie gel of the SMC secretome following thrombin stimulation. Conditioned media from CD314 cells treated with 1 nM thrombin for the time points indicated run on a 12% SDS-PAGE gel and stained with Coomassie. HT1080 fibrosarcoma cell conditioned media was used as non-SMC control.

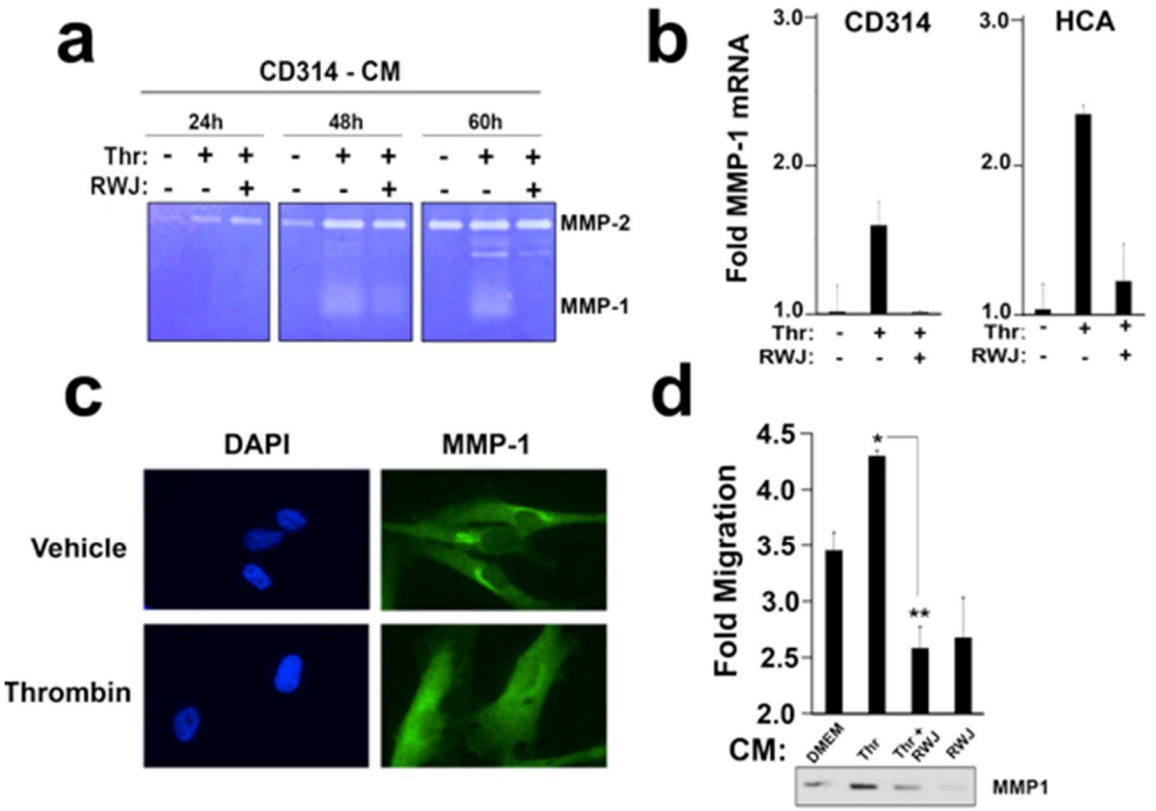

Figure 5.7. Thrombin-PAR1 signaling results in increased MMP-1 expression and secretion in SMCs. (a) Collagen zymography gel of CD314 conditioned media (CM) 24, 48, and 60 h after 5 nM thrombin treatment with and without 5 μM RWJ-56110 treatment. **(b)** RT-qPCR of MMP-1 in SMCs following 24 h treatment with 5 nM thrombin with and without 5 μM RWJ-56110. **(c)** Immunofluorescence of intracellular MMP-1 in SMCs treated with 5 nM thrombin for 30 min. **(d)** 16 h migration of CD314 towards conditioned media from cells treated with agonists indicated (5 nM thrombin, 5 μM RWJ-56110) for 60 h. * $p<0.05$; ** $p<0.01$ by ANOVA followed by Student-Newman-Keuls post-test.

VI. References

1. Adams MN, Ramachandran R, Yau M-K, Suen JY, Fairlie DP, Hollenberg MD, Hooper JD. Structure, function and pathophysiology of protease activated receptors. *Pharmacol Ther*. 2011;130:248-282

2. Katritch V, Cherezov V, Stevens RC. Structure-function of the g protein-coupled receptor superfamily. *Annu Rev Pharmacol Toxicol*. 2012

3. Hopkins AL, Groom CR. The druggable genome. *Nature reviews Drug discovery*. 2002;1:727-730

4. Southan C. A genomic perspective on human proteases. *FEBS Lett*. 2001;498:214-218

5. Ossovskaya VS, Bunnett NW. Protease-activated receptors: Contribution to physiology and disease. *Physiological Reviews*. 2004;84:579-621

6. Berndt MC, Phillips DR. Interaction of thrombin with platelets: Purification of the thrombin substrate. *Ann N Y Acad Sci*. 1981;370:87-95

7. Vu TK, Hung DT, Wheaton VI, Coughlin SR. Molecular cloning of a functional thrombin receptor reveals a novel proteolytic mechanism of receptor activation. *Cell*. 1991;64:1057-1068

8. Vu TK, Wheaton VI, Hung DT, Charo I, Coughlin SR. Domains specifying thrombin-receptor interaction. *Nature*. 1991;353:674-677

9. Liu LW, Vu TK, Esmon CT, Coughlin SR. The region of the thrombin receptor resembling hirudin binds to thrombin and alters enzyme specificity. *J Biol Chem*. 1991;266:16977-16980

10. Rasmussen SGF, Choi H-J, Rosenbaum DM, Kobilka TS, Thian FS, Edwards PC, Burghammer M, Ratnala VRP, Sanishvili R, Fischetti RF, Schertler GFX, Weis WI, Kobilka BK. Crystal structure of the human β2 adrenergic g-protein-coupled receptor. *Nature*. 2007;450:383-387

11. Santulli RJ, Derian CK, Darrow AL, Tomko KA, Eckardt AJ, Seiberg M, Scarborough RM, Andrade-Gordon P. Evidence for the presence of a protease-activated receptor distinct from the thrombin receptor in human keratinocytes. *Proc Natl Acad Sci U S A*. 1995;92:9151-9155

12. Vouret-Craviari V, Van Obberghen-Schilling E, Rasmussen UB, Pavirani A, Lecocq JP, Pouyssegur J. Synthetic alpha-thrombin receptor peptides activate g protein-coupled signaling pathways but are unable to induce mitogenesis. *Mol Biol Cell*. 1992;3:95-102

13. Nystedt S, Emilsson K, Wahlestedt C, Sundelin J. Molecular cloning of a potential proteinase activated receptor. *Proc Natl Acad Sci U S A*. 1994;91:9208-9212

14. Connolly AJ, Ishihara H, Kahn ML, Farese RV, Jr., Coughlin SR. Role of the thrombin receptor in development and evidence for a second receptor. *Nature*. 1996;381:516-519

15. Ishihara H, Connolly AJ, Zeng D, Kahn ML, Zheng YW, Timmons C, Tram T, Coughlin SR. Protease-activated receptor 3 is a second thrombin receptor in humans. *Nature*. 1997;386:502-506

16. Connolly TM, Condra C, Feng DM, Cook JJ, Stranieri MT, Reilly CF, Nutt RF, Gould RJ. Species variability in platelet and other cellular responsiveness to thrombin receptor-derived peptides. *Thromb Haemost*. 1994;72:627-633

17. Nakanishi-Matsui M, Zheng YW, Sulciner DJ, Weiss EJ, Ludeman MJ, Coughlin SR. Par3 is a cofactor for par4 activation by thrombin. *Nature*. 2000;404:609-613

18. Xu WF, Andersen H, Whitmore TE, Presnell SR, Yee DP, Ching A, Gilbert T, Davie EW, Foster DC. Cloning and characterization of human protease-activated receptor 4. *Proc Natl Acad Sci USA*. 1998;95:6642-6646

19. Kahn ML, Zheng YW, Huang W, Bigornia V, Zeng D, Moff S, Farese RV, Jr., Tam C, Coughlin SR. A dual thrombin receptor system for platelet activation. *Nature*. 1998;394:690-694

20. Kahn ML, Hammes SR, Botka C, Coughlin SR. Gene and locus structure and chromosomal localization of the protease-activated receptor gene family. *J Biol Chem*. 1998;273:23290-23296

21. Schmidt VA, Nierman WC, Feldblyum TV, Maglott DR, Bahou WF. The human thrombin receptor and proteinase activated receptor-2 genes are tightly linked on chromosome 5q13. *Br J Haematol*. 1997;97:523-529

22. Lee H, Hamilton JR. Physiology, pharmacology, and therapeutic potential of protease-activated receptors in vascular disease. *Pharmacol Ther*. 2012;134:246-259

23. Schmidt VA, Nierman WC, Maglott DR, Cupit LD, Moskowitz KA, Wainer JA, Bahou WF. The human proteinase-activated receptor-3 (par-3) gene. Identification within a par gene cluster and characterization in vascular endothelial cells and platelets. *J Biol Chem*. 1998;273:15061-15068

24. Macfarlane SR, Seatter MJ, Kanke T, Hunter GD, Plevin R. Proteinase-activated receptors. *Pharmacol Rev*. 2001;53:245-282

25. Seeley S, Covic L, Jacques SL, Sudmeier J, Baleja JD, Kuliopulos A. Structural basis for thrombin activation of a protease-activated receptor: Inhibition of intramolecular liganding. *Chemistry & Biology*. 2003;10:1033-1041

26. Jacques SL, LeMasurier M, Sheridan PJ, Seeley SK, Kuliopulos A. Substrate-assisted catalysis of the par1 thrombin receptor. Enhancement of macromolecular association and cleavage. *J Biol Chem*. 2000;275:40671-40678

27. Harris JL, Backes BJ, Leonetti F, Mahrus S, Ellman JA, Craik CS. Rapid and general profiling of protease specificity by using combinatorial fluorogenic substrate libraries. *Proc Natl Acad Sci U S A*. 2000;97:7754-7759

28. Nieman MT, Schmaier AH. Interaction of thrombin with par1 and par4 at the thrombin cleavage site. *Biochemistry*. 2007;46:8603-8610

29. Jacques SL, Kuliopulos A. Protease-activated receptor-4 uses dual prolines and an anionic retention motif for thrombin recognition and cleavage. *Biochem J*. 2003;376:733-740

30. Zhang C, Srinivasan Y, Arlow DH, Fung JJ, Palmer D, Zheng Y, Green HF, Pandey A, Dror RO, Shaw DE, Weis WI, Coughlin SR, Kobilka BK. High-resolution crystal structure of human protease-activated receptor 1. *Nature*. 2012;492:387-392

31. Audet M, Bouvier M. Restructuring g-protein- coupled receptor activation. *Cell*. 2012;151:14-23

32. McCoy KL, Traynelis SF, Hepler JR. Par1 and par2 couple to overlapping and distinct sets of g proteins and linked signaling pathways to differentially regulate cell physiology. *Mol Pharmacol*. 2010;77:1005-1015

33. Klages B, Brandt U, Simon MI, Schultz G, Offermanns S. Activation of g12/g13 results in shape change and rho/rho-kinase-mediated myosin light chain phosphorylation in mouse platelets. *J Cell Biol*. 1999;144:745-754

34. Kaneider NC, Leger AJ, Agarwal A, Nguyen N, Perides G, Derian C, Covic L, Kuliopulos A. 'Role reversal' for the receptor par1 in sepsis-induced vascular damage. *Nat Immunol*. 2007;8:1303-1312

35. Ishii K, Hein L, Kobilka B, Coughlin SR. Kinetics of thrombin receptor cleavage on intact cells. Relation to signaling. *J Biol Chem*. 1993;268:9780-9786

36. Loew D, Perrault C, Morales M, Moog S, Ravanat C, Schuhler S, Arcone R, Pietropaolo C, Cazenave JP, van Dorsselaer A, Lanza F. Proteolysis of the exodomain of recombinant protease-activated receptors: Prediction of receptor activation or inactivation by maldi mass spectrometry. *Biochemistry*. 2000;39:10812-10822

37. Nakayama T, Hirano K, Shintani Y, Nishimura J, Nakatsuka A, Kuga H, Takahashi S, Kanaide H. Unproductive cleavage and the inactivation of protease-activated receptor-1 by trypsin in vascular endothelial cells. *Br J Pharmacol*. 2003;138:121-130

38. Ishii K, Chen J, Ishii M, Koch WJ, Freedman NJ, Lefkowitz RJ, Coughlin SR. Inhibition of thrombin receptor signaling by a g-protein coupled receptor kinase. Functional specificity among g-protein coupled receptor kinases. *J Biol Chem*. 1994;269:1125-1130

39. Trejo J. Protease-activated receptors: New concepts in regulation of g protein-coupled receptor signaling and trafficking. *J Pharmacol Exp Ther*. 2003;307:437-442

40. Paing MM, Stutts AB, Kohout TA, Lefkowitz RJ, Trejo J. Beta -arrestins regulate protease-activated receptor-1 desensitization but not internalization or down-regulation. *J Biol Chem*. 2002;277:1292-1300

41. Bohm SK, Khitin LM, Grady EF, Aponte G, Payan DG, Bunnett NW. Mechanisms of desensitization and resensitization of proteinase-activated receptor-2. *J Biol Chem*. 1996;271:22003-22016

42. Leger AJ, Covic L, Kuliopulos A. Protease-activated receptors in cardiovascular diseases. *Circulation*. 2006;114:1070-1077

43. Lee H, Sturgeon SA, Jackson SP, Hamilton JR. The contribution of thrombin-induced platelet activation to thrombus growth is diminished under pathological blood shear conditions. *Thromb Haemost*. 2012;107:328-337

44. Veiga Cde S, Carneiro-Lobo TC, Coelho CJ, Carvalho SM, Maia RC, Vasconcelos FC, Abdelhay E, Mencalha AL, Ferreira AF, Castro FA, Monteiro RQ. Increased expression of protease-activated receptor 1 (par-1) in human leukemias. *Blood Cells Mol Dis*. 2011;46:230-234

45. Coughlin SR. Protease-activated receptors in hemostasis, thrombosis and vascular biology. *J Thromb Haemost*. 2005;3:1800-1814

46. Ruggeri ZM. Platelets in atherothrombosis. *Nature Med.* 2002;8:1227-1234

47. Zhang P, Gruber A, Kasuda S, Kimmelstiel C, O'Callaghan K, Cox DH, Bohm A, Baleja JD, Covic L, Kuliopulos A. Suppression of arterial thrombosis without affecting hemostatic parameters with a cell-penetrating par1 pepducin. *Circulation*. 2012;126:83-91

48. Trivedi V, Boire A, Tchernychev B, Kaneider NC, Leger AJ, O'Callaghan K, Covic L, Kuliopulos A. Platelet matrix metalloprotease-1 mediates thrombogenesis by activating par1 at a cryptic ligand site. *Cell*. 2009;137:332-343

49. Fressinaud E, Sakariassen KS, Rothschild C, Baumgartner HR, Meyer D. Shear rate-dependent impairment of thrombus growth on collagen in nonanticoagulated blood from patients with von willebrand disease and hemophilia a. *Blood*. 1992;80:988-994

50. Inauen W, Baumgartner HR, Bombeli T, Haeberli A, Straub PW. Dose- and shear rate-dependent effects of heparin on thrombogenesis induced by rabbit aorta subendothelium exposed to flowing human blood. *Arteriosclerosis*. 1990;10:607-615

51. Gast A, Tschopp TB, Baumgartner HR. Thrombin plays a key role in late platelet thrombus growth and/or stability. Effect of a specific thrombin inhibitor on thrombogenesis induced by aortic subendothelium exposed to flowing rabbit blood. *Arterioscler Thromb*. 1994;14:1466-1474

52. Okorie UM, Denney WS, Chatterjee MS, Neeves KB, Diamond SL. Determination of surface tissue factor thresholds that trigger coagulation at venous and arterial shear rates: Amplification of 100 fm circulating tissue factor requires flow. *Blood*. 2008;111:3507-3513

53. Griffin CT, Srinivasan Y, Zheng YW, Huang W, Coughlin SR. A role for thrombin receptor signaling in endothelial cells during embryonic development. *Science*. 2001;293:1666-1670

54. McGuire JJ, Dai J, Andrade-Gordon P, Triggle CR, Hollenberg MD. Proteinase-activated receptor-2 (par2): Vascular effects of a par2-derived activating peptide via a receptor different than par2. *J Pharmacol Exp Ther*. 2002;303:985-992

55. Wilcox JN, Rodriguez J, Subramanian R, Ollerenshaw J, Zhong C, Hayzer DJ, Horaist C, Hanson SR, Lumsden A, Salam TA, et al. Characterization of thrombin receptor expression during vascular lesion formation. *Circ Res*. 1994;75:1029-1038

56. Nelken NA, Soifer SJ, O'Keefe J, Vu TK, Charo IF, Coughlin SR. Thrombin receptor expression in normal and atherosclerotic human arteries. *J Clin Invest*. 1992;90:1614-1621

57. Maeda Y, Hirano K, Kai Y, Hirano M, Suzuki SO, Sasaki T, Kanaide H. Up-regulation of proteinase-activated receptor 1 and increased contractile responses to thrombin after subarachnoid haemorrhage. *Br J Pharmacol*. 2007;152:1131-1139

58. McNamara CA, Sarembock IJ, Gimple LW, Fenton JW, 2nd, Coughlin SR, Owens GK. Thrombin stimulates proliferation of cultured rat aortic smooth muscle cells by a proteolytically activated receptor. *J Clin Invest*. 1993;91:94-98

59. Andrade-Gordon P, Derian CK, Maryanoff BE, Zhang H-C, Addo MF, Cheung W-M, Damiano BP, D'Andrea MR, Darrow AL, DeGaravilla L, Eckardt AJ, Giardino EC, Haertlein BJ, McComsey DF. Administration of a potent antagonist of protease-activated receptor-1 (par-1) attenuates vascular restenosis following balloon angioplasty in rats. *J. Pharm. Exp. Therap.* 2001;298:34-42

60. Dabbagh K, Laurent GJ, McAnulty RJ, Chambers RC. Thrombin stimulates smooth muscle cell procollagen synthesis and mrna levels via a par-1 mediated mechanism. *Thromb Haemost*. 1998;79:405-409

61. Cucina A, Borrelli V, Di Carlo A, Pagliei S, Corvino V, Santoro-D'Angelo L, Cavallaro A, Sterpetti AV. Thrombin induces production of growth factors from aortic smooth muscle cells. *J Surg Res*. 1999;82:61-66

62. Cheung WM, D'Andrea MR, Andrade-Gordon P, Damiano BP. Altered vascular injury responses in mice deficient in protease-activated receptor-1. *Arterioscler Thromb Vasc Biol*. 1999;19:3014-3024

63. Sevigny LM, Austin KM, Zhang P, Kasuda S, Koukos G, Sharifi S, Covic L, Kuliopulos A. Protease-activated receptor-2 modulates protease-activated receptor-1-driven neointimal hyperplasia. *Arteriosclerosis, Thrombosis, and Vascular Biology*. 2011;31:e100-106

64. Damiano BP, D'Andrea MR, de Garavilla L, Cheung WM, Andrade-Gordon P. Increased expression of protease activated receptor-2 (par-2) in balloon-injured rat carotid artery. *Thromb Haemost*. 1999;81:808-814

65. Tennant GM, Wadsworth RM, Kennedy S. Par-2 mediates increased inflammatory cell adhesion and neointima formation following vascular injury in the mouse. *Atherosclerosis*. 2008;198:57-64

66. Sharma A, Tao X, Gopal A, Ligon B, Andrade-Gordon P, Steer ML, Perides G. Protection against acute pancreatitis by activation of protease-activated receptor-2. *Am J Physiol Gastrointest Liver Physiol*. 2005;288:G388-395

67. Hansen KK, Sherman PM, Cellars L, Andrade-Gordon P, Pan Z, Baruch A, Wallace JL, Hollenberg MD, Vergnolle N. A major role for proteolytic activity and proteinase-activated receptor-2 in the pathogenesis of infectious colitis. *Proc Natl Acad Sci U S A*. 2005;102:8363-8368

68. Kassel KM, Owens AP, 3rd, Rockwell CE, Sullivan BP, Wang R, Tawfik O, Li G, Guo GL, Mackman N, Luyendyk JP. Protease-activated receptor 1 and hematopoietic cell tissue factor are required for hepatic steatosis in mice fed a western diet. *Am J Pathol*. 2011;179:2278-2289

69. Fiorucci S, Antonelli E, Distrutti E, Severino B, Fiorentina R, Baldoni M, Caliendo G, Santagada V, Morelli A, Cirino G. Par1 antagonism protects against experimental liver fibrosis. Role of proteinase receptors in stellate cell activation. *Hepatology*. 2004;39:365-375

70. Knight V, Tchongue J, Lourensz D, Tipping P, Sievert W. Protease-activated receptor 2 promotes experimental liver fibrosis in mice and activates human hepatic stellate cells. *Hepatology*. 2012;55:879-887

71. Jesmin SZ, S; Shimojo, J; Sultana, S; Iwashima, Y; Yamaguchi, N; Gando, S. Blockade of protease activated receptor-2 ameliorates acute liver injry through the suppression of upregulated levesl of endothelin-1 and tnf-alpha in a rat model of endotoxemia. *Circulation*. 2008

72. Whitehead I, Kirk H, Kay R. Expression cloning of oncogenes by retroviral transfer of cdna libraries. *Mol Cell Biol*. 1995;15:704-710

73. Liu J, Schuff-Werner P, Steiner M. Thrombin/thrombin receptor (par-1)-mediated induction of il-8 and vegf expression in prostate cancer cells. *Biochem Biophys Res Commun*. 2006;343:183-189

74. Andrade-Gordon P, Maryanoff BE, Derian CK, Zhang H-C, Addo MF, Darrow AL, Eckardt AJ, Hoekstra WJ, McComsey DF, Oksenberg D, Reynolds EE, Santulli RJ, Scarborough RM, Smith CE, White KB. Design, synthesis, and biological characterization of a peptide-mimetic antagonist for a tethered-ligand receptor. *Proc. Natl. Acad. Sci. (USA)*. 1999;96:12257-12262

75. Zhang HC, Derian CK, Andrade-Gordon P, Hoekstra WJ, McComsey DF, White KB, Poulter BL, Addo MF, Cheung WM, Damiano BP, Oksenberg D, Reynolds EE, Pandey A, Scarborough RM, Maryanoff BE. Discovery and optimization of a novel series of thrombin receptor (par-1) antagonists: Potent, selective peptide mimetics based on indole and indazole templates. *J Med Chem*. 2001;44:1021-1024

76. Maryanoff BE, Zhang HC, Andrade-Gordon P, Derian CK. Discovery of potent peptide-mimetic antagonists for the human thrombin receptor, protease-activated receptor-1 (par-1). *Curr Med Chem Cardiovasc Hematol Agents*. 2003;1:13-36

77. Kahn ML, Nakanishi-Matsui M, Shapiro MJ, Ishihara H, Coughlin SR. Protease-activated receptors 1 and 4 mediate activation of human platelets by thrombin. *J Clin Invest*. 1999;103:879-887

78. Covic L. TB, Jacques S., Kuliopulos A. . Handbook of cell-penetrating peptides. 2007:2

79. Covic L, Gresser AL, Talavera J, Swift S, Kuliopulos A. Activation and inhibition of g protein-coupled receptors by cell-penetrating membrane-tethered peptides. *Proc Natl Acad Sci USA*. 2002;99:643-648

80. Covic L, Misra M, Badar J, Singh C, Kuliopulos A. Pepducin-based intervention of thrombin-receptor signaling and systemic platelet activation. *Nat Med*. 2002;8:1161-1165

81. Zhang P, Gruber A, Kasuda S, Kimmelstiel C, O'Callaghan K, Cox DH, Bohm A, Baleja JD, Covic L, Kuliopulos A. Suppression of arterial thrombosis without affecting hemostatic parameters with a cell-penetrating par1 pepducin. *Circulation*.126:83-91

82. Adams MN, Ramachandran R, Yau MK, Suen JY, Fairlie DP, Hollenberg MD, Hooper JD. Structure, function and pathophysiology of protease activated receptors. *Pharmacol Ther*.130:248-282

83. Perez M, Lamothe M, Maraval C, Mirabel E, Loubat C, Planty B, Horn C, Michaux J, Marrot S, Letienne R, Pignier C, Bocquet A, Nadal-Wollbold F, Cussac D, de Vries L, Le Grand B. Discovery of novel protease activated receptors 1 antagonists with potent antithrombotic activity in vivo. *J Med Chem*. 2009;52:5826-5836

84. Lee H, Hamilton JR. Physiology, pharmacology, and therapeutic potential of protease-activated receptors in vascular disease. *Pharmacol Ther*.134:246-259

85. Chintala M, Strony J, Yang B, Kurowski S, Li Q. Sch 602539, a protease-activated receptor-1 antagonist, inhibits thrombosis alone and in combination with cangrelor in a folts model of arterial thrombosis in cynomolgus monkeys. *Arterioscler Thromb Vasc Biol*. 2010;30:2143-2149

86. Executive TC, Steering C. The thrombin receptor antagonist for clinical event reduction in acute coronary syndrome (tra*cer) trial: Study design and rationale. *Am Heart J*. 2009;158:327-334 e324

87. Morrow DA, Braunwald E, Bonaca MP, Ameriso SF, Dalby AJ, Fish MP, Fox KAA, Lipka LJ, Liu X, Nicolau JC, Oude Ophuis AJ, Paolasso E, Scirica BM, Spinar J, Theroux P, Wiviott SD, Strony J, Murphy SA, Investigators tTPTSCa. Vorapaxar in the secondary prevention of atherothrombotic events. *N Engl J Med*. 2012

88. Morrow DA, Braunwald E, Bonaca MP, Ameriso SF, Dalby AJ, Fish MP, Fox KA, Lipka LJ, Liu X, Nicolau JC, Ophuis AJ, Paolasso E, Scirica BM, Spinar J, Theroux P, Wiviott SD, Strony J, Murphy SA, Committee TPTS, Investigators. Vorapaxar in the secondary prevention of atherothrombotic events. *N Engl J Med*. 2012;366:1404-1413

89. Scirica BM, Bonaca MP, Braunwald E, De Ferrari GM, Isaza D, Lewis BS, Mehrhof F, Merlini PA, Murphy SA, Sabatine MS, Tendera M, Van de Werf F, Wilcox R, Morrow DA, Investigators TRAdP-TSC. Vorapaxar for secondary prevention of thrombotic events for patients with previous myocardial infarction: A prespecified subgroup analysis of the tra 2 degrees p-timi 50 trial. *Lancet*. 2012;380:1317-1324

90. Serebruany VL, Kogushi M, Dastros-Pitei D, Flather M, Bhatt DL. The in-vitro effects of e5555, a protease-activated receptor (par)-1 antagonist, on platelet

biomarkers in healthy volunteers and patients with coronary artery disease. *Thromb Haemost*. 2009;102:111-119

91. Goto S, Ogawa H, Takeuchi M, Flather MD, Bhatt DL. Double-blind, placebo-controlled phase ii studies of the protease-activated receptor 1 antagonist e5555 (atopaxar) in japanese patients with acute coronary syndrome or high-risk coronary artery disease. *Eur Heart J*.31:2601-2613

92. Newby AC. Matrix metalloproteinase inhibition therapy for vascular diseases. *Vascul Pharmacol*.56:232-244

93. Manka SW, Carafoli F, Visse R, Bihan D, Raynal N, Farndale RW, Murphy G, Enghild JJ, Hohenester E, Nagase H. Structural insights into triple-helical collagen cleavage by matrix metalloproteinase 1. *Proc Natl Acad Sci U S A*. 2012;109:12461-12466

94. Shoulders MD, Raines RT. Collagen structure and stability. *Annu Rev Biochem*. 2009;78:929-958

95. Newby AC. Matrix metalloproteinase inhibition therapy for vascular diseases. *Vascul Pharmacol*. 2012;56:232-244

96. Jones CB, Sane DC, Herrington DM. Matrix metalloproteinases: A review of their structure and role in acute coronary syndrome. *Cardiovasc Res*. 2003;59:812-823

97. Nagase H, Visse R, Murphy G. Structure and function of matrix metalloproteinases and timps. *Cardiovasc Res*. 2006;69:562-573

98. Parks WC, Wilson CL, Lopez-Boado YS. Matrix metalloproteinases as modulators of inflammation and innate immunity. *Nat Rev Immunol*. 2004;4:617-629

99. Sternlicht MD, Werb Z. How matrix metalloproteinases regulate cell behavior. *Annu. Rev. Cell Dev. Biol.* 2001;17:463-516

100. Boire A, Covic L, Agarwal A, Jacques S, Sherifi S, Kuliopulos A. Par1 is a matrix metalloprotease-1 receptor that promotes invasion and tumorigenesis of breast cancer cells. *Cell*. 2005;120:303-313

101. Tressel SL, Kaneider NC, Kasuda S, Foley C, Koukos G, Austin K, Agarwal A, Covic L, Opal SM, Kuliopulos A. A matrix metalloprotease-par1 system regulates vascular integrity, systemic inflammation and death in sepsis. *EMBO Mol Med*. 2011;3:370-384

102. Foley CJ, Luo C, O'Callaghan K, Hinds PW, Covic L, Kuliopulos A. Matrix metalloprotease-1a promotes tumorigenesis and metastasis. *J Biol Chem*. 2012;287:24330-24338

103. Jaffre F, Friedman AE, Hu Z, Mackman N, Blaxall BC. Beta-adrenergic receptor stimulation transactivates protease-activated receptor 1 via matrix metalloproteinase 13 in cardiac cells. *Circulation*. 2012;125:2993-3003

104. Galis ZS, Sukhova GK, Lark MW, Libby P. Increased expression of matrix metalloproteinases and matrix degrading activity in vulnerable regions of human atherosclerotic plaques. *J Clin Invest*. 1994;94:2493-2503

105. Brinckerhoff CE, Rutter JL, Benbow U. Interstitial collagenases as markers of tumor progression. *Clin Cancer Res*. 2000;6:4823-4830

106. Galt SW, Lindemann S, Allen L, Medd DJ, Falk JM, McIntyre TM, Prescott SM, Kraiss LW, Zimmerman GA, Weyrich AS. Outside-in signals delivered by matrix metalloproteinase-1 regulate platelet function. *Circ Res*. 2002;90:1093-1099

107. Giambernardi TA, Grant GM, Taylor GP, Hay RJ, Maher VM, McCormick JJ, Klebe RJ. Overview of matrix metalloproteinase expression in cultured human cells. *Matrix Biol*. 1998;16:483-496

108. Kiili M, Cox SW, Chen HY, Wahlgren J, Maisi P, Eley BM, Salo T, Sorsa T. Collagenase-2 (mmp-8) and collagenase-3 (mmp-13) in adult periodontitis: Molecular forms and levels in gingival crevicular fluid and immunolocalisation in gingival tissue. *J Clin Periodontol*. 2002;29:224-232

109. Moilanen M, Sorsa T, Stenman M, Nyberg P, Lindy O, Vesterinen J, Paju A, Konttinen YT, Stenman UH, Salo T. Tumor-associated trypsinogen-2 (trypsinogen-2) activates procollagenases (mmp-1, -8, -13) and stromelysin-1 (mmp-3) and degrades type i collagen. *Biochemistry*. 2003;42:5414-5420

110. Sukhova GK, Schonbeck U, Rabkin E, Schoen RJ, Poole AR, Billinghurst RC, Libby P. Evidence for increased collagenolysis by interstitial collagenases-1 and -3 in vulnerable human atheromatous plaques. *Circulation*. 1999;99

111. Rodriguez D, Morrison CJ, Overall CM. Matrix metalloproteinases: What do they not do? New substrates and biological roles identified by murine models and proteomics. *Biochim Biophys Acta*. 2010;1803:39-54

112. Agnihotri R, Crawford HC, Haro H, Matrisian LM, Havrda MC, Liaw L. Osteopontin, a novel substrate for matrix metalloproteinase-3 (stromelysin-1) and matrix metalloproteinase-7 (matrilysin). *J Biol Chem*. 2001;276:28261-28267

113. Jin F, Zhai Q, Qiu L, Meng H, Zou D, Wang Y, Li Q, Yu Z, Han J, Zhou B. Degradation of bm sdf-1 by mmp-9: The role in g-csf-induced hematopoietic stem/progenitor cell mobilization. *Bone Marrow Transplant*. 2008;42:581-588

114. Lu X, Wang Q, Hu G, Van Poznak C, Fleisher M, Reiss M, Massague J, Kang Y. Adamts1 and mmp1 proteolytically engage egf-like ligands in an osteolytic signaling cascade for bone metastasis. *Genes Dev*. 2009;23:1882-1894

115. Ito A, Mukaiyama A, Itoh Y, Nagase H, Thogersen IB, Enghild JJ, Sasaguri Y, Mori Y. Degradation of interleukin 1beta by matrix metalloproteinases. *J Biol Chem*. 1996;271:14657-14660

116. Blackburn JS, Brinckerhoff CE. Matrix metalloproteinase-1 and thrombin differentially activate gene expression in endothelial cells via par-1 and promote angiogenesis. *Am J Pathol*. 2008;173:1736-1746

117. Yang E, Boire A, Agarwal A, Nguyen N, O'Callaghan K, Tu P, Kuliopulos A, Covic L. Blockade of par1 signaling with cell-penetrating pepducins inhibits akt survival pathways in breast cancer cells and suppresses tumor survival and metastasis. *Cancer Res*. 2009;69:6223-6231

118. Netzel-Arnett S, Fields GB, Birkedal-Hansen H, Van Wart HE. Sequence specificities of human fibroblast and neutrophil collagenases. *J Biol Chem*. 1991;266:6747-6755

119. Turk BE, Huang LL, Piro ET, Cantley LC. Determination of protease cleavage site motifs using mixture-based oriented peptide libraries. *Nat Biotechnol*. 2001;19:661-667

120. Lovejoy B, Welch AR, Carr S, Luong C, Broka C, Hendricks RT, Campbell JA, Walker KA, Martin R, Van Wart H, Browner MF. Crystal structures of mmp-1 and -13 reveal the structural basis for selectivity of collagenase inhibitors. *Nat Struct Biol*. 1999;6:217-221

121. Bode W, Reinemer P, Huber R, Kleine T, Schnierer S, Tschesche H. The x-ray crystal structure of the catalytic domain of human neutrophil collagenase inhibited by a substrate analogue reveals the essentials for catalysis and specificity. *EMBO J*. 1994;13:1263-1269

122. Berman J, Green M, Sugg E, Anderegg R, Millington DS, Norwood DL, McGeehan J, Wiseman J. Rapid optimization of enzyme substrates using defined substrate mixtures. *J Biol Chem*. 1992;267:1434-1437

123. Chang JY. Thrombin specificity. Requirement for apolar amino acids adjacent to the thrombin cleavage site of polypeptide substrate. *Eur J Biochem*. 1985;151:217-224

124. Austin KM, Covic L, Kuliopulos A. Matrix metalloproteases and par1 activation. *Blood*. 2013;121:431-439

125. Nesi A, Fragai M. Substrate specificities of matrix metalloproteinase 1 in par-1 exodomain proteolysis. *Chembiochem*. 2007;8:1367-1369

126. Kuliopulos A, Covic L, Seeley SK, Sheridan PJ, Helin J, Costello CE. Plasmin desensitization of the par1 thrombin receptor: Kinetics, sites of truncation, and implications for thrombolytic therapy. *Biochemistry*. 1999;38:4572-4585

127. Schuepbach RA, Madon J, Ender M, Galli P, Riewald M. Protease activated receptor-1 cleaved at r46 mediates cytoprotective effects. *J Thromb Haemost*. 2012;10:1657-1684

128. Sevigny LM, Austin KM, Zhang P, Kasuda S, Koukos G, Sharifi S, Covic L, Kuliopulos A. Protease-activated receptor-2 modulates protease-activated receptor-1-driven neointimal hyperplasia. *Arterioscler Thromb Vasc Biol*. 2011;31:e100-106

129. Ayoub MA, Maurel D, Binet V, Fink M, Prezeau L, Ansanay H, Pin JP. Real-time analysis of agonist-induced activation of protease-activated receptor 1/galphai1 protein complex measured by bioluminescence resonance energy transfer in living cells. *Mol Pharmacol*. 2007;71:1329-1340

130. Ayoub MA, Trinquet E, Pfleger KD, Pin JP. Differential association modes of the thrombin receptor par1 with galphai1, galpha12, and beta-arrestin 1. *FASEB J*.24:3522-3535

131. Bae JS, Yang L, Rezaie AR. Lipid raft localization regulates the cleavage specificity of protease activated receptor 1 in endothelial cells. *J Thromb Haemost*. 2008;6:954-961

132. Jackson SP. Arterial thrombosis--insidious, unpredictable and deadly. *Nat Med*. 2011;17:1423-1436

133. Heidenreich PA, Trogdon JG, Khavjou OA, Butler J, Dracup K, Ezekowitz MD, Finkelstein EA, Hong Y, Johnston SC, Khera A, Lloyd-Jones DM, Nelson SA, Nichol G, Orenstein D, Wilson PW, Woo YJ. Forecasting the future of cardiovascular disease in the united states: A policy statement from the american heart association. *Circulation*. 2011;123:933-944

134. Stone GW, Maehara A, Lansky AJ, de Bruyne B, Cristea E, Mintz GS, Mehran R, McPherson J, Farhat N, Marso SP, Parise H, Templin B, White R, Zhang Z, Serruys PW. A prospective natural-history study of coronary atherosclerosis. *N Engl J Med*. 2012;364:226-235

135. Sawicki G, Salas E, Murat J, Miszta-Lane H, Radomski MW. Release of gelatinase a during platelet activation mediates aggregation. *Nature*. 1997;386:616-619

136. Kazes I, Elalamy I, Sraer JD, Hatmi M, Nguyen G. Platelet release of trimolecular complex components mt1-mmp/timp2/mmp2: Involvement in mmp2 activation and platelet aggregation. *Blood*. 2000;96:3064-3069

137. Chesney CM, Harper E, Colman RW. Human platelet collagenase. *J Clin Invest*. 1974;53:1647-1654

138. Eckart RE, Uyehara CF, Shry EA, Furgerson JL, Krasuski RA. Matrix metalloproteinases in patients with myocardial infarction and percutaneous revascularization. *J. Interv. Cardiol.* 2004;17:27-31

139. Gaubatz JW, Ballantyne CM, Wasserman BA, He M, Chambless LE, Boerwinkle E, Hoogeveen RC. Association of circulating matrix metalloproteinases with carotid artery characteristics: The atherosclerosis risk in communities carotid mri study. *Arterioscler Thromb Vasc Biol*. 2010;30:1034-1042

140. Nikkari ST, O'Brien KD, Ferguson M, Hatsukami T, Welgus HG, Alpers CE, Clowes AW. Interstitial collagenase (mmp-1) expression in human carotid atherosclerosis. *Circulation*. 1995;92:1393-1398

141. Lee RT, Schoen FJ, Loree HM, Lark MW, Libby P. Circumferential stress and matrix metalloproteinase 1 in human coronary atherosclerosis. Implications for plaque rupture. *Arterioscler Thromb Vasc Biol*. 1996;16:1070-1073

142. Djuric T, Stojkovic L, Zivkovic M, Koncar I, Stankovic A, Djordjevic A, Alavantic D. Matrix metalloproteinase-1 promoter genotypes and haplotypes are associated with carotid plaque presence. *Clin Biochem*. 2012;45:1353-1356

143. Pearce EG, Laxton RC, Pereira AC, Ye S. Haplotype effects on matrix metalloproteinase-1 gene promoter activity in cancer cells. *Molecular Cancer Research*. 2007;5:221-227

144. Esmon CT. The impact of the inflammatory response on coagulation. *Thromb Res*. 2004;114:321-327

145. Pawlinski R, Mackman N. Tissue factor, coagulation proteases, and protease-activated receptors in endotoxemia and sepsis. *Crit Care Med*. 2004;32:S293-297

146. van der Poll T, de Boer JD, Levi M. The effect of inflammation on coagulation and vice versa. *Curr Opin Infect Dis*. 2011;24:273-278

147. Kaneider NC, Leger AJ, Kuliopulos A. Therapeutic targeting of molecules involved in leukocyte-endothelial cell interactions. *FEBS J.* 2006;273:4416-4424

148. Garcia JG, Davis HW, Patterson CE. Regulation of endothelial cell gap formation and barrier dysfunction: Role of myosin light chain phosphorylation. *J Cell Physiol*. 1995;163:510-522

149. Vouret-Craviari V, Bourcier C, Boulter E, van Obberghen-Schilling E. Distinct signals via rho gtpases and src drive shape changes by thrombin and sphingosine-1-phosphate in endothelial cells. *J Cell Sci*. 2002;115:2475-2484

150. Pawlinski R, Pedersen B, Schabbauer G, Tencati M, Holscher T, Boisvert W, Andrade-Gordon P, Frank RD, Mackman N. Role of tissue factor and protease-activated receptors in a mouse model of endotoxemia. *Blood*. 2004;103:1342-1347

151. Zempo N, Koyama N, Kenagy RD, Lea HJ, Clowes AW. Regulation of vascular smooth muscle cell migration and proliferation in vitro and in injured rat arteries by a synthetic matrix metalloproteinase inhibitor. *Arterioscler Thromb Vasc Biol*. 1996;16:28-33

152. de Smet BJ, de Kleijn D, Hanemaaijer R, Verheijen JH, Robertus L, van Der Helm YJ, Borst C, Post MJ. Metalloproteinase inhibition reduces constrictive arterial remodeling after balloon angioplasty: A study in the atherosclerotic yucatan micropig. *Circulation*. 2000;101:2962-2967

153. Johnson C, Galis ZS. Matrix metalloproteinase-2 and -9 differentially regulate smooth muscle cell migration and cell-mediated collagen organization. *Arterioscler Thromb Vasc Biol*. 2004;24:54-60

154. Cho A, Reidy MA. Matrix metalloproteinase-9 is necessary for the regulation of smooth muscle cell replication and migration after arterial injury. *Circ Res*. 2002;91:845-851

155. Bendeck MP, Irvin C, Reidy MA. Inhibition of matrix metalloproteinase activity inhibits smooth muscle cell migration but not neointimal thickening after arterial injury. *Circ Res*. 1996;78:38-43

156. Prescott MF, Sawyer WK, Von Linden-Reed J, Jeune M, Chou M, Caplan SL, Jeng AY. Effect of matrix metalloproteinase inhibition on progression of atherosclerosis and aneurysm in ldl receptor-deficient mice overexpressing mmp-3, mmp-12, and mmp-13 and on restenosis in rats after balloon injury. *Ann N Y Acad Sci*. 1999;878:179-190

157. Cherr GS, Motew SJ, Travis JA, Fingerle J, Fisher L, Brandl M, Williams JK, Geary RL. Metalloproteinase inhibition and the response to angioplasty and stenting in atherosclerotic primates. *Arterioscler Thromb Vasc Biol*. 2002;22:161-166

158. Peterson JT. The importance of estimating the therapeutic index in the development of matrix metalloproteinase inhibitors. *Cardiovasc Res*. 2006;69:677-687

159. Margolin L, Fishbein I, Banai S, Golomb G, Reich R, Perez LS, Gertz SD. Metalloproteinase inhibitor attenuates neointima formation and constrictive remodeling after angioplasty in rats: Augmentative effect of alpha(v)beta(3) receptor blockade. *Atherosclerosis*. 2002;163:269-277

160. Fingleton B. Matrix metalloproteinases as valid clinical targets. *Curr Pharm Des*. 2007;13:333-346

161. Axisa B, Loftus IM, Naylor AR, Goodall S, Jones L, Bell PR, Thompson MM. Prospective, randomized, double-blind trial investigating the effect of doxycycline

on matrix metalloproteinase expression within atherosclerotic carotid plaques. *Stroke*. 2002;33:2858-2864

162. Pires PW, Rogers CT, McClain JL, Garver HS, Fink GD, Dorrance AM. Doxycycline, a matrix metalloprotease inhibitor, reduces vascular remodeling and damage after cerebral ischemia in stroke-prone spontaneously hypertensive rats. *Am J Physiol Heart Circ Physiol*. 2011;301:H87-97

163. Bendeck MP, Conte M, Zhang M, Nili N, Strauss BH, Farwell SM. Doxycycline modulates smooth muscle cell growth, migration, and matrix remodeling after arterial injury. *Am J Pathol*. 2002;160:1089-1095

164. Brown DL, Desai KK, Vakili BA, Nouneh C, Lee HM, Golub LM. Clinical and biochemical results of the metalloproteinase inhibition with subantimicrobial doses of doxycycline to prevent acute coronary syndromes (midas) pilot trial. *Arterioscler Thromb Vasc Biol*. 2004;24:733-738

165. Marx SO, Totary-Jain H, Marks AR. Vascular smooth muscle cell proliferation in restenosis. *Circ Cardiovasc Interv*. 2011;4:104-111

166. Gomez D, Owens GK. Smooth muscle cell phenotypic switching in atherosclerosis. *Cardiovasc Res*. 2012;95:156-164

167. Owens GK, Kumar MS, Wamhoff BR. Molecular regulation of vascular smooth muscle cell differentiation in development and disease. *Physiol Rev*. 2004;84:767-801

168. Geary RL, Wong JM, Rossini A, Schwartz SM, Adams LD. Expression profiling identifies 147 genes contributing to a unique primate neointimal smooth muscle cell phenotype. *Arterioscler Thromb Vasc Biol*. 2002;22:2010-2016

169. Mack CP. Signaling mechanisms that regulate smooth muscle cell differentiation. *Arterioscler Thromb Vasc Biol*. 2011;31:1495-1505

170. Leveen P, Pekny M, Gebre-Medhin S, Swolin B, Larsson E, Betsholtz C. Mice deficient for pdgf b show renal, cardiovascular, and hematological abnormalities. *Genes Dev*. 1994;8:1875-1887

171. Soriano P. Abnormal kidney development and hematological disorders in pdgf beta-receptor mutant mice. *Genes Dev*. 1994;8:1888-1896

172. Yang Q, Guan KL. Expanding mtor signaling. *Cell Res*. 2007;17:666-681

173. Giordano A, Romano A. Inhibition of human in-stent restenosis: A molecular view. *Curr Opin Pharmacol*. 2011;11:372-377

174. Sidhu S, Shafiq N, Malhotra S, Pandhi P, Grover A. A meta-analysis of trials comparing cypher and taxus stents in patients with obstructive coronary artery disease. *Br J Clin Pharmacol*. 2006;61:720-726

175. Kastrati A, Mehilli J, von Beckerath N, Dibra A, Hausleiter J, Pache J, Schuhlen H, Schmitt C, Dirschinger J, Schomig A, Investigators I-DS. Sirolimus-eluting stent or paclitaxel-eluting stent vs balloon angioplasty for prevention of recurrences in patients with coronary in-stent restenosis: A randomized controlled trial. *JAMA*. 2005;293:165-171

176. Fujii H, Kawada N. Inflammation and fibrogenesis in steatohepatitis. *J Gastroenterol*. 2012;47:215-225

177. Sanyal AJ, Banas C, Sargeant C, Luketic VA, Sterling RK, Stravitz RT, Shiffman ML, Heuman D, Coterrell A, Fisher RA, Contos MJ, Mills AS. Similarities and differences in outcomes of cirrhosis due to nonalcoholic steatohepatitis and hepatitis c. *Hepatology*. 2006;43:682-689

178. Marchesini G, Marzocchi R. Metabolic syndrome and nash. *Clin Liver Dis*. 2007;11:105-117, ix

179. Day CP, James OF. Steatohepatitis: A tale of two "hits"? *Gastroenterology*. 1998;114:842-845

180. Malinowski SS, Byrd JS, Bell AM, Wofford MR, Riche DM. Pharmacologic therapy for nonalcoholic fatty liver disease in adults. *Pharmacotherapy*. 2013

181. Hellerbrand C. Hepatic stellate cells-the pericytes in the liver. *Pflugers Arch*. 2013

182. Aithal GP, Thomas JA, Kaye PV, Lawson A, Ryder SD, Spendlove I, Austin AS, Freeman JG, Morgan L, Webber J. Randomized, placebo-controlled trial of pioglitazone in nondiabetic subjects with nonalcoholic steatohepatitis. *Gastroenterology*. 2008;135:1176-1184

183. Sanyal AJ, Chalasani N, Kowdley KV, McCullough A, Diehl AM, Bass NM, Neuschwander-Tetri BA, Lavine JE, Tonascia J, Unalp A, Van Natta M, Clark J, Brunt EM, Kleiner DE, Hoofnagle JH, Robuck PR, Nash CRN. Pioglitazone, vitamin e, or placebo for nonalcoholic steatohepatitis. *N Engl J Med*. 2010;362:1675-1685

184. Nar A, Gedik O. The effect of metformin on leptin in obese patients with type 2 diabetes mellitus and nonalcoholic fatty liver disease. *Acta Diabetol*. 2009;46:113-118

185. Uygun A, Kadayifci A, Isik AT, Ozgurtas T, Deveci S, Tuzun A, Yesilova Z, Gulsen M, Dagalp K. Metformin in the treatment of patients with non-alcoholic steatohepatitis. *Aliment Pharmacol Ther*. 2004;19:537-544

186. Li W, Zheng L, Sheng C, Cheng X, Qing L, Qu S. Systematic review on the treatment of pentoxifylline in patients with non-alcoholic fatty liver disease. *Lipids Health Dis*. 2011;10:49

187. Ip E, Farrell G, Hall P, Robertson G, Leclercq I. Administration of the potent pparalpha agonist, wy-14,643, reverses nutritional fibrosis and steatohepatitis in mice. *Hepatology*. 2004;39:1286-1296

188. Davidson MH, Hauptman J, DiGirolamo M, Foreyt JP, Halsted CH, Heber D, Heimburger DC, Lucas CP, Robbins DC, Chung J, Heymsfield SB. Weight control and risk factor reduction in obese subjects treated for 2 years with orlistat: A randomized controlled trial. *JAMA*. 1999;281:235-242

189. Hussein O, Grosovski M, Schlesinger S, Szvalb S, Assy N. Orlistat reverse fatty infiltration and improves hepatic fibrosis in obese patients with nonalcoholic steatohepatitis (nash). *Dig Dis Sci*. 2007;52:2512-2519

190. Takahashi Y, Soejima Y, Fukusato T. Animal models of nonalcoholic fatty liver disease/nonalcoholic steatohepatitis. *World J Gastroenterol*. 2012;18:2300-2308

191. Kirsch R, Clarkson V, Shephard EG, Marais DA, Jaffer MA, Woodburne VE, Kirsch RE, Hall Pde L. Rodent nutritional model of non-alcoholic steatohepatitis: Species, strain and sex difference studies. *J Gastroenterol Hepatol*. 2003;18:1272-1282

192. Tiwari S, Siddiqi SA. Intracellular trafficking and secretion of vldl. *Arterioscler Thromb Vasc Biol*. 2012;32:1079-1086

193. Farrell DJ, Hines JE, Walls AF, Kelly PJ, Bennett MK, Burt AD. Intrahepatic mast cells in chronic liver diseases. *Hepatology*. 1995;22:1175-1181

194. Gaca MD, Zhou X, Benyon RC. Regulation of hepatic stellate cell proliferation and collagen synthesis by proteinase-activated receptors. *J Hepatol*. 2002;36:362-369

195. Gaca MD, Pickering JA, Arthur MJ, Benyon RC. Human and rat hepatic stellate cells produce stem cell factor: A possible mechanism for mast cell recruitment in liver fibrosis. *J Hepatol*. 1999;30:850-858

196. Badeanlou L, Furlan-Freguia C, Yang G, Ruf W, Samad F. Tissue factor-protease-activated receptor 2 signaling promotes diet-induced obesity and adipose inflammation. *Nat Med*. 2011;17:1490-1497

197. Doran AC, Meller N, McNamara CA. Role of smooth muscle cells in the initiation and early progression of atherosclerosis. *Arterioscler Thromb Vasc Biol*. 2008;28:812-819

198. Sukhova GK, Schonbeck U, Rabkin E, Schoen FJ, Poole AR, Billinghurst RC, Libby P. Evidence for increased collagenolysis by interstitial collagenases-1 and -3 in vulnerable human atheromatous plaques. *Circulation*. 1999;99:2503-2509

199. Lehrke M, Greif M, Broedl UC, Lebherz C, Laubender RP, Becker A, von Ziegler F, Tittus J, Reiser M, Becker C, Goke B, Steinbeck G, Leber AW, Parhofer KG. Mmp-1 serum levels predict coronary atherosclerosis in humans. *Cardiovasc Diabetol*. 2009;8:50

200. Wu YW, Yang WS, Chen MF, Lee BC, Hung CS, Liu YC, Jeng JS, Huang PJ, Kao HL. High serum level of matrix metalloproteinase-1 and its rapid surge after intervention in patients with significant carotid atherosclerosis. *J Formos Med Assoc*. 2008;107:93-98

201. Adams MN, Ramachandran R, Yau MK, Suen JY, Fairlie DP, Hollenberg MD, Hooper JD. Structure, function and pathophysiology of protease activated receptors. *Pharmacol Ther*. 2011;130:248-282

202. Rasmussen UB, Vouret-Craviari V, Jallat S, Schlesinger Y, Pages G, Pavirani A, Lecocq JP, Pouyssegur J, Van Obberghen-Schilling E. Cdna cloning and expression of a hamster alpha-thrombin receptor coupled to ca2+ mobilization. *FEBS Lett*. 1991;288:123-128

203. Ragosta M, Gimple LW, Gertz SD, Dunwiddie CT, Vlasuk GP, Haber HL, Powers ER, Roberts WC, Sarembock IJ. Specific factor xa inhibition reduces restenosis after balloon angioplasty of atherosclerotic femoral arteries in rabbits. *Circulation*. 1994;89:1262-1271

204. Chieng-Yane P, Bocquet A, Letienne R, Bourbon T, Sablayrolles S, Perez M, Hatem SN, Lompre AM, Le Grand B, David-Dufilho M. Protease-activated receptor-1 antagonist f 16618 reduces arterial restenosis by down-regulation of tumor necrosis factor alpha and matrix metalloproteinase 7 expression, migration, and proliferation of vascular smooth muscle cells. *J Pharmacol Exp Ther*. 2010;336:643-651

205. Takada M, Tanaka H, Yamada T, Ito O, Kogushi M, Yanagimachi M, Kawamura T, Musha T, Yoshida F, Ito M, Kobayashi H, Yoshitake S, Saito I. Antibody to thrombin receptor inhibits neointimal smooth muscle cell accumulation without causing inhibition of platelet aggregation or altering hemostatic parameters after angioplasty in rat. *Circ Res*. 1998;82:980-987

206. Jordan SW, Chaikof EL. Simulated surface-induced thrombin generation in a flow field. *Biophys J*. 2011;101:276-286

207. Sukhova GK, Schönbeck U, Rabkin E, Schoen FJ, Poole AR, Billinghurst RC, Libby P. Evidence for increased collagenolysis by interstitial collagenases-1 and -3 in vulnerable human atheromatous plaques. *Circulation*. 1999;99:2503-2509

208. Zhang J, Nie L, Razavian M, Ahmed M, Dobrucki LW, Asadi A, Edwards DS, Azure M, Sinusas AJ, Sadeghi MM. Molecular imaging of activated matrix metalloproteinases in vascular remodeling. *Circulation*. 2008;118:1953-1960

209. Stouffer GA, Sarembock IJ, McNamara CA, Gimple LW, Owens GK. Thrombin-induced mitogenesis of vascular smc is partially mediated by autocrine production of pdgf-aa. *Am J Physiol*. 1993;265:C806-811

210. Ceruso MA, McComsey DF, Leo GC, Andrade-Gordon P, Addo MF, Scarborough RM, Oksenberg D, Maryanoff BE. Thrombin receptor-activating peptides (traps): Investigation of bioactive conformations via structure-activity, spectroscopic, and computational studies. *Bioorg Med Chem*. 1999;7:2353-2371

211. Al-Ani B, Hansen KK, Hollenberg MD. Proteinase-activated receptor-2: Key role of amino-terminal dipeptide residues of the tethered ligand for receptor activation. *Mol Pharmacol*. 2004;65:149-156

212. Gerthoffer WT. Actin cytoskeletal dynamics in smooth muscle contraction. *Can J Physiol Pharmacol*. 2005;83:851-856

213. Parmacek MS. Myocardin: Dominant driver of the smooth muscle cell contractile phenotype. *Arterioscler Thromb Vasc Biol*. 2008;28:1416-1417

214. Thomson S, Buck E, Petti F, Griffin G, Brown E, Ramnarine N, Iwata KK, Gibson N, Haley JD. Epithelial to mesenchymal transition is a determinant of sensitivity of non-small-cell lung carcinoma cell lines and xenografts to epidermal growth factor receptor inhibition. *Cancer Res*. 2005;65:9455-9462

215. Antonino MJ, Jeong YH, Tantry US, Bliden KP, Gurbel PA. Role of genotype-based personalized antiplatelet therapy in the era of potent p2y(12) receptor inhibitors. *Expert Rev Cardiovasc Ther*. 2012;10:1011-1022

216. Singla A, Bliden KP, Jeong YH, Abadilla K, Antonino MJ, Muse WC, Mathew DP, Bailon O, Tantry US, Gurbel PA. Platelet reactivity and thrombogenicity in postmenopausal women. *Menopause*. 2012

217. Eckart RE, Uyehara CF, Shry EA, Furgerson JL, Krasuski RA. Matrix metalloproteinases in patients with myocardial infarction and percutaneous revascularization. *J Interv Cardiol*. 2004;17:27-31

218. Pearce E, Tregouet DA, Samnegard A, Morgan AR, Cox C, Hamsten A, Eriksson P, Ye S. Haplotype effect of the matrix metalloproteinase-1 gene on risk of myocardial infarction. *Circ Res*. 2005;97:1070-1076

219. Navarese EP, Kubica J, Gurbel PA. "Sirolimus or paclitaxel drug eluting stent in left main disease: The winner is... ". *Int J Cardiol*. 2011;152:387

220. Andrade-Gordon P, Derian CK, Maryanoff BE, Zhang HC, Addo MF, Cheung W, Damiano BP, D'Andrea MR, Darrow AL, de Garavilla L, Eckardt AJ, Giardino EC, Haertlein BJ, McComsey DF. Administration of a potent antagonist of protease-activated receptor-1 (par-1) attenuates vascular restenosis following balloon angioplasty in rats. *J Pharmacol Exp Ther*. 2001;298:34-42

221. Gurbel PA, Jeong YH, Tantry US. Vorapaxar: A novel protease-activated receptor-1 inhibitor. *Expert Opin Investig Drugs*. 2011;20:1445-1453

222. Tricoci P, Huang Z, Held C, Moliterno DJ, Armstrong PW, Van de Werf F, White HD, Aylward PE, Wallentin L, Chen E, Lokhnygina Y, Pei J, Leonardi

S, Rorick TL, Kilian AM, Jennings LH, Ambrosio G, Bode C, Cequier A, Cornel JH, Diaz R, Erkan A, Huber K, Hudson MP, Jiang L, Jukema JW, Lewis BS, Lincoff AM, Montalescot G, Nicolau JC, Ogawa H, Pfisterer M, Prieto JC, Ruzyllo W, Sinnaeve PR, Storey RF, Valgimigli M, Whellan DJ, Widimsky P, Strony J, Harrington RA, Mahaffey KW. Thrombin-receptor antagonist vorapaxar in acute coronary syndromes. *N Engl J Med*. 2012;366:20-33

223. Adam SS, McDuffie JR, Ortel TL, Williams Jr JW. Comparative effectiveness of warfarin and new oral anticoagulants for the management of atrial fibrillation and venous thromboembolism: A systematic review. *Ann Intern Med*. 2012

224. Serruys PW, Herrman JP, Simon R, Rutsch W, Bode C, Laarman GJ, van Dijk R, van den Bos AA, Umans VA, Fox KA, et al. A comparison of hirudin with heparin in the prevention of restenosis after coronary angioplasty. Helvetica investigators. *N Engl J Med*. 1995;333:757-763

225. Burchenal JE, Marks DS, Tift Mann J, Schweiger MJ, Rothman MT, Ganz P, Adelman B, Bittl JA. Effect of direct thrombin inhibition with bivalirudin (hirulog) on restenosis after coronary angioplasty. *Am J Cardiol*. 1998;82:511-515

226. Preisack MB, Baildon R, Eschenfelder V, Foley D, Garcia E, Kaltenbach M, Meisner C, Selbmann HK, Serruys PW, Shiu MF, Sujatta M, Bonan R, Karsch KR. [low molecular weight heparin, reviparin, after ptca: Results of a randomized double-blind, standard heparin and placebo controlled multicenter study (reduce study]. *Z Kardiol*. 1997;86:581-591

227. Te Sligte K, Bourass I, Sels JP, Driessen A, Stockbrugger RW, Koek GH. Non-alcoholic steatohepatitis: Review of a growing medical problem. *Eur J Intern Med*. 2004;15:10-21

228. Yilmaz Y. Review article: Is non-alcoholic fatty liver disease a spectrum, or are steatosis and non-alcoholic steatohepatitis distinct conditions? *Aliment Pharmacol Ther*. 2012;36:815-823

229. Promrat K, Kleiner DE, Niemeier HM, Jackvony E, Kearns M, Wands JR, Fava JL, Wing RR. Randomized controlled trial testing the effects of weight loss on nonalcoholic steatohepatitis. *Hepatology*. 2010;51:121-129

230. Younossi ZM. Review article: Current management of non-alcoholic fatty liver disease and non-alcoholic steatohepatitis. *Aliment Pharmacol Ther*. 2008;28:2-12

231. Haukeland JW, Damas JK, Konopski Z, Loberg EM, Haaland T, Goverud I, Torjesen PA, Birkeland K, Bjoro K, Aukrust P. Systemic inflammation in nonalcoholic fatty liver disease is characterized by elevated levels of ccl2. *J Hepatol*. 2006;44:1167-1174

232. Tosello-Trampont AC, Landes SG, Nguyen V, Novobrantseva TI, Hahn YS. Kuppfer cells trigger nonalcoholic steatohepatitis development in diet-induced mouse model through tumor necrosis factor-alpha production. *J Biol Chem*. 2012;287:40161-40172

233. Schuepbach RA, Madon J, Ender M, Galli P, Riewald M. Protease-activated receptor-1 cleaved at r46 mediates cytoprotective effects. *J Thromb Haemost*. 2012;10:1675-1684

234. Woo AY-H, Song Y, Zhu W, Xiao R-P. Advances in receptor conformation research: The quest for functionally selective conformations focusing on the β2-adrenoceptor. *British Journal of Pharmacology*. 2014:n/a-n/a

235. Ayoub MA, Maurel D, Binet V, Fink M, Pr√¯©zeau L, Ansanay H, Pin J-P. Real-time analysis of agonist-induced activation of protease-activated receptor 1/gœ±i1 protein complex measured by bioluminescence resonance energy transfer in living cells. *Molecular Pharmacology*. 2007;71:1329-1340

236. Ayoub MA, Trinquet E, Pfleger KDG, Pin J-P. Differential association modes of the thrombin receptor par1 with gœ±i1, gœ±12, and œ≤-arrestin 1. *The FASEB Journal*. 2010;24:3522-3535

237. Zheng H, Loh HH, Law P-Y. Agonist-selective signaling of g protein-coupled receptor: Mechanisms and implications. *IUBMB Life*. 2010;62:112-119

238. Yang L, Dong W, Yan F, Ren X, Hao X. Recombinant bovine pancreatic trypsin inhibitor protects the liver from carbon tetrachloride-induced acute injury in mice. *J Pharm Pharmacol*. 2010;62:332-338

239. Bourd-Boittin K, Bonnier D, Leyme A, Mari B, Tuffery P, Samson M, Ezan F, Baffet G, Theret N. Protease profiling of liver fibrosis reveals the adam metallopeptidase with thrombospondin type 1 motif, 1 as a central activator of transforming growth factor beta. *Hepatology*. 2011;54:2173-2184

240. Wang Z, Yao T, Song Z. Extracellular signal-regulated kinases 1/2 suppression aggravates transforming growth factor-beta1 hepatotoxicity: A potential mechanism for liver injury in methionine-choline deficient-diet-fed mice. *Exp Biol Med (Maywood)*. 2010;235:1347-1355

241. Foley CJ, Luo C, O'Callaghan K, Hinds PW, Covic L, Kuliopulos A. Matrix metalloprotease-1a promotes tumorigenesis and metastasis. *J Biol Chem*. 2012;287:24330-24338

242. Cullen P, Baetta R, Bellosta S, Bernini F, Chinetti G, Cignarella A, von Eckardstein A, Exley A, Goddard M, Hofker M, Hurt-Camejo E, Kanters E, Kovanen P, Lorkowski S, McPheat W, Pentikainen M, Rauterberg J, Ritchie A, Staels B, Weitkamp B, de Winther M, Consortium M. Rupture of the atherosclerotic plaque: Does a good animal model exist? *Arterioscler Thromb Vasc Biol*. 2003;23:535-542

243. Shireman PK. The chemokine system in arteriogenesis and hind limb ischemia. *J Vasc Surg*. 2007;45 Suppl A:A48-56

244. Selvin E, Erlinger TP. Prevalence of and risk factors for peripheral arterial disease in the united states: Results from the national health and nutrition examination survey, 1999-2000. *Circulation*. 2004;110:738-743

245. Abdulhannan P, Russell DA, Homer-Vanniasinkam S. Peripheral arterial disease: A literature review. *Br Med Bull*. 2012;104:21-39

246. Milia AF, Salis MB, Stacca T, Pinna A, Madeddu P, Trevisani M, Geppetti P, Emanueli C. Protease-activated receptor-2 stimulates angiogenesis and accelerates hemodynamic recovery in a mouse model of hindlimb ischemia. *Circ Res*. 2002;91:346-352

247. Chen HT, Tsou HK, Tsai CH, Kuo CC, Chiang YK, Chang CH, Fong YC, Tang CH. Thrombin enhanced migration and mmps expression of human chondrosarcoma cells involves par receptor signaling pathway. *J Cell Physiol*. 2010;223:737-745

248. Radjabi AR, Sawada K, Jagadeeswaran S, Eichbichler A, Kenny HA, Montag A, Bruno K, Lengyel E. Thrombin induces tumor invasion through the induction and association of matrix metalloproteinase-9 and beta1-integrin on the cell surface. *J Biol Chem*. 2008;283:2822-2834

249. Bar-Shavit R, Eldor A, Vlodavsky I. Binding of thrombin to subendothelial extracellular matrix. Protection and expression of functional properties. *J Clin Invest*. 1989;84:1096-1104